Prions, autophagy, ageing and actin cytoskeleton in yeast

A thesis submitted to the University of Manchester

for the degree of

DOCTOR OF PHILOSOPHY

in the Faculty of Biology,

Medicine, and Health

2016

SHAUN H. SPELDEWINDE

School of Biological Sciences

Thesis Contents:

Word Count: 46,534

List of Figures

List of Tables

List of Abbreviations

µ:	micro
ADE:	Adenine
ATG:	Autophagy-related gene
ATP:	Adenosine triphosphate
BSE:	Bovine spongiform encephalopathy
C. elegans	*Caenorhabditis elegans*
cAMP:	cyclic adenosine monophosphate
CFP:	Cerulean fluorescent protein
CJD:	Creutzfeldt-Jakob disease
CLS:	Chronological lifespan
CR:	Calorie restriction
Cvt:	Cytoplasm-to-vacuole targeting
DNA:	Deoxyribonucleic acid
DNPH:	2,4-dinitrophenyl-hydrazine
DTT:	Dithiothreitol
EDTA:	Ethlenediaminetetraacetic acid
ER:	Endoplasmic reticulum
ERC:	Extra-chromosomal rDNA circles
F-actin:	Filamentous actin
FITC	Fluorescein isothiocyanate
g:	gram
G-actin:	Globular actin
GA:	Golgi apparatus
GAL:	Galactose
GdnHCl:	Guanidine hydrochloride
GFP:	Green fluorescent protein
h:	hour
HEPES:	4-(2-hydroxyethyl-)-1-piperazineethanesulfonic acid
HRP:	Horseradish peroxidase
HSD:	Honest significant difference
HSP:	Heat shock protein
H_2O_2:	Hydrogen peroxide
IPOD:	Insoluble protein deposit

JUNQ:	Juxta nuclear quality control compartment
l:	litre
LB:	Luria-Bertani media
LTA:	Latrunculin A
m:	milli
M:	Molar
MetO	Oxidized methionine
MetSO:	Methionine sulfoxide
mRNA:	messenger ribonucleic acid
mTOR:	mammalian target of rapamycin
Myo:	Myosin
N:	Asparagine
NPF:	Nucleation promoting factor
OD:	Optical density
OR:	Oligopeptide repeats
PAGE:	Polyacrylamide gel electrophoresis
PAP:	Peroxidase anti-peroxidase
PAS:	Pre-autophagosomal structure
PCR:	Polymerase chain reaction
PE:	Phosphatidylethanolamine
Pgk1:	Phosphoglycerate kinase
PI:	Propidium iodide
PI3K:	phosphatidylinositol-3-phosphate kinase
PKA:	Protein Kinase A
PMSF:	Phenylmethylsufonylfluoride
PQC:	Protein quality control
PrD:	Prion forming domain
PrP^{c} :	Native prion protein
PrP^{Sc}:	Prion protein scrapie form
Prx:	Peroxiredoxin
PVDF:	Polyvinlyidene fluoride
Q:	Glutamine
Raf:	Raffinose
rDNA:	ribosomal deoxyribonucleic acid

RFP:	Red fluorescent protein
RLS:	Replicative lifespan
ROS:	Reactive oxygen species
Rpm:	Revolutions per minute
SCD:	Synthetic complete dextrose
SD:	Synthetic minimal
SDD-AGE:	Semidenaturing detergent agarose gel electrophoresis
SDS:	Sodium dodecyl sulphate
SIR:	Silent Information Regulator
SOD:	Superoxide dismutase
Spd:	Spermidine
SUPX:	Suppressor
TAP:	Tandem affinity purification
TCA:	Trichloroacetic acid
TOR:	Target of rapamycin
TSE:	Transmissible spongiform encephalopathies
Ubl:	Ubiquitin-like
WAS:	Wiskott-Aldrich Syndrome
WT:	wild-type
YEPD:	Yeast extract peptone dextrose

Declaration:

No portion of the work referred to in the thesis has been submitted in support of an application for another degree or qualification of this or any other university or other institute of learning

Acknowledgements

A PhD is the culmination of a significant amount of effort, time and energy expended on a particular subject(s) of interest. It is a representation of a collective body of work that involves the support from many parties that ultimately enables the manifestation of a PhD. For this, I would like to express my gratitude and utmost appreciation to all parties who have been key figures throughout my PhD. First and foremost, I would like to dedicate my sincere thanks and gratitude towards my supervisor, Professor Chris Grant for his continued invaluable guidance, constructive support and for being an outstanding supervisor throughout the progression of my PhD. To Dr Mark Ashe, Prof Graham Pavitt, and my advisor Prof Stephen High, your constructive advice and feedback are most appreciated. I would also like to extend my thanks to Dr Mike Speed, Dr Nigel Jones, Dr James Wilson and Dr Daimark Bennett for your excellent tutorship, advice and support during my undergraduate degree in Liverpool. I would also like to thank Wellcome Trust for supporting my PhD studentship.

To members of the Grant lab past and present: Irina, Karin, AKS007, Pari, Alan, Fadilah, Yaya, Sarah, Jana, Henry, and Rae, thank you so very much for all your tremendous support and making the lab an enjoyable place to work in. Special thanks goes to Dr Vicky D who has initiated me into the world of prion biology and ArunKumar who has been a wonderful friend to me. I would also like to express my thanks and appreciation to all members in the Ashe lab, and the Pavitt lab: Nkechi, Vicky P, Reem, Jenny, Jess, Gabbie, Gbengus, Hassan, Tawni, Fabian, Sarah MQ, Lydia, Joe C, Chris K, Martin, Zhou, Thomas, Rehana, Patrick, Ebele and Kazz for their excellent contributions and assistance.

To the WT tutorial group: S.C., M.V.P., and E.P.R., thanks for all the superb outings and camaraderie. Many thanks to the Costa Club: IriFaYaSa and Greggs Club: H.P.O&O.G Ogbehni for all your contributions and encouragement, much appreciated indeed. To the FLS Asean Group, thank you for all the great outings and sustained support. To Ananda Marga Manchester:

BABA, Sister Subhra, Kerry, Brother Kalyana, Kumar, Devashisha, Devesha, Baskar, Jivamrita, LiilaMaya, AkashaDiipa and Dada Ravi, thank you for always sharing a positive and elevating space together.

Especial thanks goes to Aunty Saro, Uncle Kevin, Sharmini and William whom all have been like a family to me in the UK. To Auntie Nimmi, my sincerest thanks for all your guidance and belief in me. Massive thank yous to my relatives back home, in Singapore, Denmark, and Australia for each and every one of your continuous support and encouragement.

I would also like to extend my sincere appreciation to my dear friends and buddies whom have given their encouragement in many ways which holds special significance to me. Big thank yous to the Selamaians: YcYean, Wan Chyn, WeiGe, SoonBro, Amsyar, Thiru, Ah Toi, Kia Hui, Sze Kee, Ah Heng, and many others for your support and staying connected since 15 years ago and hopefully for 'Selamanya'. To the NYJC Drummers: XinXian, TieZheng, YongHwa, Sherm, and Aiky, thanks for all your Jiayos and encouragement. To my Liverpool crew: YangYang, Hussain, Niedharsen, PengPeng, XiaoYang, Tairan, TJ, Soom, Rachel Q, XinXin, SiQian, and Flat B4 Sister and Brothers: Rachel L, Keerthi Bhai, and Kumail Bhai, thank you for the memorable times, support and for keeping in touch.

Most importantly, my greatest gratitude to my Parents and my Sisters, Sasha and Sheryn for all the Jiayos, Ganbates, and for always believing in me, for this thesis is especially dedicated to you all. Deepest gratitude to my Ah Ma, Grandpa, Nanny and Auntie Bunchie for always rooting for me, taking special care of me and for all the invaluable life lessons you have imparted to me. My PhD journey is only possible through you all and I hold each of you dearly in my heart ♥

Thank you, 谢谢, Terima Kasih, Rumbu Nandri All! I am indeed fortunate to have made a connection with each and everyone of you, may we stay in touch and I wish you all the very Best ☺

Yours sincerely,

Shaun Harold Speldewinde, Jaivira

PhD Communications

Conferences:

British Yeast Group Meeting, Carl Singer Foundation Session 1st Runner-Up: Autophagy protects against *de novo* [*PSI*$^{+}$] formation in yeast. Manchester 2015.
Oral Presentation

Faculty of Life Sciences PhD Conference: Autophagy protects against *de novo* [*PSI*$^{+}$] formation in yeast. University of Manchester, 2015
Oral Presentation

Faculty of Life Sciences Symposium: Autophagy protects against *de novo* [*PSI*$^{+}$] formation in yeast. University of Manchester, 2015
Poster Presentation

Gordon Research Conference: Autophagy protects against *de novo* [*PSI*$^{+}$] formation in yeast. Stress Proteins in Growth, Development and Disease. Barga, Italy, 2015
Poster Presentation and Flash Talk

Cold Spring Harbor Conference: Autophagy protects against *de novo* [*PSI*$^{+}$] formation in yeast. Protein Homeostasis in Health and Disease, Cold Spring Harbor, New York, US
Poster Presentation

Publications:

Victoria A Doronina, Gemma L Staniforth, Shaun H Speldewinde, Mick F Tuite, and Chris M Grant. (2015). "Oxidative stress conditions increase the frequency of de novo formation of the yeast [PSI+] prion."*Mol Microbiol*., **96**(1): 163–174.
DOI: 10.1111/mmi.12930

Shaun H. Speldewinde, Victoria A. Doronina, and Chris M. Grant (2015). "Autophagy protects against de novo formation of the [PSI+] prion in yeast." *Mol. Biol. Cell,* **26** no.25: 4541-4551.
DOI: 10.1091/mbc.E15-08-0548

Shaun H. Speldewinde, and Chris M. Grant (2015). "Spermidine cures yeast of prion." MICROREVIEWS: *Microbial Cell*, **3**, No. 1: 46 – 48.
DOI: 10.15698/mic2016.01.474

University of Manchester
Shaun Harold Speldewinde
Doctor of Philosophy
Prions, autophagy, ageing and actin cytoskeleton in yeast
2016

Abstract

Prions are infectious protein entities capable of self-replication. Prions are the causal agents behind the transmissible spongiform encephalopathies causing neurodegeneration and death in affected organisms. Prions have been identified in yeast with the best-characterized prions being [*PSI*$^+$] and [*PIN*$^+$], whose respective native proteins are the Sup35 translation termination factor and Rnq1 (function unknown). Autophagy is a cellular housekeeping mechanism mediating the degradation of damaged proteins and superfluous organelles. It is a highly sequential process regulated by autophagy related genes (*ATG*s). Autophagy has also been implicated in the clearance of amyloidogenic proteins including prions. However, the mechanistic basis underlying this activity is poorly understood, and a key objective of this project was to characterize how autophagy prevents spontaneous prion formation.

Our study found that the deletion of core *ATG*s correlated with an increase in *de novo* [*PSI*$^+$] and [*PIN*$^+$] formation as well as Sup35 aggregation. Enhancement of autophagic flux through spermidine treatment attenuated the increased levels of *de novo* [*PSI*$^+$] formation in mutants that normally show elevated levels of [*PSI*$^+$] formation. Defective autophagy correlated with increased oxidatively damaged Sup35 in an *atg1* mutant whereas anaerobic growth abrogated the increased [*PSI*$^+$] formation in the *atg1* mutant to wild-type levels. Our data suggest that autophagy serves a protective role in the clearance of oxidatively damaged Sup35 proteins that otherwise has a higher propensity towards [*PSI*$^+$] prion formation. We also investigated the role of prion formation and autophagy during yeast chronological ageing which is the time that non-dividing cells remain viable. Prion diseases are associated with advanced age which correlates with a decline in cellular protective mechanisms including autophagy. Our study found an age dependent increase in the frequency of *de novo* [*PSI*$^+$] formation with chronological age of yeast cells, more so in an *atg1* mutant relative to the wild-type. Autophagy competent cells carrying the [*PSI*$^+$] and [*PIN*$^+$] prions also had improved chronological lifespan relative to prion free cells and *atg1* cells. Cells carrying the [*PSI*$^+$] prion elicited elevated autophagic flux that may promote improved lifespan thus suggesting a beneficial role of the [*PSI*$^+$] prion during chronological ageing.

The actin cytoskeleton provides the structural framework essential for a multitude of cellular processes to occur. We investigated the role of the Arp2/3 complex responsible for branching of actin filaments towards prion formation. Knockout mutants of the nucleation promoting factors of the Arp2/3 complex, in particular the *abp1* mutant, showed reduced *de novo* [*PSI*$^+$] formation and Sup35 aggregation under basal and oxidative stress conditions. Similarly, treatment with latrunclin A, an actin monomer-sequestering drug also abrogated *de novo* [*PSI*$^+$] formation. Colocalization studies revealed that Sup35 often does not colocalize with Rnq1, a marker for the insoluble protein deposit (IPOD) in an *abp1* mutant. This suggests a role for the Abp1 protein in the efficient transport of Sup35 molecules to the IPOD that may facilitate *de novo* [*PSI*$^+$] prion formation under vegetative states and oxidant challenges.

Chapter 1: General Introduction:

1.1 Yeast Prions.

Prions are altered protein conformations that have transmissible and infectious properties. Prions are central in the manifestation of a group of diseases known as the transmissible spongiform encephalopathies (TSEs) that include Creutzfeldt-Jakob disease (CJD) in humans, bovine spongiform encephalopathy (BSE) in cattle and scrapie in sheep (Prusiner et al, 1982; Prusiner, 1998). Underlying its pathogenicity, is the aberrant β-sheet rich prion protein, PrP^{Sc} that captures and converts native soluble α-helix rich prion protein, PrP^{C} into the amyloidogenic prion form in a positive feedback loop like manner thus further replicating the prion form (Aguzzi, 2008). The defining physical characteristics of prions include a cross-beta strand structure as shown by X-Ray crystallography, high stability of protein structure in the presence of denaturing SDS and high heat treatment, and affinity to hydrophobic dyes such as thioflavin T and Congo Red (Otzen, 2010). Transmission of prions between cells or organisms also occurs independently of genetic material and represents *bona fide* epigenetic inheritance. Studies of prion-infected brain samples revealed that there is specific sequestration of aggregated prion proteins in parts of the central nervous system. Over time, the accumulation of these aberrant prions results in spongiform changes in neuronal tissue followed by progressive neurodegeneration that finally culminates in organismal fatality (Kovacs and Budka, 2008). In addition, many neurodegenerative diseases such as Alzheimer's and Parkinson's have been likened to prions in terms of their formation and disease progression. These diseases are typified by the coalescence of misfolded forms of the respective proteins (αβ42 and tau proteins, for Alzheimer's, and α-synuclein for Parkinson's) into highly structured

aggregates that progressively spread to parts of the neuronal network eventually leading to progressive neurodegeneration (Costanzo and Zurzolo, 2013; Prusiner, 2013). However, unlike prions, these proteins are not infectious in nature and have not been shown to transmit between individuals or species. There are at present, no effective therapies to counteract prion diseases and the molecular mechanisms underpinning prion formation and its pathogenicity are also not comprehensively characterized.

The existence of prions in *Saccharomyces cerevisiae* was first proposed by Wickner in 1994 to describe a series of non-Mendelian phenotypes observed in yeast. This included the [*URE3*] prion which together with [*PIN*$^+$] and [*PSI*$^+$] prions are the best-characterized yeast prions (Derkatch et al, 1997; Tuite and Cox, 2003). At present, 8 proteins have been established to form prions in yeast with at least 20 other proteins classified as potential prion candidates (Alberti et al, 2009; Tuite and Serio, 2010) (Table 1.1).

Table 1.1: Examples of yeast prions with their corresponding functions and phenotypes [Adapted from (Chernova et al, 2014)].

Protein/Prion	Protein function	Prion phenotype
Ure2 / [*URE3*]	Nitrogen metabolism regulatory protein	Poor nitrogen source utilization
Sup35 / [*PSI*$^+$]	Translation termination factor	Increased nonsense suppression
Rnq1 / [*PIN*$^+$]	Uncharacterized	Promote *de novo* formation of other prions
Swi1 / [*SWI*$^+$]	Chromatin remodeling	Alternative carbon source usage
Mot3 / [*MOT*$^+$]	Transcriptional Co-repressor	Altered cell wall
Mod5 / [*MOD*$^+$]	tRNA modifier	Increased ergosterol production and antifungal drug resistance
Sfp1/[ISP$^+$]	Global transcription regulator	Anti-suppression of specific Sup35 mutations
Cys/[*OCT*$^+$]	Transcriptional repressor	Transcriptional repression of multiple genes

Yeast prions are cytoplasmic elements inherited through either cellular division or via cytoduction (transfer of cytoplasmic content from cell to another without nuclear material) with the prion phenotype being reconstituted in the daughter/recipient cells respectively (Liebman and Chernoff, 2012). This is distinct from that of mammalian prions, whose propagation is through extracellular infection. Most yeast and mammalian prions also form stable aggregates structures known as amyloid fibres. The yeast prion phenotypes are generally manifested as either a loss or gain of function via altered function/activity of the corresponding prion protein. For example, [*PSI*$^{+}$] is the altered conformation of the protein Sup35 which functions as a translation termination factor during mRNA translation. When Sup35 is in the [*PSI*$^{+}$] prion form, it causes a loss of function phenotype since it sequesters and converts soluble eRF3 (Sup35) into its non-functional [*PSI*$^{+}$] prion form. This leads to inefficient translational termination and read-through of nonsense codons by near-cognate tRNAs, thus leading to the aberrant extension of the translated polypeptide by the ribosome (Tuite and Cox, 2007) (Figure 1.1A).

The defining criteria of prions in yeast are: i) reversible curability, ii) induced overexpression of the native form of the prion protein promotes the appearance of the prion form, and iii) the prion phenotype mimics the genetic mutation of the prion protein (Wickner et al, 2015). For example, addition of guanidine hydrochloride (GdnHCl) (see section 1.1.2 [*PSI*$^{+}$] prion formation and propagation) can cure i.e. clear cells of the [*URE3*] prion that can reappear again albeit at low rates from the cured clones. The spontaneous appearance of [*URE3*] positive clones can also be induced by the overexpression of Ure2 by almost a 100-fold and the [*URE3*] prion phenotype observed also resembles the gene knockout of *URE2*. Although there is no yeast protein homolog of PrP^{C}

(Liebman and Chernoff, 2012), both mammalian and fungal prions can adopt unique and stable conformational structures that are self-replicating (Collinge and Clarke, 2007; Wickner et al, 2007). These stable conformers may individually, have different abilities in propagation efficiency and manifestation of their phenotypes and can be categorized either as ‘strong’ or ‘weak’ strains/variants (Tanaka et al, 2006). More specifically, strong prion variants have higher efficiency during propagation and fully reconstitutes the prion phenotype to the subsequent generations and generally form smaller aggregates in comparison to ‘weak’ variants. ‘Weak variant’ on the other hand, form larger prion aggregates that are preferentially retained within the mother cell and thus, are less efficiently propagated to their subsequent progeny and exhibit a weaker prion phenotype (Liebman and Chernoff, 2012). In cases of mating between different cells with variants of the same prion, it is observed that prion variants that have faster replication rates and elevated aggregate formation will ‘outcompete’ the weaker prion variant within the population (Bradley et al, 2002; Tanaka et al, 2006). Furthermore, different prions can co-exist in a yeast cell simultaneously and remarkably, one prion may also exert promoting or conversely, antagonizing affects on the appearance and stability of other prion variants or distinct prions *in vivo* (Liebman and Chernoff, 2012).

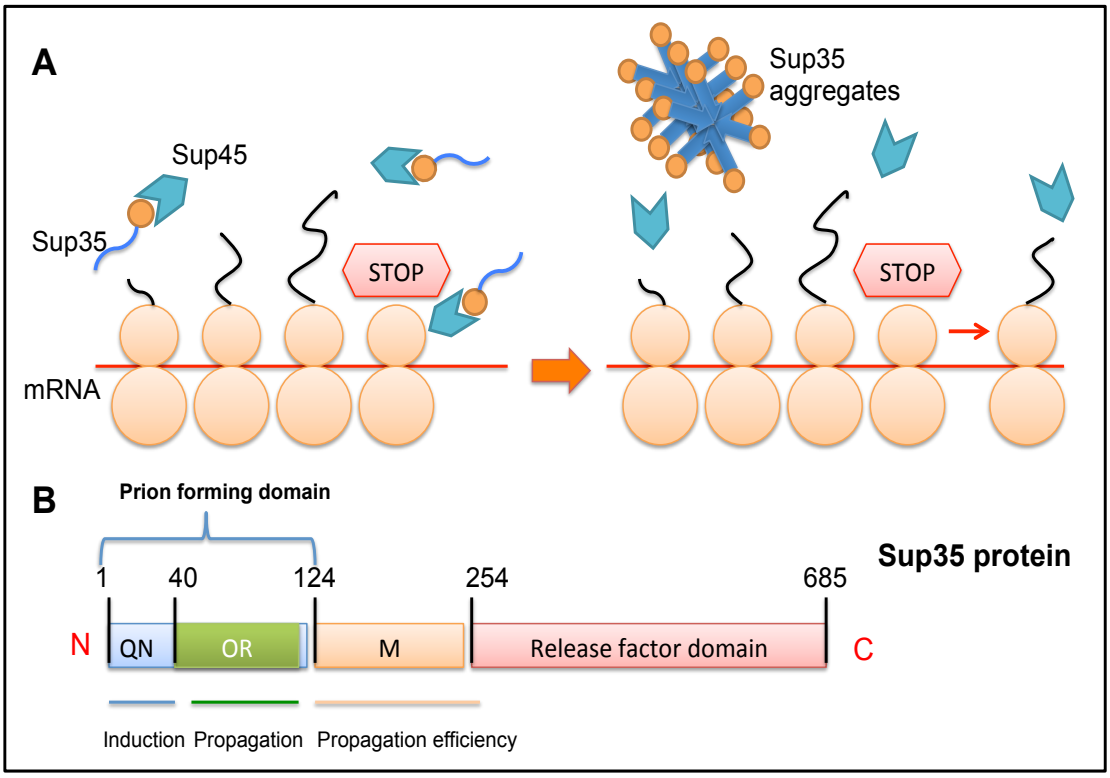

Figure 1.1: Conversion of Sup35 to the [*PSI*$^+$] prion and organisation of the Sup35 protein. **(A)** In native conditions, soluble Sup35 along with Sup45 recognizes stop codons and terminates translation. Conversely, once Sup35 is converted into its prion form, it aggregates into [*PSI*$^+$] polymers and loses its binding to Sup45 as well as its translation termination function thus enabling ribosomal read-through past the stop codon. **(B)** Schematic of Sup35 showing the prion forming domain which is composed of a glutamine/asparagine rich (QN) rich region and an oligopeptide repeat (OR) region necessary for [*PSI*$^+$] formation and propagation respectively. In addition to its N-termini PrD, Sup35 contains a middle domain (M) which is responsible for stable maintenance of certain [*PSI*$^+$] variants (Sondheimer and Lindquist, 2000; Bradley and Liebman, 2004). The release factor domain required for Sup35 translation termination function is located at the C-terminus of the protein.

1.1.1 Prion forming domain (PrD).

Common to all prions is the presence of a prion forming domain (PrD) that can singularly drive prion formation without requiring the rest of the protein being present. For example, expression of the PrD of Sup35 alone correlated with an increase in the frequency of [*PSI*$^+$] formation by 66-fold compared with overexpression of full-length Sup35 protein (Kochneva-Pervukhonva et al, 1998). The yeast PrDs are also inherently disordered regions of protein with

enrichment in glutamine (Q) and asparagine (N) residues with their length correlating with prion transmission efficiency (Vitrenko et al, 2007). It is important to note that, contrary to other prions, the PrD of *Podospora anserine* Het-s prion as well as the Mod5 prion in yeast lack any Q/N rich domains but still have the capacity to form amyloid structures that are stably propagated (Saupe, 2007; Suzuki et al, 2012). In addition, certain prions may have other domains such as the oligopeptide repeats (OR) found in the Sup35 protein that are required for the stable propagation of the prion once it is formed (Figure 1.1B). The OR domain is also typically associated with the Hsp104 chaperone that plays a critical role in prion propagation (Osherovich et al, 2004) (refer to section 1.1.2 [*PSI*$^+$] prion formation and propagation). In addition, the fusion of yeast PrDs to another protein may also facilitate the prion formation of the chimeric protein construct. The prion forming domains may also exert other functions beside prion formation. For example, the PrD of Sup35 is found to influence mRNA stability via its association with the poly(A)-binding protein (Hosoda et al, 2003).

1.1.2 [*PSI*$^+$] prion formation and propagation.

The *de novo* formation of [*PSI*$^+$] prion is dependent on the presence of another prion, [*PIN*$^+$] ([*PSI*$^+$ Inducible]), which is the altered conformation of the Rnq1 protein whose native protein function is as yet uncharacterized (Derkatch et al, 2001; Bradley et al, 2002). The discovery of Rnq1 as a prion determinant emerged from studies of a heritable cytoplasmic element that reconstituted the [*PSI*$^+$] status in [*psi*$^-$] cells, whereas loss of [*PIN*$^+$] status from cells corresponded with deletion of the *RNQ1* gene. Furthermore, transformation of *in vitro* generated Rnq1 amyloid fibrils also recovered the [*PIN*$^+$] status in [*pin*$^-$] cells

thus confirming its infectious and transmissible nature (Osherovich and Weissman, 2001; Patel and Liebman, 2007). The C-termini PrD of Rnq1 spans amino acid residues 153-405 together with a non-prion domain forming the rest of the protein. Furthermore, [*PSI*$^{+}$] prion propagation is absolutely requisite of a molecular chaperone, Hsp104, that is similarly essential for propagation of most characterized yeast prions to date (Grimminger-Marquardt and Lashuel, 2010).

According to the heterologous cross-seeding model, pre-existing [*PIN*$^{+}$] prion aggregates serves as nucleation sites for the misfolding of soluble Sup35 molecules to assemble and further form larger prion aggregates resulting in more efficient [*PSI*$^{+}$] induction (Derkatch et al, 2001; Derkatch et al, 2004). In yeast, misfolded Sup35 proteins are detected by the protein quality control machinery and sent to the IPOD, located adjacent to the PAS (pre-autophagosomal structure) (Parzych and Klionsky, 2014). IPOD is the localization site for aggregated proteins including Rnq1 and Ure2 in their prion forms as well as oxidatively damaged proteins (Tyedmers et al, 2010a; Tyedmers et al, 2010b). The concentration of such proteins in a localized manner in a [*PIN*$^{+}$] cell, together with Rnq1 aggregates, serves as a prion-seeding site. This promotes further aggregation of prion proteins that first form non-transmissible long polymers followed by their fragmentation through the disaggregase activity of Hsp104 into shorter, transmissible units termed ‘propagons’. These propagons reconstitute the prion phenotype when they are passed onto daughter cells (Tyedmers et al, 2010a; Tyedmers et al, 2010b) (Figure 1.2). The role of Hsp104 in yeast prion propagation has been elucidated using the chaotropic agent, guanidine hydrochloride (GdnHCl) that inactivates the disaggregase activity of Hsp104 through inhibition of its ATPase activity. Hsp104 inactivation leads to uninterrupted extension of prion polymers

forming non-heritable aggregates that are preferentially retained by the mother cell and are not passed onto the daughter cells thus preventing prion propagation (Ferreira et al, 2001; Jung and Masison, 2001). Besides Sup35, Rnq1/[*PIN*$^{+}$] also serves as a nucleating site that facilitates the *de novo* formation of other yeast prion proteins including [*URE3*] (Bradley et al, 2002), and this ability is extended to the polymerization of non-Q/N rich aggregation-prone proteins such as the polyglutamine rich huntingtin protein in a yeast model (Meriin et al, 2002) and the [Het-s] prion in *Podospora anserina* (Taneja et al, 2007).

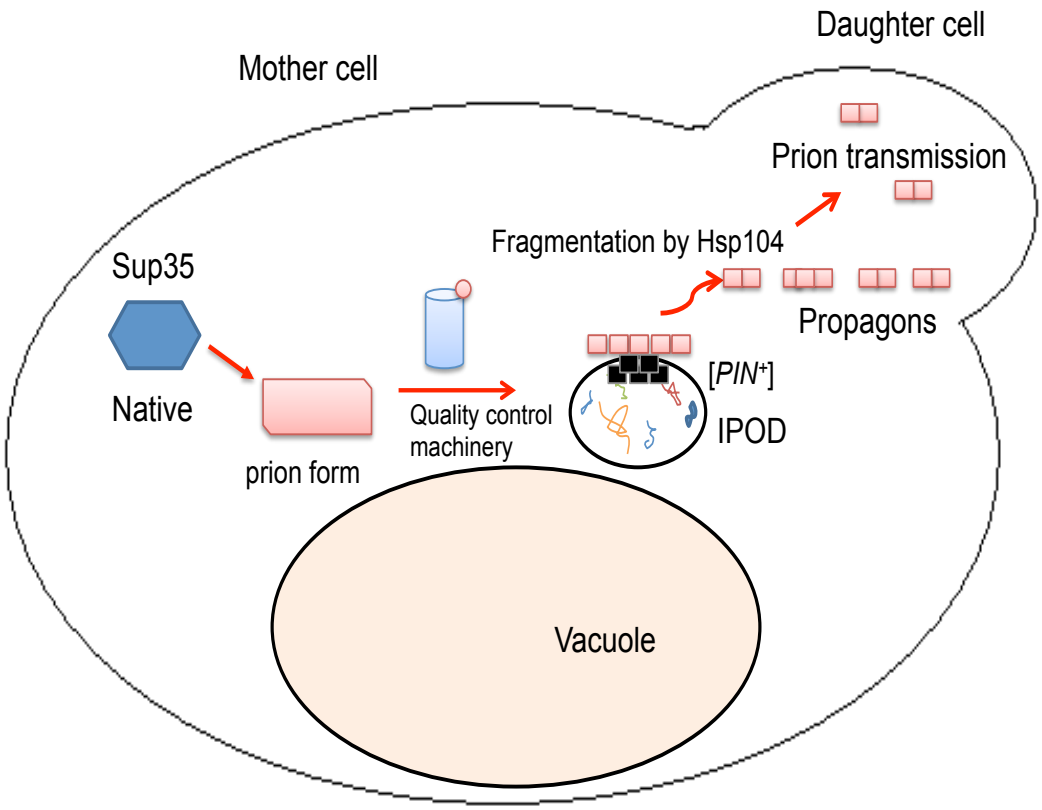

Figure 1.2: A model for [*PSI*$^+$] prion propagation. Soluble Sup35 protein is misfolded into an altered conformation that can potentially convert other soluble Sup35 into the misfolded form (self-replication). Misfolded Sup35 proteins are detected by the cellular quality control machinery and are sent to the insoluble protein deposit (IPOD) located adjacent to the vacuole. [*PIN*$^+$] prions and Rnq1 aggregates which are also stored in the IPOD can serve as seeding sites for extended polymerization of misfolded Sup35. These extended polymers are fragmented by Hsp104 into smaller units termed 'propagons' which are transmissible into daughter cells during cell division thereby propagating the [*PSI*$^+$] prion. Addition of GdnHCl inhibits the disaggregase activity of Hsp104 which prevents prion polymer fragmentation i.e. no propagons produced, thus stopping continued prion propagation into the subsequent generations (Tyedmers et al, 2010a; Tyedmers et al, 2010b).

1.1.3 Prion induction.

The process of prion induction can be investigated via overexpression of prion proteins tagged with a fluorescent protein such as Sup35-GFP and its visualization through fluorescence microscopy. Using this approach, prion induction has been suggested to take place in two steps that require the role of the actin cytoskeleton. The first step is the formation of the peripheral ring by [*PSI*$^+$] prion aggregates at the cell membrane cortex. The second step is the

collapse of the peripheral ring forming an internal ring encompassing the vacuole (Manogaran et al, 2011) (Figure 1.3A). Bimolecular fluorescence studies by Arslan et al (2015) also revealed that the first stage involves the initial formation of a few dots composed of prion aggregates where one of the dots is located adjacent to the vacuole. The perivacuolar dot further progresses to form the peripheral ring which then collapse into the internal ring surrounding the vacuole (Figure 1.3B). The rest of the prion dots were also found to dissolve during this process. Furthermore, the prion aggregates forming the internal ring around the vacuole are subsequently sequestered at the insoluble protein deposit (IPOD).

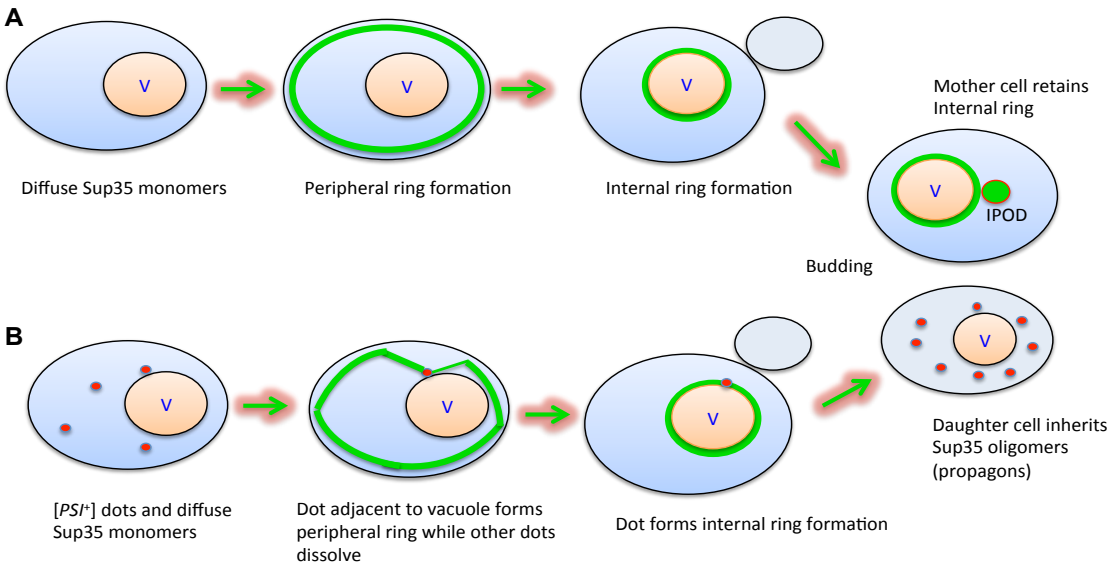

Figure 1.3: [*PSI*$^+$] induction process. (A) The [*PSI*$^+$] prion is induced in at least two stages. Firstly, prion induction begins with the formation of the peripheral ring at the cell cortex. Secondly, the peripheral ring further collapses into an internal ring encompassing the vacuole. **(B)** Arslan et al, 2015 suggests that prion induction involves the formation of [*PSI*$^+$] dots, whereby one of the dots further forms the peripheral ring followed by the internal ring. The Sup35 aggregates are further localized at the IPOD. During cellular budding, the mother cell will retain the internal ring while the daughter cells receives the Sup35 oligomers (V denotes the vacuole, the green rings are the peripheral ring beneath the cell membrane and the internal ring around the vacuole, and the red ovals are [*PSI*$^+$] dots).

1.1.4 Role of Heat shock proteins (HSPs) in the propagation of yeast prions.

Other than acting as essential components of the cellular protein homeostasis network that ensure the proper folding and thus function of proteins, chaperones also function to detect misfolded proteins including amyloid proteins and aggregated proteins. Chaperones have also been found to mediate the formation, stability and heritability of prions. Hsp104 is a key chaperone involved in the propagation of most yeast prions including [*PSI*$^{+}$] as first shown by Chernoff et al (1995). As mentioned above, Hsp104 acts to sever prion polymers into smaller units to generate new prion ends that reconstitute the prion phenotype when transmitted to daughter cells. Overproduction of Hsp104 was shown to cure the [*PSI*$^{+}$] prion presumably by excessive fragmentation of the prion polymers into non-prion monomers (Paushkin et al, 1996). Conversely, Hsp104 abrogation results in formation of extended large molecular weight polymers of Sup35 that are preferentially retained by the mother cell during budding (Newnam et al, 2011). Additionally, the fragmentation ability of Hsp104 requires the assistance of members of the Hsp70 and Hsp40 chaperone families that are essential for prion propagation as well as the disaggregation and remodelling of stress-damaged proteins (Glover and Lindquist, 1998).

The yeast Hsp70 family is mainly composed of 2 major subfamilies: Ssa (encoded by *SSA1-4*) that function in conjunction with the Hsp40 co-chaperones, Ydj1 and Sis1 (Verghese et al, 2012) and the other subfamily being Ssb (encoded by *SSB1* and *SSB2*) that is assisted by Hsp40-Zuo1 and the co-chaperone Ssz1 (Gautschi et al, 2002). Interestingly, both Ssa and Ssb exhibit differential effects on [*PSI*$^{+}$] propagation. Excess Ssa levels leads to

enhanced [*PSI*$^{+}$] propagation rates when Hsp104 is simultaneously overexpressed (Newnam et al, 1999). In addition, *ssa2* genetic knockout was found to promote the loss of weak [*PSI*$^{+}$] variants during mild heat shock (Newnam et al, 2011). Conversely, overexpression of Ssb was found to antagonize [*PSI*$^{+}$] propagation, and this effect was abrogated by the deletion of both *SSB1 and SSB2* (Chernoff et al*,* 1995). Allen et al (2005) reported that when both Ssa and Ssb are present in excess levels, they promoted the elimination of [*PSI*$^{+}$] when Sup35 is overproduced albeit through different mechanisms. More specifically, Ssa promotes the growth and stabilization of Sup35 amyloid fibers that may lose its prion heritability while Ssb stimulates the refolding of Sup35 prion aggregates into non-prion conformations or targets Sup35 prion aggregates to protein degradation pathways thereby counteracting [*PSI*$^{+}$] formation and propagation. Using chimeric constructs of Ssa and Ssb in different combinations, it was found that the peptide-binding domain of Ssa and Ssb was the main determinant in the differential effects on [*PSI*$^{+}$] curing by Hsp104 (Allen et al, 2005).

Bacterial homologs of Hsp70 and Hsp40 chaperones are able to substitute for their equivalent yeast chaperones in propagating yeast prions when they are expressed in yeast host (Reidy et al, 2012). Furthermore, Hsp70 and Hsp40 are also conserved in higher eukaryotes including humans (Young, 2010). Although, orthologs of Hsp104 have been found in bacteria and plants, they are not conserved in animals and humans. However, the human Hsp110, which is a Hsp70-related chaperone, can function in conjunction with Hsp70 and Hsp40 to disaggregate proteins reminiscent of yeast Hsp104 but Hsp110 has not been proven to recapitulate the yeast prion propagation activity of Hsp104 (Shorter, 2011). It has also been postulated that the balance between

the Hsp104-Hsp70-Hsp40 chaperones is an important modulator of yeast prion propagation. Short or long-term heat shock was found to either antagonize or stabilize [*PSI*$^{+}$] propagation, respectively, due to the differential levels of Hsp104 and Ssa that are expressed in response to a range of thermal challenges (Newnam et al*,* 2011). Thus, the chaperone machinery that functions in the defense against protein dysregulation and misfolding during environmental insults, also regulates prion propagation and enables prions to become self-transmissible entities.

1.1.5 Prions: A boon or bane for their yeast host?

Fungal prions are generally not associated with disease *per se* as compared to mammalian prions and their phenotypes manifest as either loss or gain of function via altered function/activity of the specific prion forming protein involved. For example, the [*SWI*$^{+}$] and [*OCT*$^{+}$] prions, whose normal proteins (Swi1 and Cyc8) function in the regulation of chromatin remodeling and transcription, allows alternative carbon source utilization in their prion forms. Conversely, [*PIN*$^{+}$] prion (soluble protein: Rnq1) confers a gain of function phenotype in which it promotes the *de novo* formation of other prions including [*PSI*$^{+}$] (Liebman and Chernoff, 2012). The [HET-s] prion identified in the filamentous fungus, *Podospora anserina*, regulates vegetative compatibility by inducing the death of non-prion mycelium of other genetically incompatible strains at points of contact, and is the first prion proven to be host-beneficial (Saupe, 2011). In addition, prions have been proposed to provide a mechanism of adaptive homeostasis in yeast which may confer a selective advantage under specific environmental conditions (Tyedmers et al*,* 2008). This idea was further corroborated with the identification of fungal prions in wild yeast isolates

including [*PIN*$^+$] and [*MOT3*$^+$] that were found in 6-12% of wild yeast screened. This also included the isolation of [*PSI*$^+$] in certain strains that may confer a selective advantage under specific milieus including salt and oxidative stresses (Halfmann et al, 2012). Furthermore, cells carrying the [*MOD*$^+$] prion were found to exhibit increased resistance to antifungal drugs and against 5-fluorouracil (Suzuki et al, 2012). Additionally, the conversion of the misfolded Sup35 into insoluble amyloid structures has also been proposed to be an adaptive mechanism for cells to counteract the toxicity of elevated levels of misfolded/damaged amyloidogenic Sup35 molecules that may normally overwhelm protein quality control mechanisms within the cell (Ganusova et al, 2006). Thus, the conservation of prions in certain fungi has been regarded as a possible adaptive mechanism or molecular switch via epigenetic means that is both rapid and transient that allows the host to mount a rapid response to certain environmental cues to ensure overall cell survival (Tuite et al, 2011). Once the challenge has been removed, cells can then revert back to the non-prion state and resume normal cellular activities.

Alternatively, yeast prions may be thought of as pathogenic much like their mammalian counterpart. This has been suggested based on the idea that yeast prions can exert harmful effects on the host depending upon the prion variants, genetics and environmental conditions involved (Joseph and Kirkpatrick, 2008). For example, induced overproduction of Sup35 is toxic as it sequesters associated proteins into non-functional aggregates such as the Sup45 termination release factor, and overexpressed Rnq1 similarly sequesters spindle body components (Treusch and Lindquist 2012). Yeast prions have also been suggested to negatively affect their hosts and therefore, are rarely found in the wild and may be an anomalous product of laboratory strains and

conditions (Wickner et al, 2011). The ability to generate prions is also not a ubiquitous feature in the fungal family, with only a select few species retaining prion forming capacity.

1.1.6 Oxidative stress and prion formation.

Several studies have found that oxidative stress is a common feature in mammalian prion diseases (Kim et al, 2001; Milhavet and Lehmann, 2002). For example, brain tissues originating from scrapie-infected mice as well as humans with Creutzfeldt-Jakob disease showed a significant rise in several oxidative stress markers (Yun et al, 2006; Pamplona et al, 2008). Oxidative insults on cells are commonly caused from elevated levels of ROS (Reactive Oxygen Species) that induces widespread oxidative damage to amino acid residues on proteins, hence promoting their misfolding (Dean et al, 1997). For example, methionine residues on the α-helices of PrP^{C} were found to be targets of ROS-induced damage and were postulated to promote the spontaneous conformational change to β-sheet rich structures that may represent a 'generic misfolding mechanism' in the formation of the PrP^{Sc} (Canello et al, 2008; Wolschner et al, 2009). Protein carbonylation, an indicator of oxidative stress, is also suggested to promote protein misfolding and carbonylated proteins have similarly been found to accumulate in protein aggregates (Stadtman and Levine, 2000; Maisonneuve et al, 2008). Sideri et al (2010; 2011) have demonstrated that the frequency of *de novo* [*PSI*$^{+}$] prion formation is increased upon hydrogen peroxide (H_2O_2) exposure and is greatly elevated in mutants of the antioxidant peroxiredoxin (Prx) proteins *tsa1 tsa2*. Conversely, growth under anaerobic conditions prevents [*PSI*$^{+}$] prion formation in *tsa1 tsa2* mutants indicating that molecular oxygen is absolutely required for [*PSI*$^{+}$] formation.

Tsa1 is the principal 2-Cysteine Prx with multiple niches in stress protection including oxidative stress defense functioning as an antioxidant in hydroperoxide detoxification (Garrido and Grant, 2002; Wong et al, 2004). The Tsa2 Prx is functionally similar and highly homologous to Tsa1 (86% amino acid similarity). Despite low Tsa2 basal expression levels relative to Tsa1, it is strongly induced upon exposure to hydrogen peroxide and other organic hydroperoxides (Park et al, 2000; Munhoz and Netto, 2004). Both Tsa1 and Tsa2 colocalize to ribosomes and were suggested to suppress [*PSI*$^{+}$] formation. Sideri et al (2010) and Doronina et al (2015) also demonstrated that oxidative stress is a general trigger in yeast prion formation. The authors found that antioxidant mutants such as those lacking superoxide dismutase 1 (*sod1* mutant) and conditions that induce oxidative stress (hydrogen peroxide and superoxide anion exposure) resulted in an increased frequency in *de novo* prion formation in yeast. Furthermore, overexpression of methionine sulfoxide reductase, an antioxidant enzyme, abrogated the increased levels of prion formation in these antioxidant mutants. Taken together, ROS appear to represent an initial stage in prion formation where they cause oxidative damage to prion-forming proteins thus increasing their propensity to misfold into non-native forms or the amyloid state. Once these stable amyloid forms are generated, they may self-perpetuate and propagate into subsequent generations.

1.2 Autophagy in yeast.

Most cellular activities are mediated through the actions of proteins and protein complexes. However, proteins are also known to be targets of a variety of stresses that may trigger the loss of their native structures and hence cellular function. Therefore, a defensive network of various protein homeostasis mechanisms is in place to prevent or minimize such occurrences. One such mechanism is autophagy, which is an evolutionary conserved housekeeping pathway that regulates the turnover of damaged or toxic proteins, and is the sole cellular mechanism capable of disposing of superfluous organelles (Yang and Klionsky, 2010; Reggiori and Klionsky, 2013). Yeast has been a particularly important model organism in uncovering our knowledge of the autophagy machinery and its mechanistic process (Yorimitsu and Klionsky, 2007). Thus far, 41 genes have been identified to be involved in autophagy and are collectively classified as the autophagy-related genes (*ATG*) (Reggiori and Klionsky, 2013; Yao et al, 2015). The products of *ATG* genes form multi-factor complexes that have specific roles in the autophagy pathway and can be grouped functionally: 1) the Atg1 kinase complex, 2) the Atg9 cycling complex, 3) the Vps34/class III PI3K complexes, and 4) the ubiquitin-like conjugation (Ubl) systems of Atg8 and Atg12 (Xie and Klionsky, 2007) (Table 1.2).

Unlike other vesicular-dependent processes, autophagy involves the *de novo* synthesis of double membrane vesicles that mature into an autophagosome that fully entraps cytosolic waste that is then targeted to the vacuole (yeast) or lysosomes (higher eukaryotes) for subsequent degradation (Reggiori and Klionsky, 2002). Autophagy plays a key role during conditions of nutrient deprivation when the rechanneling of intracellular nutrients/macromolecules into critical cellular processes is favoured in order to

preserve overall cell viability (Gonzalez-Polo et al, 2005). Furthermore, autophagy plays a critical role in a multitude of processes in mammals such as cell development and cell differentiation and the immune response (Ravikumar et al, 2010). Autophagy is constitutively activated and is highly induced when cells face stress stimuli such as nutrient challenges, oxidative stress (Kiffin et al, 2006), and ER stress (Yorimitsu and Klionsky, 2007). In addition, refined regulation of autophagy is critical as its dysregulation is harmful to cells and has been implicated in a variety of human diseases including age-related neurodegeneration, metabolic defects and cancer (Wirawan et al, 2012).

Table 1.2: Core autophagy components and their roles in the autophagy pathway.

Core Autophagy Components		**Roles**
Atg1 Kinase complex: Atg1-Atg13 with non-core Atg17-Atg29-Atg31 sub-complex		Autophagy Induction, formation of PAS (pre-autophagosomal structure)
PI3K complex: Atg6-Atg14 with Vps34 and Vps15		PAS nucleation
Atg9 cycling complex: Atg9/Atg2-Atg18 complex		Membrane recruitment for PAS expansion
Atg12 Ubl system:	Atg12-Atg5-Atg16 Atg12 is processed by Atg7 and Atg10	Conjugation of Atg8 to phosphatidylethanolamine (PE)
Atg8 Ubl system:	Atg8-PE Atg8 is processed by Atg4, Atg7, and Atg3	PAS elongation and maturation to autophagosome

(Ubl: Ubiquitin-like)

1.2.1 The progression of autophagy.

The autophagy pathway is a highly sequential process that can be separated into **i)** PAS (pre-autophagosomal structure) induction and nucleation, **ii)** PAS elongation/autophagosome formation, **iii)** autophagosome maturation, **iv)** autophagosome fusion with vacuoles/lysosomes, and **v)** the degradation and recycling of the autophagic cargo (Figure 1.4). The process of autophagy begins with the induction of the Atg1 kinase complex that initiates the generation of the double-membrane PAS. The Atg1 kinase complex is composed of Atg1, the only known serine/threonine kinase in the autophagy pathway (ULK1/ULK2 in mammals) (Matsuura et al, 1997), and the Atg13 regulatory kinase in conjunction with an additional sub-complex formed by Atg17, Atg29 and Atg31 (Kamada et al, 2000). In yeast, the PAS is generated at a single site near the periphery of the vacuole while conversely, multiple PAS formation can occur concurrently in mammals (Chen and Klionsky, 2011).

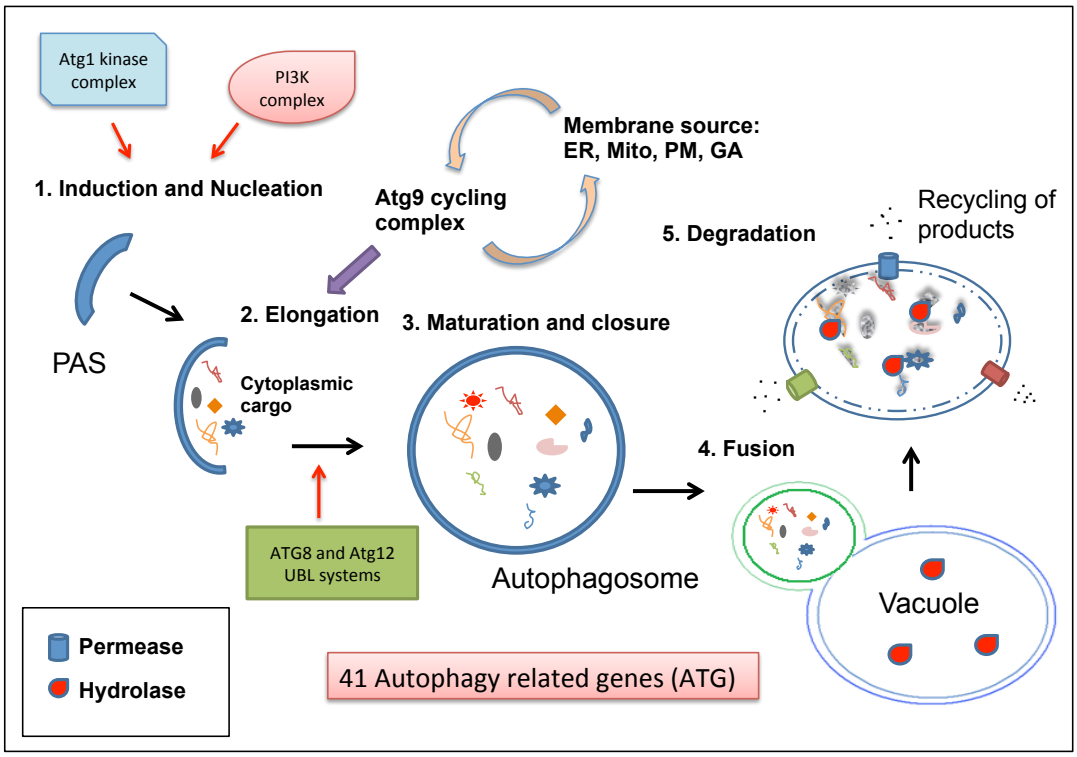

Figure 1.4: Overview of the autophagy pathway. Autophagy functions in the degradation and recycling of cytosolic macromolecules and is the sole cellular system mediating organelle turnover. The process of autophagy begins with the induction and formation of an isolation membrane, termed the PAS, which is mediated by the Atg1 kinase complex and the phosphatidylinositol-3-phosphate kinase (PI3K) complex. The PAS undergoes expansion encompassing bulk cytoplasm in non-selective autophagy or a selected substrate in selective autophagy with supply of membranes by the Atg9 cycling complex. This is followed by the maturation and full closure of the isolation membrane forming a double-membrane enclosed autophagosome aided by ATGs such as the Atg8 and Atg12 ubiquitin-like (Ubl) conjugation systems. The autophagosome then fuses with the vacuole. Degradation of the autophagosome and its contents occurs via resident hydrolytic enzymes to produce basic building blocks that are exported into the cytosol for recycling into anabolic pathways or for production of energy. [ER: Endoplasmic reticulum; Mito: Mitochondria; PM: Plasma membrane; GA: Golgi apparatus].

1.2.1.1 Atg1 kinase complex regulation and PAS induction.

Under non-induced conditions, Atg1 and Atg13 activity is repressed by phosphorylation via multiple regulatory factors such as the serine/threonine protein kinase TOR (target of rapamycin) and the Ras/cAMP/protein kinase A pathway (Figure 1.5). The TORC1 (TOR complex 1) during nutrient rich conditions negatively regulates autophagy by decreasing the affinity of Atg13 for Atg1 kinase, thus impairing the activation of the autophagy pathway. TORC1

is also capable of inhibiting autophagy via alteration of the phosphorylation status of several proteins essential for autophagy activity through the proteins Tap42 and protein phosphatase 2A (He and Klionsky, 2009; Yorimitsu et al, 2009). The interplay of the nutrient sensing network and autophagy also involves the kinases PKA (protein kinase A) and Sch9 which function as negative modifiers of autophagy (Yorimitsu et al, 2007). High uptake of glucose induces production of cAMP (cyclic adenosine monophosphate) which binds and inactivates Bcy1, a negative regulator of PKA. De-repression of PKA activity leads to inhibition of autophagy by causing the dissociation of Atg1 from the PAS (Budovskaya et al, 2004). Excessive induction of PKA and Sch9 activity also leads to inactivation of autophagy despite inhibition of the TOR pathway via rapamycin treatment or nutrient deficiency thus showcasing a co-ordination of TORC1, Sch9 and PKA signals in integrating cellular nutrient status with autophagy regulation (Stephan et al, 2009).

Atg17 is required for optimal efficiency of Atg1 kinase activity (Kamada et al, 2000) and may play a role in co-coordinating the recruitment of other Atg proteins to the PAS during autophagy induction (Cheong and Klionsky, 2008). However, the actual mechanism by which Atg13 or Atg17 exerts their regulatory roles on Atg1 function still remains elusive. Hypophosphorylated Atg13 activates the Atg1 kinase and this is followed by the binding of the Atg17-Atg29-Atg31 subcomplex that is able to homodimerize through Atg17. The assembly of this multimeric complex initiates the *de novo* generation of the isolation membrane, PAS, by a poorly understood mechanism and represents the first stage of autophagy.

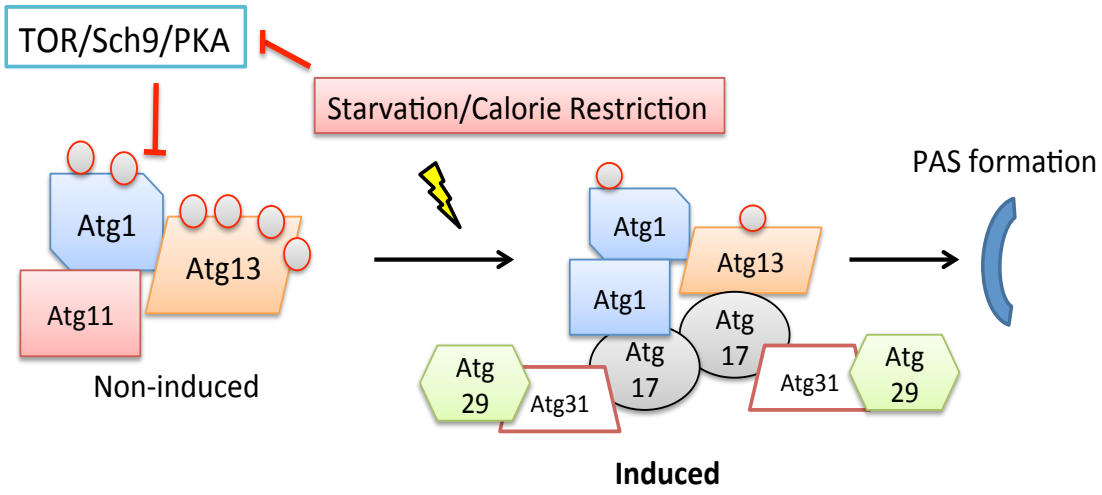

Figure 1.5: Autophagy induction by the Atg1 kinase complex. Under non-induced conditions, Atg1 and Atg13 activity is repressed by phosphorylation via multiple regulatory factors such as the kinases TOR, Sch9 and protein kinase A that are negative modifiers of autophagy. Atg11, an adaptor protein, is found to be associated with the Atg1 kinase complex. Nutrient limitation is a known trigger of autophagy induction through the inactivation of TOR/Sch9/PKA kinases and the dephosphorylation of Atg1 and Atg13 by yet unidentified phosphatases. A hypophosphorylated Atg13 activates the Atg1 kinase followed by the binding of Atg17-Atg29-Atg31 subcomplex that is able to homodimerize through Atg17. The assembly of this multimeric complex initiates the *de novo* generation of the isolation membrane, PAS, by poorly understood mechanisms and represents the first stage of autophagy. [Circles with red outline indicate protein phosphorylation].

1.2.1.2 Autophagosome maturation.

After the generation of the PAS, the progressive elongation of the PAS then occurs that is facilitated by the phosphatidylinositol-3-phosphate kinase (PI3K) complex. In yeast, PI3P (phosphatidylinositol-3-phosphate) is synthesized by two complexes formed by Vps34 (the PI3K), and Vps15 (kinase), and Vps30/Atg6 (function unknown) respectively (Kihara et al, 2001). Mammalian cells, on the other hand, regulate autophagy via class I and class III PI3K complexes (Kamada et al, 2000). Atg14 is known to be part of complex I and also interacts with Vps30/Atg6 with the former facilitating the recruitment of the complex to the PAS (Kihara et al, 2001). PI3P is suggested to serve as a platform for the recruitment of Atg proteins involved in the maturation of the

PAS into the fully-fledged autophagosome (Krick et al, 2006; Nair et al, 2010). For example, one known protein recruited to PI3P is Atg18, which is a PI3P binding protein that plays a role in the movement of Atg9 (see below).

The maturation of the PAS into the autophagosome is mediated by the activity of the Atg9 cycling complex. Atg9 is the only known *ATG* transmembrane protein (Noda et al, 2000) that together with Atg18 and Atg2 constitutes the Atg9 cycling complex. This complex serves to facilitate PAS elongation through the recruitment of vesicular membrane during early phases of autophagy. Additionally, the Atg9 cycling complex also regulates the retrograde movement of vesicles during autophagosome disassembly at the final stages of the autophagy pathway. The Atg1 kinase complex and oligomerization of Atg9 itself appears to regulate the cellular localization of Atg9 (He et al, 2008). In addition, Atg41, a recently characterized protein, facilitates the movement of Atg9 to the PAS (Yao et al, 2015). The source of the membranes for PAS synthesis is still not fully known with various research groups proposing that the Atg9 cycling complex sources its vesicles from the ER (Yla-Anttila et al, 2009), Golgi (Takahashi et al, 2009) and even the plasma membrane (Ravikumar et al, 2010) or mitochondria (Hailey et al, 2010).

The maturation of the PAS into an autophagosome is further aided by the two ubiquitin-like (Ubl) conjugation systems: the Atg8 (mammalian homolog, LC3) and the Atg12 Ubl complexes (Geng and Klionsky, 2008). In the Atg8 system, the Atg8 ubiquitin-like protein is processed into its functional form by Atg4, a cysteine protease (Kirisako et al, 1999), and is activated by the E1 activating enzyme, Atg7. Atg8 is subsequently conjugated to phosphatidylethanolamine (PE) via its C-terminal glycine through the action of the Atg3 conjugating enzyme (Kirisako et al, 2000) and this process is aided by

the Atg12 Ubl system (Hanada et al, 2007; Fujita et al, 2008). Atg12 is also activated by Atg7 and is irreversibly conjugated to an internal lysine on Atg5 via the action of the E2 conjugation enzyme, Atg10 (Shintani et al, 1999). This complex then binds with Atg16 through Atg5 and the former homodimerises (Kuma et al, 2002). The conjugated Atg8-PE on autophagosomes plays a role in preventing premature autophagosomal fusion with the vacuole or lysosome.

1.2.1.3 Autophagosome fusion with the vacuole.

Before the fusion event of the autophagosome with the vacuole, Atg8 on the external leaflet (Atg8 is initially located on both sides of the autophagosme membrane) is removed from PE by Atg4-dependent cleavage in an event termed as 'deconjugation'. This event is thought to be a signal for the disassembly of other Atg protein complexes as they are not associated with the fully matured autophagosome. The fully mature autophagosome that has entrapped cellular waste/cargo targeted for degradation then fuses with the vacuole. It appears that the disassembly of the Atg machinery from the mature autophagosome is essential before fusion with the vacuole/lysosome can occur. The hydrolysis of PI3P on Atg complexes by the PI3-phosphatase Ymr1 (Cebollero et al, 2012) facilitates the disassembly of the Atg machinery from the mature autophagosome. Vacuolar fusion releases the inner membrane of autophagosomes and its cargo into the vacuolar lumen and it is now termed an 'autophagic body'. Atg15 (a lipase) degrades the inner membrane of the autophagic body thus enabling the release of its contents (Epple et al, 2001) that can be accessed and degraded by resident vacuolar hydrolases. The resultant breakdown products are exported back to the cytosol via membrane permeases such as Atg22 (Yang et al, 2006) and are ultimately funneled into

biosynthetic pathways for anabolic processes or channeled into metabolic pathways for energy generation.

Besides the core Atg proteins mentioned above, there are several other Atg proteins that mediate selective types of autophagy (Figure 1.6). These include the accessory Atg proteins Atg19, Atg32, Atg34, and Atg36 (Mijaljica et al, 2012). Atg19 and Atg34 act as receptors in the Cvt (cytoplasm-to-vacuole targeting) pathway, which functions in the transportation of hydrolases (aminopeptidase, mannosidase) into the yeast vacuole where they function to degrade macromolecules in the vacuole (Hutchins and Klionsky, 2001). On the other hand, Atg32 and Atg36 are receptor proteins that mediate selective autophagy of the mitochondria (mitophagy), and peroxisomes (pexophagy) respectively. In addition, the core autophagy machinery is also essential in the process for selective autophagy to occur.

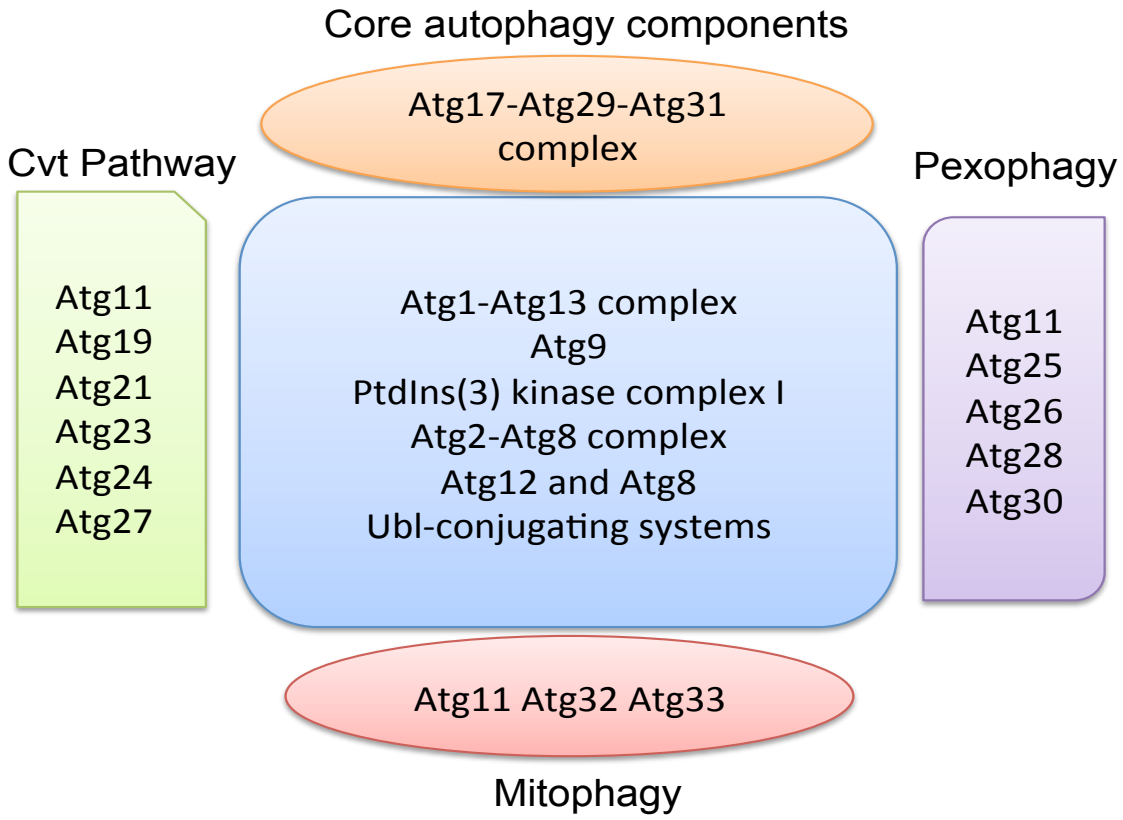

Figure 1.6: Classification of the Atg Proteins. The core machinery is requisite for the initiation and the *de novo* synthesis of the PAS and the subsequent elongation and maturation of the autophagosome (Highlighted in blue). Other Atg proteins are involved in selective types of autophagy: the Cvt pathway, mitophagy and pexophagy and interact with the core machinery to coordinate non-selective and selective autophagy, respectively.

1.2.2 The role of autophagy in protection against prions and other protein-aggregation diseases.

Increasing evidence has highlighted the important roles for autophagy in the defense against protein aggregation and in ageing-associated diseases. This protective function is particularly important for neurons, as they are post-mitotic cells that cannot dilute the accumulation of misfolded proteins and dysfunctional organelles by cellular division. The connection between prion disease and autophagy was first proposed based on the finding that neurons in mouse and cell models of prion disease often had large autophagic vacuoles (Boellaard et al, 1991; Liberski et al, 2004). In addition, PrP^{Sc} was also found to

colocalize with lysosomal markers indicating that the clearance of prions may occur via the autophagy pathway (Dearmond and Bajsarowicz, 2010). The first direct evidence that autophagy is capable of mediating cellular PrP^{Sc} degradation came from studies by Aguib et al (2009) and Heiseke et al (2009). In these studies, downregulation of autophagy using either pharmacological inhibition or siRNA knockdown of Atg5 (essential for autophagy to occur) was correlated with impaired clearance of intracellular PrP^{Sc} levels in mice. Furthermore, application of other autophagy promoting agents such as imatinib, rapamycin and trehalose was also shown to result in reduced levels of prions and, in certain instances, delayed incubation time of prions as well as the onset of the disease (Aguib et al, 2009; Heiseke et al, 2009; Cortes et al, 2012). Rapamycin, an mTOR (mammalian target of rapamycin) inhibitor treatment, was shown to have a clearing effect on the levels of prion accumulation thus indicating that upregulating autophagy may promote degradation of PrP^{Sc}. Similarly, application of resveratrol, which induces autophagy via upregulation of Sirt1 activity, was found to attenuate prion-mediated toxicity in human cell lines (Jeong et al, 2012) and in *C.elegans* (Bizat et al, 2010).

A protective role of autophagy also extends to other neurodegenerative diseases caused by the aberrant accumulation of protein aggregates including Parkinson's disease, Alzheimer's disease, and Huntington's disease (Ravikumar et al, 2002; Qin et al, 2003; Iwata et al, 2005; Rubinsztein et al, 2005; Berger et al, 2006; Hara et al, 2006; Ventruti and Cuervo, 2007). For example, the degradation of mutant huntingtin and α-synuclein was promoted upon upregulation of autophagy via treatment with lithium or trehalose (Sarkar et al, 2005; Sarkar et al, 2007). Specific knockdown of *atg5* and *atg7* in the brain gave rise to sporadic neurodegeneration not unlike that observed for

Alzheimer's and Parkinson's diseases whose symptoms include impaired motor function, poly-ubiquinated protein aggregates accumulation and neurodegeneration (Nassif et al, 2010). Rapamycin-mediated induction of autophagy also promotes the degradation of aberrant toxic proteins in animal models of Huntington's and other proteinopathies (Qin et al, 2003; Ravikumar et al, 2004; Iwata et al, 2005; Berger et al, 2006). Impairment of the autophagy system may also underlie the increased accumulation of α-synuclein protein aggregates in neurons as has been demonstrated in a mice model harbouring a deletion of Atg7 which is essential for autophagy to occur (Friedman et al, 2012). Furthermore, promotion of autophagy via inhibition of the TOR pathway exerts positive effects on the degradation of a human polyglutamine huntingtin protein in *Drosophila* (Wang et al, 2009). Although there is mounting evidence to suggest a cytoprotective role for autophagy against prions and other proteinopathies, it is unclear which stage of the autophagy pathway is crucial for prion clearing (i.e. protection against prions) and whether a defective autophagy pathway corresponds to increased *de novo* prion formation and prion propagation.

1.2.3 The link between autophagy and ageing.

Ageing is the progressive decline of organisms in various cellular processes and in resistance against stress and disease. It is also associated with a loss of proteostasis, and increase accumulation of aggregate-prone proteins including tau (Alzheimer's), huntingtin (Huntington's) and α-synuclein (Parkinson's) (Levine and Kroemer, 2008). A decline in autophagy activity has been correlated with ageing and is suggested to contribute to different aspects of the ageing phenotype including ageing-related diseases (Rubinsztein et al,

2011). A number of studies have also reported that Atg proteins together with their regulators such as Sirtuin1 have diminished expression in aged cells/tissues. For example, downregulation of the essential autophagy components Atg5, Atg7, Beclin1/Atg6 is observed in human brain ageing (Lipinski et al, 2010). In addition, a multitude of short-lived mutants with impaired autophagy (10 *ATG* genetic aberrations out of 117 short-lived mutants) were identified in an unbiased screen to identify chronological ageing factors in yeast (Matecic et al, 2010).

The connection between autophagy and lifespan extending phenotypes/factors has been found in species ranging from invertebrates to mice models (Madeo et al, 2010). For instance, regulatory systems mediating yeast lifespan such as the critical components of nutrient-sensing pathways including protein kinase A, Sch9 and target of rapamycin (TOR) are also common regulators of autophagy. Increased expression of Atg5 was also demonstrated to induce autophagy and improve the lifespan of mice in conjunction with anti-ageing phenotypes such as enhanced resistance to oxidative stress and apoptosis in fibroblasts, improved motor function and insulin resistance (Pyo et al, 2013). Application of spermidine, a polyamine, has also been reported to promote lifespan extension in models of yeast, worms and flies predominantly via induction of autophagy (Eisenberg et al, 2009). The role of autophagy in increasing lifespan via calorie restriction has also been validated in worm models (Jia and Levine, 2007) and the FOXO-transcription factor mediates lifespan extension in *C. elegans* via upregulation of autophagy (Salih and Brunet, 2008).

The links between ROS regulation and autophagy has important implications for the ageing process. For instance, *atg7 Drosophila* mutants

show decreased resistance against challenges to oxidative stress-inducing compounds such as paraquat and hydrogen peroxide and have reduced lifespan relative to wild-type flies (Juhasz et al, 2007). Conversely, overexpression of *Atg8*a in *Drosophila* was found to extend lifespan in addition to improving resistance to ROS challenges and reducing the accumulation of oxidatively damaged proteins (Simonsen et al, 2008). Similarly in the same study, specific overexpression of autophagy genes in the brains of adult *Drosophila* showed significantly improved lifespan and increased resistance to oxidative stress. Despite numerous studies linking autophagy with the ageing process, it is still not clearly characterized how autophagy declines with age. Based on the stochastic nature of ageing and the complexity of the autophagy pathway, the reasons for such a decline may be multi-factorial. Therefore, more strategic and comprehensive studies will be required to dissect the interplay between autophagy and ageing.

There is also the possibility that the dysregulation of upstream signaling events during normal ageing could potentially disrupt autophagy and other proteostasis mechanisms and thus accelerate the ageing process. Notably, the mTOR pathway is often hyperactivated during ageing and as a result inhibits autophagy as well (Cornu et al, 2013). Similarly, suppression of mTOR via rapamycin treatment was shown to increase the lifespan of murine models (Harrison et al, 2009) and slowed a variety of age-related defects in the cardiovascular, blood, liver and general neuronal health in mice (Wilkinson et al, 2012). The majority of manipulations of the autophagy pathway via genetic or pharmacological means exhibit pleiotropic effects indicating that autophagy genes and their products have roles outside of autophagy. For example, mTOR inhibition also affects many other processes including mRNA translation,

ribosome formation, angiogenesis, mitochondrial metabolism, adipogenesis and cellular growth that may modulate the ageing phenotype (Dennis et al, 2001; Rubinsztein et al, 2011). How these additional effects may influence ageing and ageing-associated diseases requires further investigation. Therefore, the therapeutic application of autophagy promoting pharmacological compounds must first be tested out with caution as the consequences of long-term induction of autophagy has not been fully clarified. Nonetheless, the contribution of autophagy in the degradation and clearance of abnormal proteins, dysfunctional organelles and superfluous material suggests its importance in providing new material for maintenance of cellular health and fitness (Kenyon, 2010).

1.3 Ageing in Yeast.

Ageing in the cell is the progressive deterioration of a multitude of cellular processes resulting in the increased probability of cell death. The study of ageing is of paramount importance due to the increase in average lifespan across the human population coupled with the rise in age-related diseases and the consequent socioeconomic burden entailed. Understanding the mechanisms and causes of ageing could help devise preventative or ameliorative strategies to bring about healthier ageing and improved general wellbeing. Yeast was first used as a model organism around 50 years ago by Mortimer and Johnson (1959) to study the effects of ageing. However, it was only in the 1990s that yeast was actively used to investigate ageing. Since then, yeast as a model organism has been instrumental in uncovering the genetic and epigenetic mechanisms through which ageing is modulated. Several of the ageing mechanisms or ageing genes found in yeast also appear to be correlated and conserved with their respective counterparts in higher eukaryotes. There are currently two main paradigms that ageing is studied in yeasts, namely: replicative lifespan (RLS), and chronological lifespan (CLS) (Figure 1.7).

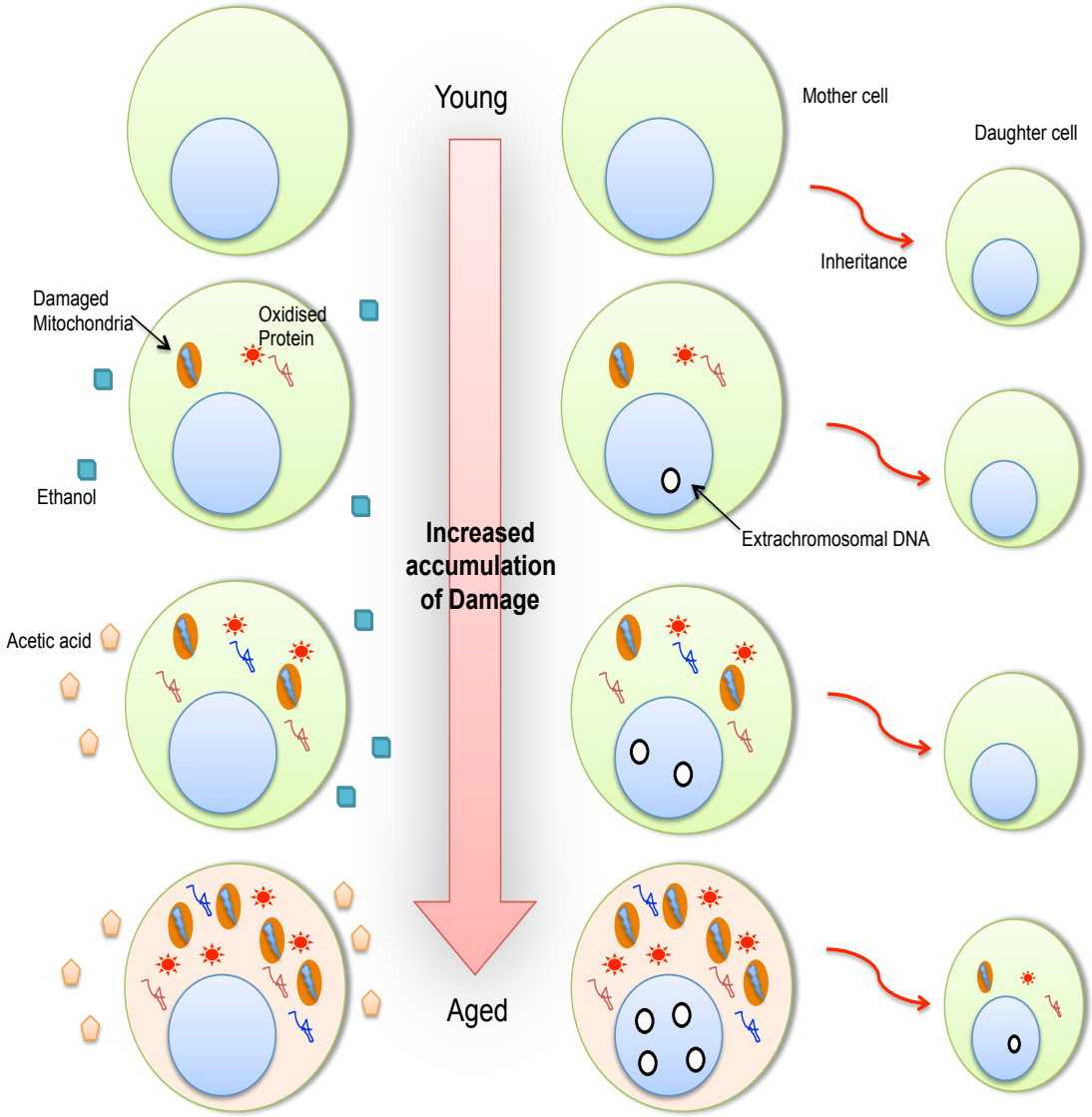

Figure 1.7: Schematic representation of chronological ageing and replicative ageing. Both chronological ageing and replicative ageing are associated with an increased accumulation of damage in the form of oxidatively damaged proteins and dysfunctional mitochondria with the progress of time. During chronological ageing, extracellular glucose is metabolised into ethanol which is then converted to acetic acid as cells age further. In replicative ageing, other than damaged proteins and organelles, cells also accumulate extrachromosomal DNA which are predominantly rDNA (ribosomal DNA) circles. As the mother cells age, the resultant daughter cells are also found to be increasingly prone to inherit damaged molecules and components from aged mother cells (Modified from Kaeberlein, 2010).

1.3.1 Replicative lifespan (RLS) and Sir2 (Silent Information Regulator).

Replicative lifespan is defined by the number of budding events that occurs from a single mother cell before death (Mortimer and Johnston, 1959). This assay takes advantage of the asymmetric budding of mother cells to produce daughter cells that are physically smaller to distinguish between the two. Depending on the strain background, a mother cell on average produces approximately 20-30 buds before becoming senescent. In addition, the yeast mother undergo a series of morphological changes and accumulates damage as they advance in age including increases in cell size, having longer cell cycles, fragmented nuclei and becoming sterile before going into senescence (Longo et al, 2012). This age-associated damage is asymmetrically segregated during cell division with the mother cell retaining most of the damage to ensure higher survival fitness of the new daughter cell. One of the major genetic modulators in ageing uncovered from yeast RLS experiments was that of *SIR2* which is a nicotinamide adenine dinucleotide dependent histone deacetylase of the Sirtuin family (Imai et al, 2000). Sir2 was initially discovered to silence the *HML* (Hidden MAT Left) and *HMR* (Hidden MAT Right) mating type loci. Additionally, Sir2 is also implicated in gene silencing at the telomeric ends of chromosomes as well as rDNA repeats in the nucleolus (Wierman and Smith, 2014). Overexpression of Sir2 was found to be correlated with an extension in RLS (Kaeberlein et al, 1999) and this effect is attributed to Sir2 acting as a suppressor in the formation of extra-chromosomal rDNA circles (ERCs) which are generated as a result of homologous recombination in ribosomal DNA (rDNA) repeats. ERCs are also capable of self-replication and are preferentially retained by the mother cell during cellular division (Sinclair and Guarente, 1997). The role of rDNA instability in limiting RLS was further emphasized with

the finding that *FOB1* deletion which suppresses rDNA recombination and therefore ERC formation led to the extension of lifespan and improved the RLS of *sir2* mutants (Kaeberlein et al, 1999). However, the idea that an excess of ERCs leads to reduced lifespan is being questioned as it is suggested that rDNA instability has a more pronounced effect on ageing compared to ERCs (Lindstrom et al, 2011). An ERC-independent function of Sir2 was identified that resulted in RLS extension through its histone acetylation activity to promote transcriptional silencing at certain telomeric and subtelomeric regions (Dang et al, 2009). Other than ERCs, the deletion of *SIR2* was found to lead to impairment of asymmetric segregation of oxidatively damaged proteins to daughter cells from *sir2* mother cells during budding events (Erjavec et al, 2007; Erjavec and Nystrom, 2007). Thus Sir2 was proposed to aid in generating daughter cells with an improved capacity to counteract oxidative stress (Erjavec et al, 2007). Induction of Hsp104 activity also counteracted the decrease in lifespan in the *sir2* mutant indicating that oxidative stress-induced cellular damage may contribute to accelerated ageing.

1.3.2 Chronological lifespan (CLS), and the Tor/Sch9 and Ras/cAMP/PKA pathway.

Chronological lifespan or chronological ageing is defined as the period of time that a stationary yeast cell survives. CLS experiments involves growing yeast cultures into the postdiauxic phase (normally achieved 2-3 days after inoculation) where the majority of cells no longer divide (Longo et al, 1996). Once the postdiauxic phase is reached, and most glucose in the media is depleted, yeast cells switch to mitochondrial respiration of ethanol fermented from glucose (Werner-Washburne et al, 1996). This phase is typically

characterized by reduced growth rates and an induction in stress-resistance pathways. While RLS provides a model that mimics the ageing of somatic or stem cells of higher organisms that are mitotically dividing, the CLS more closely resemble the ageing of non-dividing cells such as neurons and muscles (Fabrizio and Longo, 2008). Studies of ageing using CLS provided the first proof that the Ras/cAMP/PKA pathway is linked with improved chronological ageing and that the antioxidant protein, Sod2, is essential in these pathways to promote lifespan (Fabrizio and Longo, 2003; Wei et al, 2008). In fact, *ras2* was the first mutant found in CLS studies and leads to a doubling of CLS and is accompanied with an increase in resistance to heat shock and oxidative stress (Fabrizio and Longo, 2003). The Ras/cAMP/PKA pathway is involved the sensing of the availability of glucose and other nutrients and has been confirmed to have pro-chronological ageing effects in mice (Enns et al, 2010; Fontana et al, 2010; Borras et al, 2011).

Another major pathway identified in CLS studies to have positive effects on lifespan is the Tor/Sch9 pathway which is involved in glucose and amino acid sensing (Fabrizio et al, 2001). Interestingly, studies from both RLS and CLS led to a more comprehensive model of the pro-chronological effect during calorie restriction that is largely dependent upon downregulation of TOR/Sch9 and the Ras/cAMP/PKA pathways (Figure 1.8). Furthermore, both TOR/Sch9 and the Ras/cAMP/PKA pathways impinge on Rim15 kinase and is associated with the upregulation of the Msn2/4 and Gis1 transcription factors involved in promoting stress-resistance and in regulating metabolism and utilization of carbon (Longo et al, 2012). The importance of Msn2/4 activated response in promoting lifespan was further corroborated with the finding of its upregulation of Sir2 expression in RLS studies (Fabrizio et al, 2005; Medvedik et al, 2007).

Deletion of SK6, the mice ortholog of Sch9, also improved lifespan and reduced age-related defects (Selman et al, 2009). However, the role of Sir2 as seen in RLS analysis is not reflected to that observed in CLS studies as the deletion of *SIR2* results in lifespan extension rather than limiting it during calorie restriction. This lifespan promotion during CR (calorie restriction) is attributed to the premature depletion of ethanol in a *sir2* mutant closely resembling to that observed in *sch9* and *ras2* mutants (Fabrizio et al, 2005; Smith et al, 2007). Calorie restriction has also been validated as the only means of consistently promoting lifespan in most model organisms tested including yeasts, worms, flies and rodents (Anderson and Weindruch, 2012). Reduction of TOR activity through amino acid starvation or treatment with rapamycin was also found to result in the induction of autophagy that may enhance degradation of damaged proteins thus further improving CLS during calorie restriction (Alvers et al, 2009a). The yeast CLS model has also led to the identification of a multitude of factors that interfere with chronological ageing particularly implicating several protection mechanisms against stress including oxidative stress, mitochondrial dysfunction and generation of reactive oxygen species, nuclear DNA instability and replication stress, reduced autophagy and alterations in metabolism (Longo et al, 2012).

Changes in the composition of the extracellular environment were also another factor found to modulate CLS. For example, the accumulation of acetic acid that is generated through metabolism of ethanol in the postdiauxic phase of CLS led to a reduction of chronological lifespan (Burtner et al, 2009). Buffering the CLS culture at pH 6.0 and simultaneous removal of acetic acid from the medium or transferring the culture to water was found to be sufficient to extend CLS. However, the exact mechanism of acidification during CLS is

unclear with suggestions that it may lead to exacerbated ROS production, increase in Ras signalling and causing mitochondrial dysfunction therefore, leading to increased senescence of yeast cells (Longo and Fabrizio, 2002). It is evident that chronological ageing involves the cumulative effect of many genes and proteins that may influence each other and the ageing process. More expansive efforts are required to identify the downstream effects of the major stress responsive genes and nutrient sensing pathways implicated in chronological ageing thus allowing the construction of a more comprehensive network linking the major mechanisms that underpin chronological ageing.

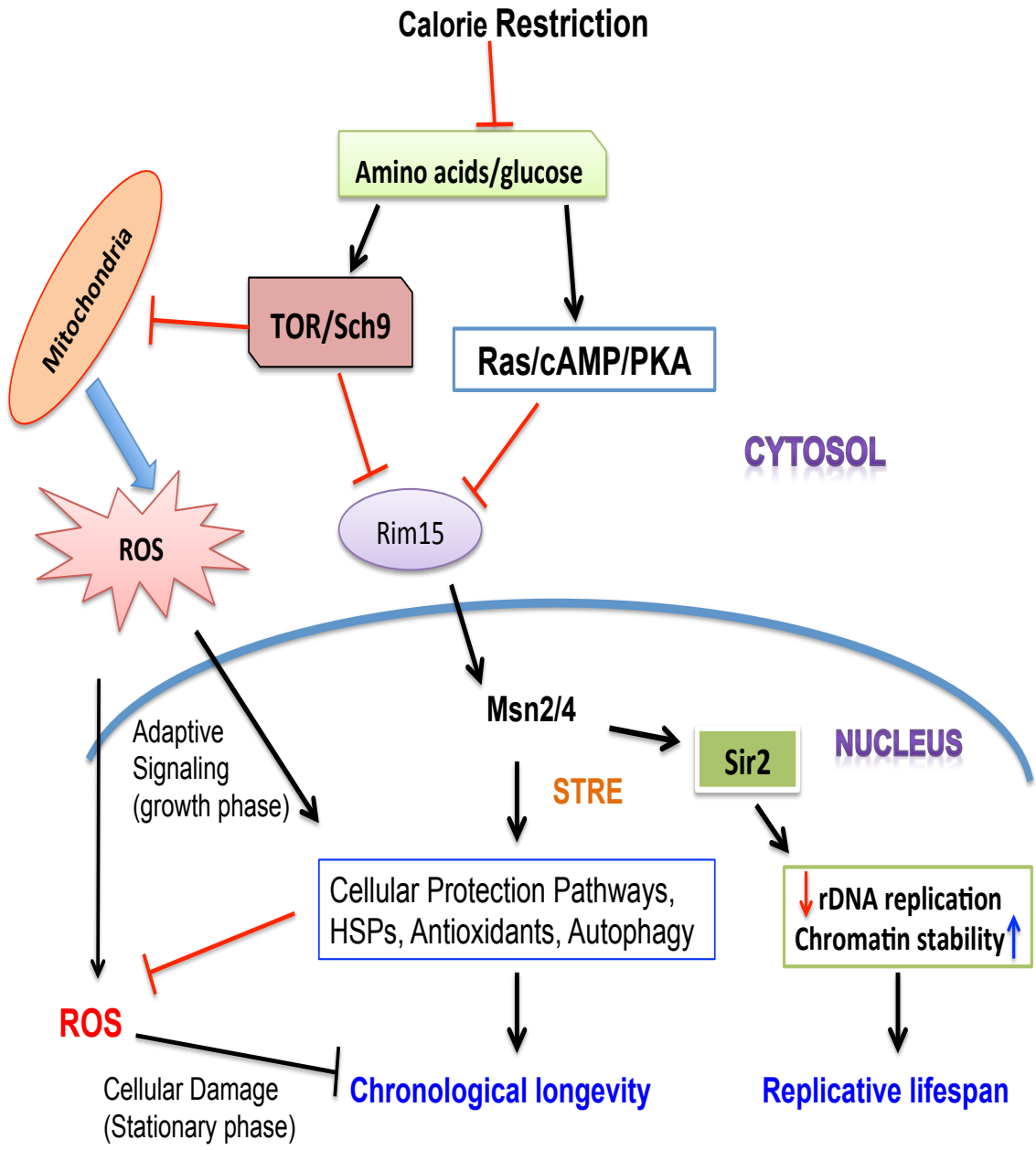

Figure 1.8: Yeast lifespan pathways and calorie restriction. The Tor/Sch9 and Ras/cAMP/PKA pathways are major nutrient sensing pathways and are inextricably implicated in calorie-restriction mediated life-span extension. Both of these pathways converge upon the Rim15 kinase that activates the Msn2/4 stress response resulting in increased resistance to various stresses and enhanced chronological longevity. In addition, the Msn2/4 stress-responsive transcription factor also promotes Sir2 activity resulting in improved rDNA and chromatin stability thus extending replicative lifespan. Reduced Tor/Sch9 activity also improves mitochondrial activity and adaptive ROS signalling during the growth phase. This results in decreased ROS production and promotion of the stress response leading to lifespan extension.

1.3.3 Mitochondria and oxidative stress in yeast ageing

The switch from high metabolic activity towards enhanced stress protection is a key feature through which reduced TOR/Sch9 activity improves yeast CLS. Interestingly, a reduction in TOR/Sch9 was found to promote the upregulation of mitochondrial translation and respiration leading to increased ROS production that extends yeast CLS (Bonawitz et al, 2007). Indeed, a mitochondrial ROS signalling adaptation mechanism has been proposed to explain the longevity promoting effect of reduced TOR/Sch9 signalling (Pan et al, 2011). The idea of a mitochondrial adaptation during ageing has been suggested based on the findings that there is increased mitochondrial respiration activity during calorie restriction through induction of the Hap4 transcription factor (Piper et al, 2006) as well as the production of ROS during stationary phase (Goldberg et al, 2009) that correlated with CLS extension. ROS generated during calorie restriction or as a result of catalase dysfunction was also found to extend lifespan through stimulation of SOD activity (Mesquita et al, 2010). This is consistent with other studies that found overexpression of *SOD1* and *SOD2* is linked with extension of yeast CLS (Fabrizio and Longo, 2003) and enhancing lifespan in flies (Sohal et al, 1995; Sun et al, 2004). Furthermore, increases in early stages but ablated levels during later stages in mitochondrial ROS is associated with longevity promotion in *C. elegans* (Schulz et al, 2007). It is important to note however that overexpression of antioxidant genes/enzymes only led to a modest increase in CLS compared to deletion of *sch9* or *ras2* suggesting a more complicated network involved between ROS, mitochondria activity and ageing (Fabrizio and Longo, 2003).

The link between mitochondrial function and RLS is somewhat poorly defined. Initial studies show that the activation of the retrograde response

pathway whereby the mitochondria is able to communicate stress signals to the nucleus is correlated with an increase in lifespan during RLS and is mediated via the Ras/cAMP/PKA pathway (Kirchman et al, 1999; Borghouts et al, 2004). However, studies in yeast strains with the absence of mitochondrial DNA or mitochondrial respiration showed an improvement in RLS (Kaeberlein et al, 2005). In addition, a mutant of a mitochondrial translation factor, *SOV1* which is a nuclear encoded gene, promoted longer RLS that is also partly dependent upon Sir2 activity (Caballero et al, 2011). Contrary to that found in CLS studies as well, the induction of superoxide dismutases actually reduces RLS (Fabrizio et al, 2004).

Further work is required to expand the complex connection between mitochondrial function and signalling coupled to ROS production in regulating yeast lifespan. One possibility in which the mitochondria could impact upon chronological ageing is through the activation of redox-sensitive programmes such as the DNA-damage response pathways, protein homeostasis, and autophagy by ROS generated from mitochondrial activity. Additionally, adaptive mitochondrial signalling to the nucleus during the early stages of CLS may also promote chronological ageing through the increased expression of genes involved in adaptive responses such as the genes involved in the Msn2/4 stress response pathway. Some or all of these protective pathways mentioned may directly or indirectly contribute to the amelioration of lifespan in yeast and other organisms.

1.4 Yeast actin cytoskeleton.

The actin cytoskeleton is the architectural framework of the cell and plays critical roles in a multitude of cellular processes including maintenance of cell shape, cell motility, mechanosensing, cellular division, and intracellular transport (Pollard et al., 2000). Actin is one of the most abundant proteins in the cell and exists in two forms, either as monomeric G-actin (Globular-actin) or as polymeric F-actin (Filamentous-actin). F-actin is a double-stranded helix with a fast growing barbed end where the ATP-bound G-actin is incorporated, and a pointed end that is slow growing where actin disassembly preferentially occurs (Moseley and Goode, 2006). Profilin, a ubiquitous protein within the cell, serves to inhibit the addition of ATP bound G-actin monomers to the pointed end while allowing G-actin addition to the barbed end of F-actin filaments. Thus actin polymerization is preferentially initiated at the 'free' uncapped barbed end. The generation of 'free' barbed ends can occur either through the uncapping of existing capped barbed ends, via the severing of an actin filament to reveal free ends, or by the *de novo* generation of new actin filaments from G-actin monomers. Repeated cycles of assembly and disassembly of actin is regulated by almost 100 different proteins serving to maintain the reservoir of actin monomers, promote actin nucleation and polymerization, as well as actin filament bundling. The remodelling of the actin architecture is highly regulated in a spatiotemporal manner by these actin-associated proteins in accordance with internal and external stimuli to drive processes such as vesicular trafficking or cellular movement (Pollard et al, 2000; Pollard and Cooper, 2009).

Since initial evidence that yeast contains a full actin cytoskeleton was first confirmed in 1984 (Adams and Pringle, 1984), yeast has been instrumental in the genetic identification and functional elucidation of components of the actin

cytoskeleton as well as their regulatory pathways; most of which have their respective homologs in mammals. For example, genetic screens in yeast led to the discovery of the Arp2/Arp3 (human Arp2/Arp3) complex that function to initiate and facilitate the branching of actin filaments (Higgs and Pollard, 2001) (Figure 1.9). Yeast studies also provided more definitive molecular functions for certain proteins in the regulation of actin. The role of the metazoan formin in the nucleation of linear actin filaments was confirmed in work studying its yeast homologs, Bni1p and Bnr1p (Evangelista et al, 2002; Sagot et al, 2002). Furthermore, work on the yeast actin cytoskeleton also confirmed the crucial role of the actin network in the process of endocytosis whereas studies in mammalian cells at that time provided inconclusive data. Concomitantly, examples of the conservation in actin regulatory pathways between that in humans and yeast are: Rho and Ras GTPases, protein kinases A and C, and phosphatidylinositol 4,5- bisphosphate (Mishra et al, 2014).

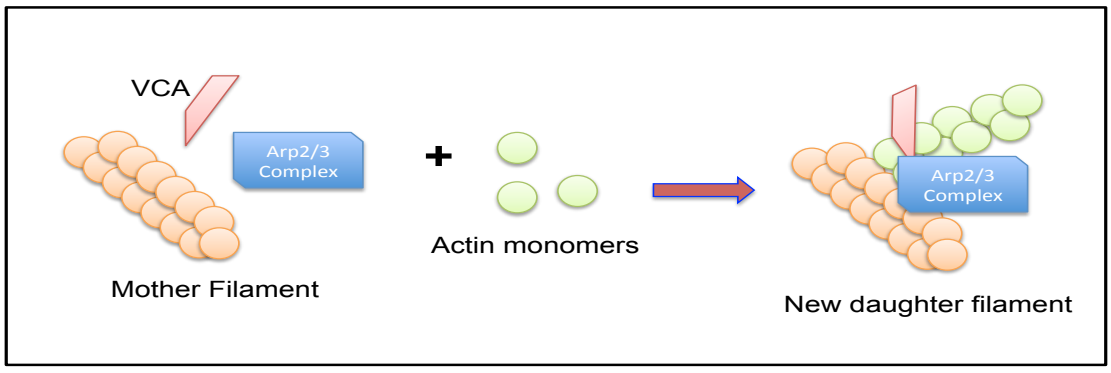

Figure 1.9: The Arp2/3 complex facilitates actin filament branching. The Arp2/3 complex together with vinculin (VCA) recruits and adds actin monomers onto pre-existing actin mother filaments at an angle of 70° to form a dense network of branched actin filaments.

The yeast actin cytoskeleton, albeit less complex than mammalian cells, is organised primarily in three distinct ways (Mishra et al, 2014):

1) Cortical actin patches are networks of branched actin filaments that can be detected as dot structures when stained with the fluorophore-conjugated phalloidin (F-actin specific). Cortical actin patches in yeast are assembled by the Arp2/3 actin nucleation complex and its accessory co-factors (Figure 1.10). Nucleation promoting factors (NPFs) including WASp (Wiskott-Aldrich syndrome) associated protein Las17, Myo3/5 (Myosin 3/5), Pan1, and Abp1 also serve to facilitate the nucleation activity of the Arp2/3 complex. Indeed, mutants of the Arp2/3 complex have also been shown to have abnormal actin patch formation (Winter et al, 1997). Actin patches are predominantly located at sites of polarized growth and are essential for clathrin-mediated endocytosis in yeast (Galletta et al, 2010).

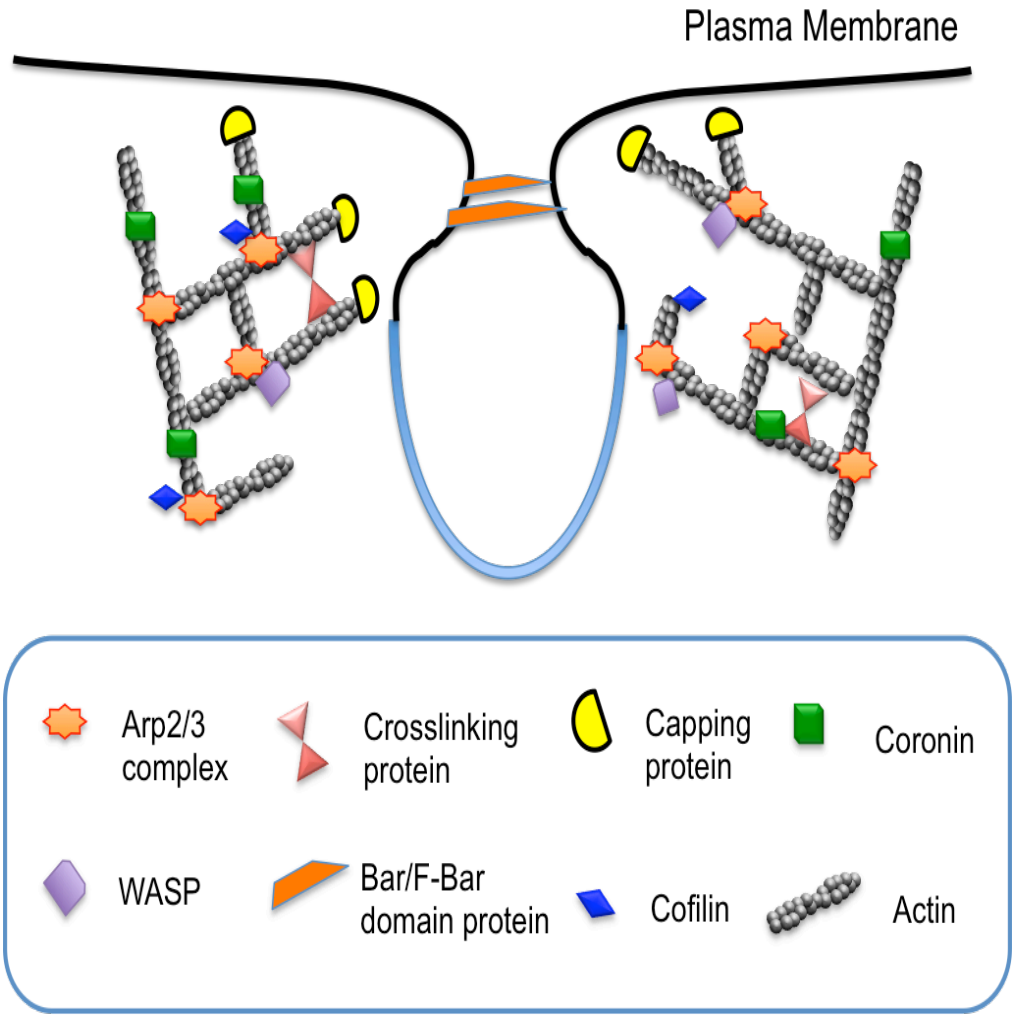

Figure 1.10: Organisation of an actin patch at an endocytic site. At sites of endocytosis, actin patch initiation begins with the arrival of clathrin and early adapter proteins followed by the Arp2/3 complex that form a branched network of actin filaments. The actin nucleation activity of the Arp2/3 complex is promoted by nucleation promoting factors including Las17 and Myo3/5. The actin filament branches are cross-linked by the action of fimbrin (crosslinking protein) whereby capping proteins bind to actin filaments and limit their growth. Filament length and actin patch dynamics are controlled by the combined activities of cofilin and coronin. Lastly, BAR- and F-BAR- domain-amphiphysin proteins then regulate membrane invagination and scission allowing intracellular internalization of the endocytic vacuole with its cargo.

2) Actin cables are long filamentous structures running along the length of the cell with their ends clustered with the cortical actin patches. Their formation is regulated by formins that function to nucleate actin filaments (Bnr1 and Bni1 in yeast) and are associated with the intracellular

transport of vesicles and organelles (cargo) including peroxisomes, golgi, secretory vesicles at the sites of polarized growth (Figure 1.11).

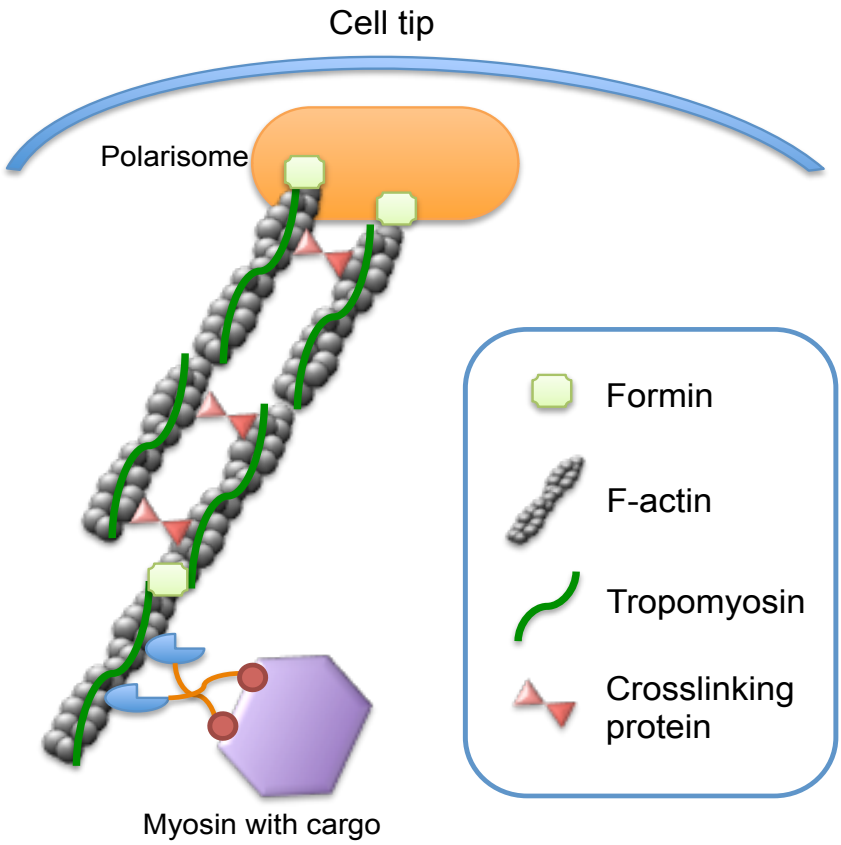

Figure 1.11: The structure of actin cables. Polarisomes are located at sites of polarised cell growth including cell tips. Formins located within the polarisome complex and its activator Rho-GTPases, Bud6 and Pob1, function to promote nucleation of new actin filaments. New actin filaments are pushed inwards by the activity of adjoining formins which nucleates other actin filaments. This forms a cable-like system of short-parallel actin filaments with the formins located at the barbed end facing the site of polarized growth. The actin filaments are cross-linked together to form thicker actin cables which are further stabilized by tropomyosin. These actin cables act as polarized tracks for type V myosins to traverse along to deliver various forms of cargo to sites of polarized growth within cells.

3) The final form of actin is the actin contractile ring located at the interface of the mother and daughter cell during budding. The ring is composed of a linear F-actin filament which is formed by formin, myosin II and is similar to mammalian actomyosin rings. The actin contractile ring serves to generate the force required to drive cellular division and also to facilitate cell wall assembly at the mother and daughter cell interface.

1.4.1 Cortical actin patches and endocytosis.

The formation and dynamics of cortical actin patches have been shown to be essential in the process of endocytosis which is responsible for the uptake of extracellular cell receptors and fluids (Moseley and Goode, 2006). The process of endocytosis can be subdivided into three distinct stages involving the sequential recruitment and activity of different cytoskeletal components (Merrifield, 2004; Kaksonen et al, 2005; Sirotkin et al, 2010) (Figure 1.12). The initial stage of endocytosis involves the recruitment of early patch components such as clathrin, and adaptor proteins such as the F-Bar domain containing protein Syp1, and Yap1810 to initiate patch formation and membrane curvature (Weinberg and Drubin, 2012). Next to follow are the adaptor proteins including Sla1, End3, Sla2, Pan1 and Ent1 that aid in linking the endocytic vesicle to clathrin and the actin cytoskeleton. Recruitment of NPFs including the yeast homologue WASp associated protein Las17 also occurs at this stage while the F-Bar proteins Syp1 and Sla1 function to inhibit the actin nucleation activity of the Arp2/3 complex and Las17 respectively to suppress their untimely activation during the early stages of endocytosis (Feliciano and Di Pietro, 2012).

The second stage of endocytosis is further patch development through the actin polymerization activity of the Arp2/3 complex and its NPFs which coincide with slow, random movements of actin patches along the membrane cortex. The activation of the Arp2/3 complex during this stage is promoted with the departure of Syp1 and Sla1. The F-Bar protein Bzz1 is also recruited and binds to Las17 thus stimulating actin polymerization (Soulard et al, 2002; Soulard et al, 2005). The Arp2/3 complex has been shown to have an elevated basal activity that is further enhanced by its NPFs (Wen and Rubenstein, 2005) with Las17 having the strongest NPF activity followed by Myo3/5 and with both Pan1 and Abp1 having minimal NPF activity. Abp1 has been shown to regulate the elongation of newly synthesized actin filaments and facilitates the departure of Sla1 from actin patches (Michelot et al, 2013). In addition, Abp1 may facilitate movement of actin patches by competitively antagonizing the activity of the more dominant NPFs (Kaksonen et al, 2005). The last stage of endocytosis is characterized by the rapid internal movement of endocytic vesicles away from the cell cortex along the polarized actin cables by passive transport and this process is aided by the Sac6 actin bundling protein. This stage also coincides with the shedding of most of the early patch components and is accompanied by membrane scission by the amphyphysin proteins Rvs161 and Rvs167 (Kaksonen et al, 2005; Kukulski et al, 2012). The internalization of actin patches is followed by the rapid disassembly of the actin patchs by cofilin, Aip1 and Crn1 (Coronin) (Chen and Pollard, 2013) thus completing the endocytosis process with fusion to the endosome.

1.4.1.1 The role of Abp1 and Crn1 in actin patch formation.

1.4.1.2 Abp1:

Abp1 is one of the NPFs involved in the regulation of the Arp2/3 complex. The NPF activity of Abp1 is dependent upon the presence of two A motifs which have high affinity to the Arp2/3 complex. In addition, Abp1 contains an actin depolymerization factor-binding domain that allows the binding of Abp1 to F-actin (Goode et al, 2001). Relative to Las17 as well as Myo3/5, Abp1 has weaker NPF ability in promoting Arp2/3 complex activity (Goode et al, 2001). During actin patch formation, the arrival of Abp1 occurs just before the progression from slow to rapid actin patch movement. However, unlike Las17, Myo3/5 and Pan1, Abp1 remains associated with the actin patch throughout the transport and internalization of the actin patch away from the cell cortex (Kaksonen et al, 2003). In addition, Abp1 activity is also required to displace Sla1 via recruitment of the Ark1 and Prk1 kinases whose phosphorylation of Pan1 disrupts the Sla1-Pan1-End3 complex (Moseley and Goode, 2006). The removal of Sla1 and other early patch components by Abp1 is also suggested to facilitate the disassembly of endocytic components at the final stages of endocytosis (Kaksonen et al, 2005) (Figure 1.12). Furthermore, Abp1 has also been shown to cooperate with Aip1 as well as capping proteins to regulate actin filament elongation as well as organization of actin polarity during Arp2/3 complex-mediated actin nucleation (Michelot et al, 2013).

1.4.1.3 Crn1:

The binding of Crn1 to cortical actin patches is mediated by a β-propeller domain and coiled-coiled domain. Crn1 serves as a negative regulator of the Arp2/3 complex through its association with the Arc35 subunit of the Arp2/3

complex (Goode et al 1999). Crn1 inhibits Arp2/3 complex activity when the complex is not bound to pre-existing actin filaments. Conversely, Crn1 permits actin nucleation activity of the Arp2/3 complex when it is bound to preformed actin filaments thus allowing the continued formation of branched actin networks (Goode et al, 1999; Humphries et al, 2002; Moseley and Goode, 2006). Similar to Abp1, Crn1 is suggested to arrive at later stages of actin patch formation possibly during the onset of rapid patch movement away from the cell cortex (Moseley and Goode, 2006) (Figure 1.12). Furthermore, deletion of *CRN1* leads to reduced actin patch movement while overexpression of *CRN1* was found to impair the formation of actin and microtubule networks (Goode et al, 1999; Galetta et al, 2008).

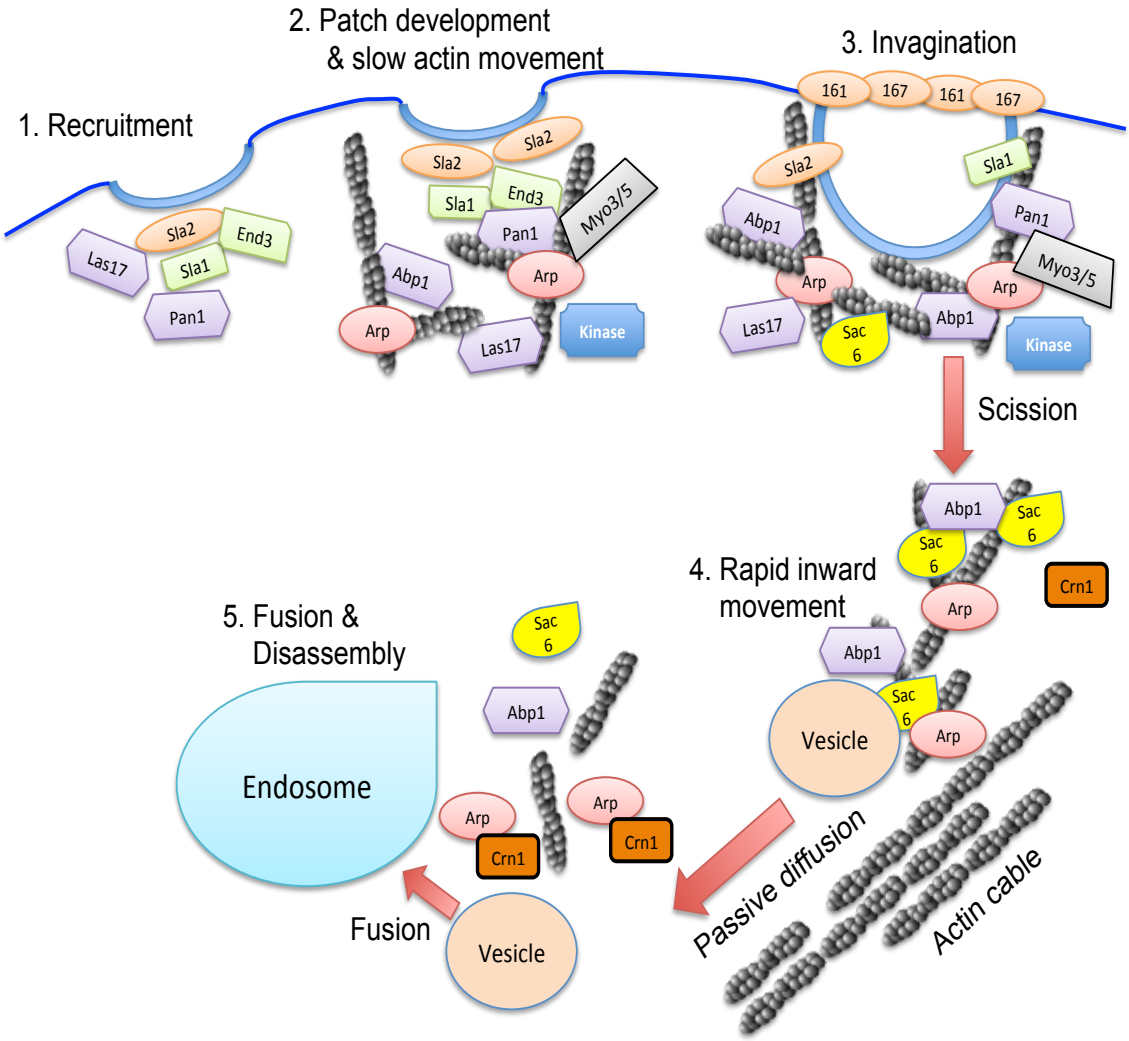

Figure 1.12: Actin patch initiation, development and the process of endocytosis. Step 1 Early patch components including clathrins, and two NPFs, Las17 and Pan1 are recruited to the cell cortex by endocytic receptors. **Step 2** Patch development proceeds with the activation and recruitment of the Arp2/3 complex by Las17 and Pan1 followed by actin nucleation and slow patch movement. Two other NPFs, Abp1 and Myo3/Myo5 are also recruited. Abp1 functions to recruit the kinases Ark1 and Prk1 which phosphorylate Pan1 which causes inhibition of Pan1-activation of Arp2/3 complex and disassembly of the Pan1 complex (Pan1, End3 and Sla1). **Step 3** Activities of Pan1, Rvs161, Rvs167 and myosins Myo3/ Myo5 facilitates vesicle scission and internalization. The Arp2/3 complex, Abp1, Sac6 and possibly other patch components remain associated with the vesicle while others such as Las17, Pan1, Sla1, Sla2 are left at the cortex. Crn1, a negative regulator of the Arp2/3 complex possibly arrives at this stage. **Step 4** The internalized vesicle moves rapidly in an anterograde manner (from bud to mother) along actin cable via passive diffusion. **Step 5** The final stage is the fusion of the endocytic vesicle with the endosome followed by the disassembly of the actin patch components. Crn1 inhibits the actin nucleation activity of the Arp2/3 complex when the Arp2/3 complex is not bound to preformed actin filaments.

1.4.2 Actin cytoskeleton and prion formation.

The yeast actin cytoskeleton has been implicated in the formation of amyloidogenic protein aggregates including prions (Table 1.3). In Sup35 overexpression studies, the actin cytoskeleton was proposed to be involved in the early conversion events from [*psi*$^-$] to [*PSI*$^+$] (the initial formation of the peripheral ring followed by its eventual collapse into a ring surrounding the vacuole) due to the physical interaction of Sup35 with actin cortical patch components (Manogaran et al, 2011; Arslan et al, 2015). Knockout mutants involved in actin filament assembly and actin-dependent endocytosis including Sla1, Sla2, End3, Las17 and Vps5 cause a reduction in visible Sup35 aggregates as well as a decreased *de novo* [*PSI*$^+$] frequency when Sup35 is overexpressed (Ganusova et al, 2006; Manogaran et al, 2011). Genes encoding products involved in the actin cytoskeleton can be categorised into two classes. Class II genes decreased peripheral and internal ring formation and reduced prion induction while class I genes only affected prion induction ability and not ring formation. Additionally, the addition of latrunculin A that disrupts the actin cytoskeleton via sequestration of actin monomers was found to destabilize weak [*PSI*$^+$] variants and their propagation (Bailleul-Winslett et al, 2000). The expression levels of the Las17 binding protein, Lsb2, during and after thermal challenge has been linked to prion induction, which is also dependent upon its association with the actin cytoskeleton (Chernova et al, 2011). Elevated levels of Lsb2 induced upon heat shock was found to trigger higher levels of [*PSI*$^+$] conversion events independently of the presence of other prions such as [*PIN*$^+$]. Conversely, Lsb2 abrogation leads to the destabilization of [*PSI*$^+$] aggregates during heat shock.

The formation and maturation of both actin filaments and amyloid fibres share similarities in that both processes initiate with a nucleation step, followed by polymer extension and the eventual fragmentation of the polymer into smaller units to trigger further filament formation. Thus it may be envisaged that events leading towards the formation of mature prions from misfolded proteins are facilitated by the actin cytoskeleton machinery. These may act to target and transport prion proteins into protein sequestration deposits for storage such as the IPOD, leading to its detoxification and subsequent degradation (Ganusova et al, 2006). In line with this, autophagy markers such as Atg8 and Atg14 have been reported to colocalize with the IPOD thus leading to eventual removal of the prion aggregates via autophagy (Treusch and Lindquist, 2012). However, endocytosis has been reported to be essential only in the initial events of prion formation as no difference was observed in peripheral ring formation between wild-type and mutants that disrupt endocytosis including knockout mutants of *end3* and *erg2* during the formation of the [Het-s] prion (Mathur et al, 2010).

Table 1.3: Proteins involved in yeast actin cytoskeleton formation and dynamics as well as actin-related proteins that are associated with prion formation.

Yeast protein (s)	Function:	Prion formation:
Act1p	Filament component/cell polarity/ endocytosis/ cytokineses/ protein translation regulation	(Bailleul-Winslett et al, 2000)
Arp2p, Arp3p, Arc40p, Arc35p, Arc19p, Arc18p, Arc15p	Nucleation of actin filaments/ filament binding/ cell polarity/ endocytosis	
Las17p	Nucleation of actin filaments/ binds actin monomers/ filament binding/ cell polarity/ endocytosis/ cytokinesis	(Manogaran et al, 2011)
Myo3p, Myo5p	Nucleation of actin filaments/ filament binding/ cytokinesis/ cell polarity/ endocytosis	
Pan1p	Nucleation of actin filaments/ filament binding/ cell polarity/ endocytosis	
Abp1p	Nucleation of actin filaments/ filament binding/ cell polarity/ endocytosis	
Bni1p, Bnr1p	Nucleation of actin filaments/ filament binding/ cytokinesis/ cell polarity/ endocytosis	
Myo1p	Nucleation of actin filaments/ filament binding/ cell polarity/ cytokinesis	
Cap1p, Cap2p	Filament binding/ filament end capping/ cell polarity/ endocytosis	
Pfy1p	Nucleation of actin filaments/ binds actin monomers/ cell polarity	
Sac6p	Bundling of actin filaments/vesicular trafficking from endosome to Golgi	
Sla2p (End4p)	Endocytosis/cell polarity/localized in actin patches	(Ganusova et al, 2006)
Sla1p	Assembly and regulation of cortical actin patches/endocytosis	
End3p	Endocytosis/actin cytoskeletal organization/cell wall morphogenesis/ complex formation with Sla1p and Pan1p	
Lsb1p Lsb2p	Inhibitors of actin polymerization through association with Las17p. Lsb2 is induced upon thermal challenge.	(Chernova et al, 2011)

1.5. Objectives of PhD:

The causal basis underlying spontaneous prion formation still remains a poorly understood process. The 2nd and 3rd chapter of this thesis aim to investigate the molecular mechanisms of autophagy in *de novo* prion formation using the [*PSI*$^{+}$] prion in yeast as a model system. We also examine whether promotion of autophagic flux through pharmacological means may exert a protective effect against prion formation as well as the accumulation of prion aggregates.

The effects of carrying prions within cells on yeast chronological ageing has also not been fully characterized which forms the second part of our study. The 4th chapter of the thesis aims to investigate the links between autophagy and prion formation in the context of chronological ageing of the cell. Does autophagy elicit a protective role against *de novo* prion formation during chronological ageing and whether carrying different prions affect yeast chronological ageing are questions we aim to address in this chapter?

The 5th chapter of this thesis focuses upon the role of the cortical actin cytoskeleton, more specifically components of the Arp2/Arp3 complex that functions in actin branching and actin patch formation towards the *de novo* formation of prions under basal as well as oxidative stress conditions. This is based on previous mass-spectrometry data from the lab which identified several components of the actin cytoskeleton that were associated with Sup35 in an antioxidant mutant.

1.6 Alternative thesis.

This thesis is presented according to the rules and the regulations of thesis policy of the University of Manchester. The four results chapters describe independent studies which are each appropriate for publication. Although each of the chapters represents independent pieces of work, they are linked by common themes and the use of similar methodologies and constitute a coherent body of work.

Chapter 2: Autophagy protects against *de novo* formation of the [*PSI*$^{+}$] prion in yeast.

Authors: Shaun H. Speldewinde, Victoria A. Doronina, and Chris M. Grant

Journal: *Molecular Biology of the Cell*

Chapter 3: Spermidine cures yeast of prions.

Authors: Shaun H. Speldewinde, and Chris M. Grant

Journal: *Microbial Cell*

Chapter 4: The yeast [*PSI*$^{+}$] prion improves chronological ageing in autophagy competent cells.

Authors: Shaun H. Speldewinde, and Chris M. Grant

Journal: To be submitted to *Microbial Cell*

Chapter 5: The cortical actin cytoskeleton is required for increased yeast [*PSI*$^{+}$] prion formation during oxidative stress conditions.

Authors: Shaun H. Speldewinde, Victoria A. Doronina, Mick Tuite and Chris M. Grant

Journal: To be submitted to *PLOS Genetics*

Chapter 2: Autophagy protects against *de novo* formation of the [*PSI*$^{+}$] prion in yeast.

Shaun H. Speldewinde, Victoria A. Doronina and Chris M. Grant*

University of Manchester, Faculty of Life Sciences, The Michael Smith Building, Oxford Road, Manchester, M13 9PT, UK.

*Address correspondence to: Chris M. Grant, The University of Manchester, Faculty of Life Sciences, The Michael Smith Building, Oxford Road, Manchester, M13 9PT, UK. Phone: (0161) 306 4192; Email: chris.grant@manchester.ac.uk

With supervision from Prof Chris M. Grant and advice from Dr Victoria A. Doronina, the author has designed the experiments, generated all the figures presented in this chapter, and wrote the manuscript.

ABSTRACT

Prions are self-propagating, infectious proteins that underlie several neurodegenerative diseases. The molecular basis underlying their sporadic formation is poorly understood. We show that autophagy protects against *de novo* formation of [*PSI*$^{+}$], which is the prion form of the yeast Sup35 translation termination factor. Autophagy is a cellular degradation system, and preventing autophagy by mutating its core components elevates the frequency of spontaneous [*PSI*$^{+}$] formation. Conversely, increasing autophagic flux by treating cells with the polyamine spermidine suppresses prion formation in mutants that normally show a high frequency of *de novo* prion formation. Autophagy also protects against the *de novo* formation of another prion, namely the Rnq1/[*PIN*$^{+}$] prion, which is not related in sequence to the Sup35/[*PSI*$^{+}$] prion. We show that growth under anaerobic conditions in the absence of molecular oxygen abrogates Sup35 protein damage and suppresses the high frequency of [*PSI*$^{+}$] formation in an autophagy mutant. Autophagy therefore normally functions to remove oxidatively damaged Sup35, which accumulates in cells grown under aerobic conditions, but in the absence of autophagy, damaged/misfolded Sup35 undergoes structural transitions favoring its conversion to the propagatable [*PSI*$^{+}$] form.

2.1 INTRODUCTION

Prions are infectious agents arising from misfolded proteins. They cause transmissible spongiform encephalopathies (TSEs) typified by Creutzfeldt-Jakob disease in humans and bovine spongiform encephalopathy in cattle. Conversion of the normal prion protein (PrP^{C}) into its infectious PrP^{Sc} confirmation underlies the pathogenesis of TSEs (Collinge and Clarke, 2007). This protein-only mechanism of infectivity can also explain the unusual genetic behavior of several prions found in the yeast *Saccharomyces cerevisiae* (Wickner, 1994; Alberti et al, 2009). [*PIN*$^{+}$] and [*PSI*$^{+}$] are the best-studied yeast prions and are formed from the Rnq1 and Sup35 proteins, respectively (Wickner, 1994; Derkatch et al, 1997). [*PSI*$^{+}$] is the altered conformation of the Sup35 protein, which normally functions as a translation termination factor during protein synthesis. The *de novo* formation of [*PSI*$^{+}$] is enhanced by the presence of the [*PIN*$^{+}$] prion (Derkatch et al, 1996; Derkatch et al, 2001; Osherovich and Weissman, 2001), which is the altered form of the Rnq1 protein, whose native protein function is unknown (Treusch and Lindquist, 2012).

Yeast Sup35 normally functions in translation termination in its soluble form but is sequestered away from this function in its amyloid or aggregated form (Wickner, 1994). Recently, aggregated Sup35 has been shown to retain its translation termination function, and alterations in amyloid heterogeneity have been shown to underlie changes in Sup35 protein–only phenotypes (Pezza et al, 2014).The amyloid state is a highly structured, insoluble fibrillar deposit, consisting of many repeats of the same protein. This type of aggregation is

central to the pathology of many neurodegenerative diseases, including Alzheimer's, Parkinson's, Huntington's, and prion diseases. Although the exact point at which these disease-related proteins are toxic is debatable, it is well accepted that the process of amyloid formation is generally detrimental to human health. Fungal and mammalian prions form *de novo,* but the mechanism is poorly understood in molecular terms. An initial alternative conformational state might be instigated by spontaneous misfolding event(s) that might be triggered by mutation, mistranslation, environmental stresses, and/or disruption of the chaperone network (DeMarco and Daggett, 2005). Hence any defense systems that can eliminate these initially misfolded species might prevent conversion to the amyloid or disease-causing form of the protein.

Studies in yeast cells have identified intricate protein quality control systems in which insoluble proteins are partitioned into defined sites in the cell; amyloid and amorphous aggregates are believed to be processed separately (Sontag et al, 2014). The ubiquitin proteasome system (UPS) is the main proteolytic system that subsequently degrades misfolded and damaged proteins or proteins that are no longer required in cells. Proteins destined for degradation by the proteasome are tagged with ubiquitin, and previous studies showed that alterations in the ubiquitin system affect prion formation (Allen et al, 2007). In addition, a number of genes that affect the UPS have been identified in an unbiased genome-wide screen for factors that modify the frequency of [*PSI*$^{+}$] induction (Tyedmers et al, 2008). This suggests that the UPS normally functions to prevent conversion of misfolded Sup35 into its transmissible amyloid form. However, ubiquitinated Sup35 has not been directly detected in yeast, and it is unclear whether the proteasome plays a direct role in

suppressing [*PSI*$^{+}$] prion formation (Allen et al, 2007).

Autophagy is the cellular proteolytic system that degrades organelles and clears protein aggregates via vacuolar/lysosomal degradation (Parzych and Klionsky, 2014). During autophagy, an elongated isolation membrane sequesters cell material for degradation, forming a double-membrane-bound vesicle called the autophagosome. Fusion of the autophagosome with vacuoles/lysosomes introduces acidic hydrolases, which degrade the contained proteins and organelles. The progress of the autophagy pathway is regulated by the products of autophagy-related genes (*ATG genes*). Approximately 35 *ATG* genes have been identified in yeast, and several mammalian homologues have been functionally characterized. A number of possible links between autophagy and protein aggregation diseases have been described. For example, a link between autophagy and prion disease was first suggested by the observance of autophagic vacuoles in neurons from a scrapie hamster model (Boellaard et al, 1991). Suppression of basal autophagy in mice causes neurodegenerative diseases, suggesting that autophagy plays a role in the clearance of misfolded proteins (Hara et al, 2006; Komatsu et al, 2006), and amyloidogenic aggregates such as those formed by α-synuclein and huntingtin have been identified as substrates of autophagy (Webb et al, 2003; Ravikumar et al, 2004; Iwata et al, 2005). In addition, a correlation has been observed between pharmacological interventions that induce autophagy and enhanced cellular degradation of prions in prion-infected neuronal cell models (Heiseke et al, 2009). All of this suggests that autophagy plays a protective role against prion toxicity. However, the molecular details of how autophagy might promote prion clearance/degradation are unclear, and it is unknown whether a defective

autophagy pathway might promote increased prion formation/ accumulation.

In the present study, we analyze the role of autophagy in protecting against *de novo* [*PSI*$^{+}$] prion formation in yeast. We show that the frequency of [*PSI*$^{+}$] and [*PIN*$^{+}$] prion formation is elevated in mutants deficient in autophagy. Conversely, induction of autophagy acts to protect against *de novo* prion formation. We show that oxidatively damaged Sup35 accumulates in autophagy mutants and suggest that autophagy normally functions to remove such oxidatively damaged Sup35, preventing spontaneous prion formation. In agreement with this idea, we show that growth under anaerobic conditions suppresses the *de novo* formation of [*PSI*$^{+}$] in an autophagy mutant.

2.2 RESULTS

2.2.1 [*PSI*$^{+}$] prions are formed in autophagy mutants.

A representative range of autophagy mutants was constructed to determine whether Sup35 aggregation is elevated in the absence of autophagy. Deletion mutants were made in a [*PIN*$^{+}$][*psi*$^{-}$] version of yeast strain 74D-694, which is commonly used for prion studies (Chernoff et al., 1995). Mutants were constructed in a [*PIN*$^{+}$][*psi*$^{-}$] strain background with defects in the core autophagy machinery, including the Atg1 kinase complex (*atg1*), the PI3K complex (*atg14*), the Atg9 cycling complex (*atg9*), the Atg8 ubiquitin-like conjugation system (*atg8, atg4*), and the Atg12 ubiquitin-like conjugation system (*atg12, atg7*). Mutants were also constructed lacking a vacuolar lipase (*atg15*), a receptor protein for the cytoplasm-to-vacuole targeting (Cvt) pathway (*atg19*), an adapter protein required for cargo loading in pexophagy (*atg11*), and a mitochondrial cargo receptor required in mitophagy (*atg32*).

Sup35 aggregate formation was visualized using a Sup35NM–green fluorescent protein (GFP) fusion protein whose expression is under the control of the copper-regulatable *CUP1* promoter (Patino et al, 1995). After short-term induction of this protein, diffuse cytoplasmic fluorescence is observed in [*psi*$^-$] cells, whereas coalescence of newly made Sup35NM-GFP with preexisting Sup35 aggregates in [*PSI*$^+$] cells allows the detection of [*PSI*$^+$] foci. [*PIN*$^+$][*psi*$^-$] strains were grown for 16 h and Sup35NM-GFP induced with copper for 1 h to visualize Sup35 aggregation. As expected, diffuse cytoplasmic fluorescence was observed in the control [*psi*$^-$] strain (Figure 2.1A). Similar diffuse cytoplasmic Sup35 fluorescence was detected in the *atg11* and *atg32* mutants. In contrast, many large Sup35 puncta were detected in all of the remaining *atg* mutants (Figure 2.1A). Quantification of aggregate formation revealed that ~2–5% of mutant cells examined contained visible fluorescent foci after 16 h of growth (Figure 2.1B).

One well-defined genetic criterion for a yeast prion is its reversible curability (Wickner, 1994). This is commonly tested using guanidine hydrochloride (GdnHCl), which blocks the propagation of yeast prions by inhibiting the key ATPase activity of Hsp104, a molecular chaperone that is absolutely required for yeast prion propagation (Ferreira et al, 2001; Jung and Masison, 2001). Curing autophagy mutants with GdnHCl resulted in diffuse cytoplasmic Sup35-GFP fluorescence, with no detectable foci, indicating that these puncta may represent [*PSI*$^+$] prion formation rather than amorphous Sup35 protein aggregates (Figure 2.1C).

A.

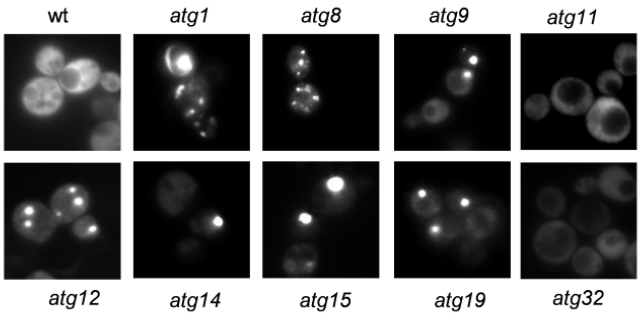

B.

Core autophagy	Mutant	puncta (%)
Atg1 kinase complex	*atg1*	3.9
PI3K complex	*atg14*	3.3
Atg9 cycling complex	*atg9*	2.1
Atg12 Ubl system	*atg12*	1.7
	atg7	2.6
Atg8 Ubl system	*atg8*	4.0
	atg4	4.7
Accessory components		
Vacuolar lipase	*atg15*	4.9
Selective macroautophagy	*atg11*	0
Receptor for Cvt pathway	*atg19*	4.8
Mitophagy	*atg32*	0
wild-type		0

C.

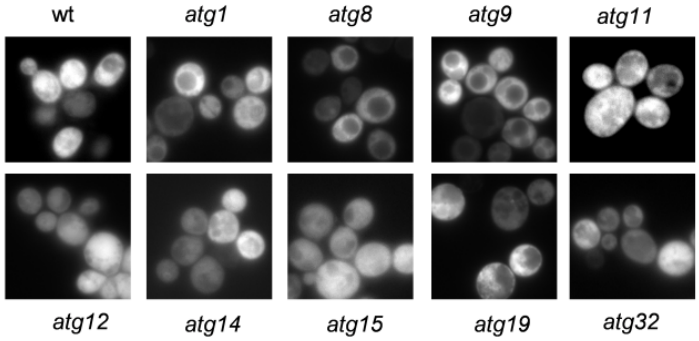

Figure 2.1: [*PSI*$^{+}$] prions are formed in autophagy mutants. (A) Representative fluorescence micrographs for the wild-type and indicated autophagy mutant strains containing plasmids expressing Sup35NM-GFP. Sup35NM-GFP expression was induced for 1 h using copper before visualizing aggregate formation after 16 h of growth. **(B)** The aggregation frequency was calculated in the indicated autophagy mutants as a percentage of the number of cells containing fluorescent foci out of ~300 cells counted. **(C)** Representative fluorescence micrographs for strains cured with GdnHCl.

2.2.2 Increased frequency of *de novo* [*PSI*$^+$] and [*PIN*$^+$] prion formation in autophagy mutants.

Strain 74D-694 contains the *ade1-14* mutant allele, which confers adenine auxotrophy due to the presence of a premature UGA stop codon in the *ADE1* gene. Thus [*psi*$^-$] *ade1-14* cells are unable to grow in the absence of exogenous adenine and accumulate an intermediate in the adenine biosynthetic pathway that causes the colonies to be red. Suppression of the *ade1-14* mutation in [*PSI*$^+$] cells allows growth in the absence of adenine, giving rise to white or pink colonies. Spontaneous white/pink Ade$^+$ colonies were isolated from *atg1*, *atg8*, and *atg19* mutants (Figure 2.2A). The Ade$^+$ phenotype was eliminated by growth in the presence of GdnHCl, giving rise to red Ade$^-$ colonies, confirming the *de novo* formation of [*PSI*$^+$] in these cells (Figure 2.2A). Semidenaturing detergent agarose gel electrophoresis (SDD-AGE) was used to provide further evidence that autophagy mutants form [*PSI*$^+$] prions. [*PSI*$^+$] prions form SDS-resistant, high–molecular weight aggregates that can be detected using SDD-AGE (Kryndushkin et al, 2003). Such Sup35 aggregates were detected in a control [*PSI*$^+$] strain (Figure 2.2B). Growth of this strain in the presence of GdnHCl shifted Sup35 back to its monomeric size due to the requirement for Hsp104 to propagate [*PSI*$^+$] prion formation. Similar SDS-resistant, high–molecular weight aggregates were detected in the [*PSI*$^+$] versions of the *atg1*, *atg4*, *atg8*, and *atg15* mutants, which were also curable by growth in the presence of GdnHCl (Figure 2.2B).

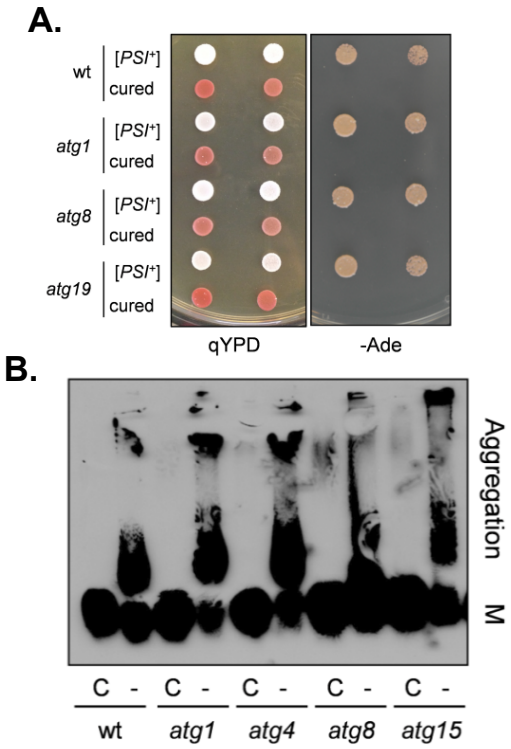

Figure 2.2: The [*PSI*$^+$] prion is formed in autophagy mutants. (A) [*PSI*$^+$] prion formation was visualized in the wild-type (74D-694) and *atg1*, *atg8*, and *atg19* mutant strains by pink/white colony formation and growth on minimal medium in the absence of adenine. Curing with GdnHCl gives rise to red Ade$^-$ colonies, confirming the *de novo* formation of [*PSI*$^+$] in these cells. **(B)** Cell extracts were prepared from exponentially growing cells and analyzed by SDD-AGE. SDS-resistant Sup35 aggregates were detected in *atg1*, *atg4*, *atg8*, and *atg15* mutant strains. Aggregate and monomer (M) forms are indicated.

To quantify [*PSI*$^+$] formation, we used a plasmid with a *ura3-14* allele containing the *ade1-14* nonsense mutation engineered into the wild-type *URA3* gene (Manogaran et al, 2006). The *ura3-14* allele allows [*PSI*$^+$] prion formation to be scored by growth on media lacking uracil, indicative of decreased translational termination efficiency in [*PSI*$^+$] cells. We used this assay rather than scoring [*PSI*$^+$] formation by suppression of the *ade1-14* nonsense mutation and growth on media lacking adenine to avoid any possible complications arising from adenine metabolism in autophagy mutants. Formation of the red pigment in adenine mutants arises due to its accumulation in vacuoles

(Chaudhuri et al, 1997), and we reasoned that autophagy mutants might affect vacuolar function. [*PSI*$^{+}$] formation was differentiated from nuclear gene mutations that give rise to uracil prototrophy by their irreversible elimination in GdnHCl. Using this assay, we estimated the frequency of *de novo* [*PSI*$^{+}$] prion formation in a control [*PIN*$^{+}$][*psi*$^{-}$] strain to be ~1×10^{-5} (Figure 2.3A), comparable to previously reported frequencies (Lund and Cox, 1981; Lancaster et al, 2010). Loss of *ATG1*, *ATG8*, or *ATG19* caused a modest increase in the frequency of *de novo* [*PSI*$^{+}$] formation of approximately twofold to threefold. Given that increased cellular concentration of Sup35 can promote [*PSI*$^{+}$] prion formation, we examined Sup35 protein levels in autophagy mutants (Figure 2.3B). This analysis confirmed that similar levels of Sup35 are present in a wild-type and *atg1*, *atg8*, and *atg19* mutant strains, ruling out any effects on Sup35 protein concentration.

Given the increased frequency of [*PSI*$^{+}$] prion formation in autophagy mutants, we examined the *de novo* formation of another yeast prion, namely the Rnq1/[*PIN*$^{+}$] prion, which is not related in sequence to the Sup35/[*PSI*$^{+}$] prion. The *de novo* formation of [*PIN*$^{+}$] prions was detected in ~6% of control [*pin*$^{-}$] cells (Figure 2.3C), comparable to previous measurements (Sideri et al, 2011). The frequency of [*PIN*$^{+}$] prion formation was elevated by approximately twofold to threefold in *atg1*, *atg8*, and *atg19* mutants (Figure 2.3C). Taken together, these data indicate that an increased frequency of *de novo* prion formation occurs in mutants defective in the core autophagy machinery, suggesting that active autophagy is required to suppress prion formation during normal growth conditions.

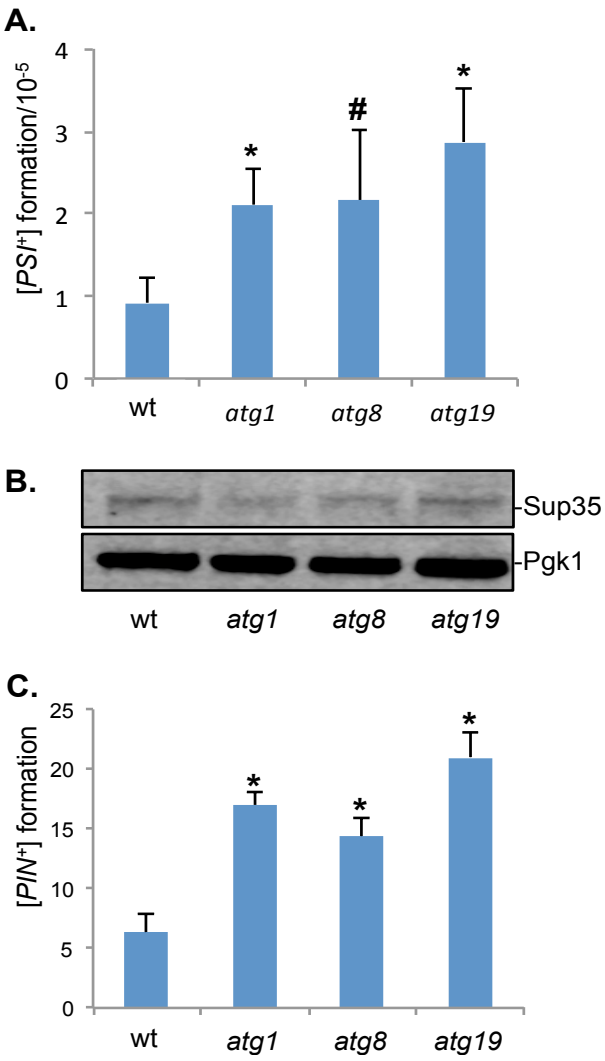

Figure 2.3: Increased frequency of *de novo* [*PSI*$^+$] and [*PIN*$^+$] prion formation in autophagy mutants. (A) [*PSI*$^+$] prion formation was quantified in the wild-type and *atg1*, *atg8*, and *atg19* mutant strains using an engineered *ura3-14* allele, which contains the *ade1-14* nonsense mutation inserted into the wild-type *URA3* gene (Manogaran et al., 2006). [*PSI*$^+$] prion formation was scored by growth on medium lacking uracil, indicative of decreased translational termination efficiency. [*PSI*$^+$] formation was differentiated from nuclear gene mutations that give rise to uracil prototrophy by their irreversible elimination in GdnHCl. Data shown are the means of at least three independent biological repeat experiments expressed as the number of colonies per 10^5 viable cells. Error bars denote the standard deviation. Statistical analysis was performed by one-way ANOVA with pair-wise comparisons using Tukey HSD (honest significant difference) test comparing the [*PSI*$^+$] prion formation in the *atg1*, *atg8*, and *atg19* mutant strains to the [*PSI*$^+$] prion formation in the wild-type strain (*$p<0.01$, $^{\#}p<0.05$). **(B)** Western blot analysis showing Sup35 protein levels in wild-type and *atg1*, *atg8*, and *atg19* mutant strains. Blots were probed with α-Pgk1 as a loading control. **(C)** [*PIN*$^+$] prion formation was quantified in wild-type and *atg1*, *atg8*, and *atg19* mutant strains and is expressed as the number of [*PIN*$^+$] colonies formed per 96 colonies examined. Data shown are the means of at least three independent biological experiments; error bars denote the standard deviation. Statistical analysis was

performed by one-way ANOVA with pair-wise comparisons using Tukey HSD test comparing the [*PIN*$^+$] prion formation in the *atg1*, *atg8*, and *atg19* mutant strains to the [*PIN*$^+$] prion formation in the wild-type strain (*p<0.01).

2.2.3 The frequency of induced [*PSI*$^+$] formation is increased in an autophagy mutant.

[*PSI*$^+$] prion formation can be induced by the overexpression of Sup35 in [*PIN*$^+$] strains since the excess Sup35 increases the possibility for prion seed formation (Wickner, 1994). Strains were initially grown overnight, before the Sup35NM-GFP was induced with copper to promote [*PSI*$^+$] prion formation. We found that overexpression of Sup35NM-GFP in a [*PIN*$^+$][*psi*$^-$] control strain resulted in detectable protein aggregates after 18 h of expression induced by copper addition, and aggregates were detected in ~4.7% of cells by 24 h (Figure 2.4A), similar to previous reports (Mathur et al, 2010). Overexpression of Sup35NM-GFP in [*PIN*$^+$][*psi*$^-$] cells facilitates the detection of ring- and ribbon-like aggregates that are believed to be characteristic of *de novo* prion formation. These structures can be found in the cell periphery or surrounding the vacuole and mature into an infectious prion state, detected as large, dot-like aggregates (Ganusova et al, 2006). Ring and ribbon-like aggregates characteristic of the *de novo* formation of [*PSI*$^+$] could be detected in 0.6% of control cells by 18 h (Figure 2.4A). When the same experiment was repeated in an *atg1* mutant, increased aggregation was detected after overnight growth and induction of Sup35NM-GFP for 1 h, as expected from Figure 2.1. Sup35 aggregation continued to increase in the *atg1* mutant, with 13.6% of cells examined containing visible aggregates after 24 h of Sup35NM-GFP expression (Figure 2.4A). Ring- and ribbon-like aggregates characteristic of the *de novo*

formation of [*PSI*$^+$] could also be detected within 12 h. Thus autophagy mutants appear to show an increased frequency of both spontaneous and induced [*PSI*$^+$] prion formation.

Sup35 Western blot analysis was used to rule out any differences in Sup35NM-GFP induction in the *atg1* mutant compared with the wild-type strain (Figure 2.4B). This analysis showed that a similar profile of increased Sup35NM-GFP was detected in both the wild-type and *atg1* mutant strains. Strains were cured with GdnHCl before Sup35NM-GFP overexpression to determine the requirement for Hsp104 for induced puncta formation. No puncta were detected in the cured wild-type strain after 2 or 24 h induction of Sup35NM-GFP (Figure 2.4C). Similarly, no puncta were detected in the *atg1* mutant after 2 h of induction of Sup35NM-GFP, but 3.6% of *atg1* mutant cells contained puncta after 24 h of induction (Figure 2.4C). These data confirm that the induced aggregate formation in the wild-type and the *atg1* mutant is largely [*PIN*$^+$] dependent.

The induction of [*PSI*$^+$] prion formation was quantified using the *ade1-14* mutant allele, which confers adenine auxotrophy and is differentiated from nuclear *SUPX* gene mutations by its irreversible elimination in guanidine hydrochloride (Tuite et al, 1981). The frequency of [*PSI*$^+$] formation was ~10-fold higher in a wild-type strain containing the plasmid expressing Sup35NM-GFP before copper induction compared with a nontransformed strain (compare Figures 2.4D and 2.3A). This presumably reflects increased basal levels of Sup35 expression from the Sup35NM-GFP plasmid. Before copper induction, the frequency of [*PSI*$^+$] formation was approximately threefold higher in the *atg1*

mutant than with the wild-type strain (Figure 2.4D). This is very similar to the difference observed between wild-type and *atg1* mutant strains using the *ura3-14* assay (Figure 2.3A). [*PSI*$^{+}$] formation was strongly induced in response to copper addition. This induction was stronger in the *atg1* mutant than with the wild-type strain, confirming that autophagy suppresses induced [*PSI*$^{+}$] prion formation (Figure 2.4D).

Overexpression of Sup35 in a [*PSI*$^{+}$] background can be toxic due to increased Sup35 aggregation titrating Sup35 away from its normal function in translation termination (Derkatch et al, 1996; Allen et al, 2007; Vishveshwara et al, 2009). We examined whether autophagy is required to protect against this toxicity. *Sup35* was overexpressed under the control of the *GAL1* promoter in [*PIN*$^{+}$][*PSI*$^{+}$] versions of the wild-type and *atg1*, *atg8*, and *atg19* mutant strains. Sup35 overexpression was more toxic in the autophagy mutants than with the wild-type strain (Figure 2.4E). This toxicity depended on the [*PSI*$^{+}$] status of the cells, since it was largely abrogated in [*PIN*$^{+}$][*psi*$^{-}$] mutants.

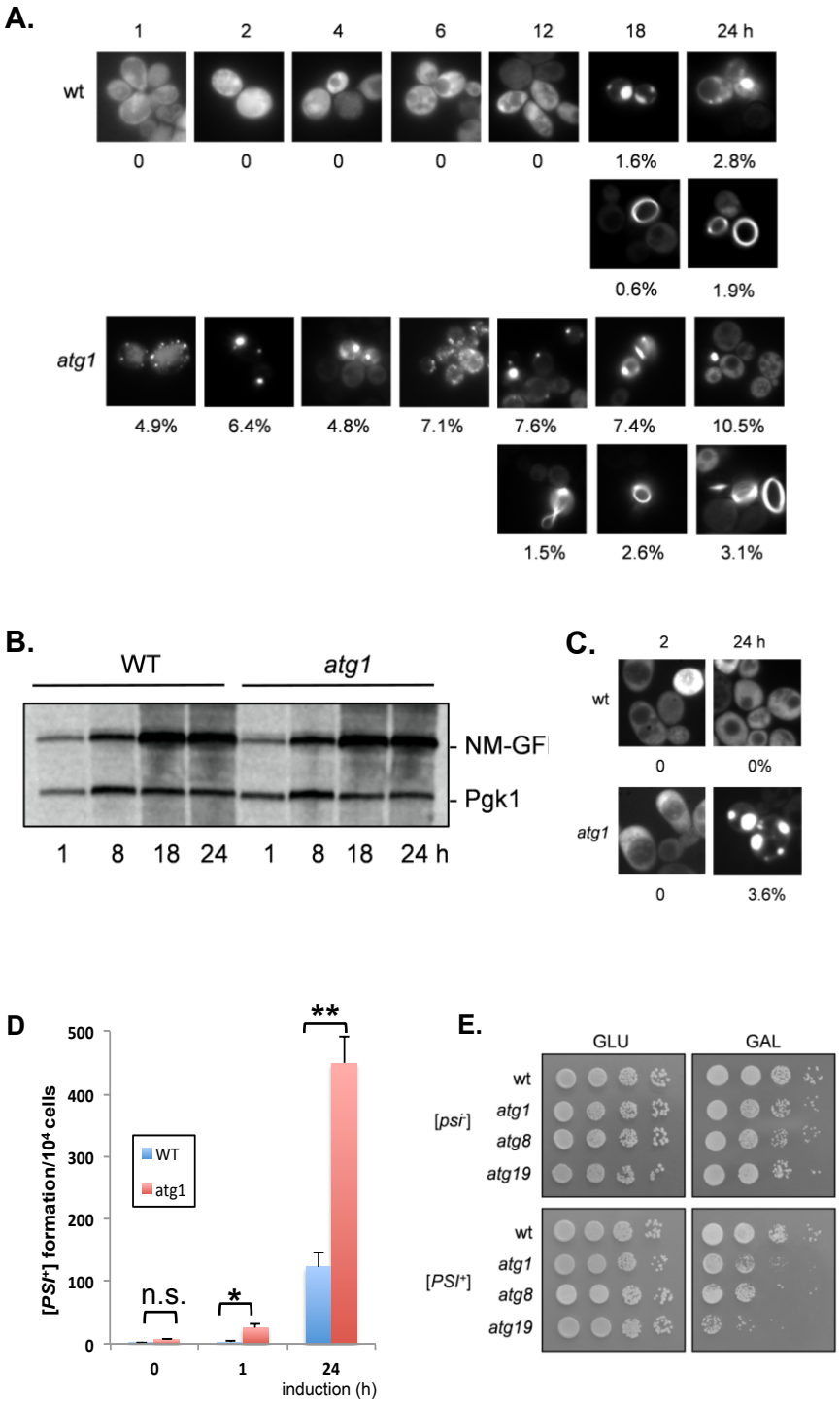

Figure 2.4: Induction of [*PSI*$^+$] prion formation in autophagy mutants. (A) Fluorescence micrographs for [*PIN*$^+$] [*psi*−] versions of the wild-type and *atg1* mutant strains containing the *CUP1-SUP35NM-GFP* plasmid induced with copper for the indicated times. Top rows, representative images in which puncta formation was first detected in the wild-type (18 h) and *atg1* (1 h) strains. Bottom rows, representative images in which ring- and ribbon-like aggregates, indicative of *de novo* prion formation, were detected in the wild-type (18 h) and *atg1* (12 h) strains. The percentage of cells containing visible puncta or ring- and ribbon-like aggregates is shown for each strain from an average of 300 cells counted. **(B)** Western blot analysis of the wild-type and

atg1 mutant strains after induction of the Sup35NM-GFP for 1, 8, 18, or 24 h. Blots were probed with αSup35 or α-Pgk1 as a loading control. **(C)** Fluorescence micrographs for cured versions of the wild-type and *atg1* mutant strains after induction of Sup35NM-GFP for 2 or 24 h. Representative images in which puncta were only detected in *atg1* mutant cells (3.6%) after 24-h induction. **(D)** [*PSI*$^+$] prion formation was quantified in the wild-type and *atg1* mutant strains containing the *CUP1-SUP35NM-GFP* plasmid after 0, 1, and 24 h of copper induction. [*PSI*$^+$] formation was quantified using the *ade1-14* mutant allele by growth on medium lacking adenine and differentiated from nuclear *SUPX* gene mutations by their irreversible elimination in GdnHCl. Data shown are the means of at least three independent biological repeat experiments expressed as the number of colonies per 10^4 viable cells. Error bars denote the standard deviation. Statistical analysis was performed by one-way ANOVA with pair-wise comparisons using Tukey HSD test comparing the [*PSI*$^+$] prion formation between the wild-type strain and the *atg1* mutant at 0, 1, and 24 h of induction ($^{n.s.}$not statistically significant, *p<0.01, **p<0.001). **(E)** Sup35 toxicity was examined in [*psi*$^-$] or [*PSI*$^+$] versions of the indicated strains containing SUP35 under the control of a *GAL* inducible promoter. Strains were initially grown overnight in raffinose-containing medium before dilution (A_{600} = 1, 0.1, 0.01, 0.001) and spotting onto agar plates containing galactose or glucose. Overexpression of Sup35 inhibits growth in the [*PSI*$^+$] versions of autophagy mutants compared with [*psi*$^-$] versions.

2.2.4 Inducing autophagy protects against *de novo* [*PSI*$^+$] prion formation.

Because loss of autophagy results in an increased frequency of prion formation, we examined whether inducing autophagy could protect *against de novo* [*PSI*$^+$] prion formation. This is difficult to examine in a wild-type strain, given the rare occurrence of spontaneous [*PSI*$^+$] prion formation. We therefore used mutants that are known to have an increased frequency of *de novo* [*PSI*$^+$] prion formation. This included a mutant lacking the Tsa1 and Tsa2 peroxiredoxins (Sideri et al, 2010). Peroxiredoxins are important cellular antioxidants, and oxidative damage to Sup35 is believed to trigger the formation of [*PSI*$^+$] prions in this mutant (Sideri et al, 2011). A number of factors that modify the frequency of [*PSI*$^+$] induction were identified in an unbiased genome-wide screen (Tyedmers et al, 2008). We used one such mutant identified in this screen that is deleted for *PPQ1* (*SAL6*), encoding a protein

phosphatase of unknown function. Ppq1 (Sal6) was originally identified as a mutant that increases the efficiency of translational suppressors, including nonsense suppressors (Vincent et al, 1994). Rather than affecting prion formation, this mutant presumably allows the detection of [*PSI*$^{+}$] strains that are normally too weak to detect. Using the *ura3-14 allele* plasmid assay, we found the frequency of *de novo* [*PSI*$^{+}$] prion formation to be elevated by approximately four-fold in a [*PIN*$^{+}$][*psi*$^{-}$] *tsa1 tsa2* mutant and by 20-fold in a [*PIN*$^{+}$][*psi*$^{-}$] *ppq1* mutant (Figure 2.5A). Autophagy can be stimulated by a number of pharmacological agents including the naturally occurring polyamine spermidine (Eisenberg et al, 2009; Morselli et al, 2011). Growth of the *tsa1 tsa2* and *ppq1* mutants in the presence of 4 mM spermidine significantly reduced the elevated frequency of *de novo* [*PSI*$^{+}$] prion formation normally observed in these mutants but not in an *atg1* mutant (Figure 2.5A).

A GFP-Atg8 construct was used as a control to confirm that spermidine induces autophagy in these mutants (Noda et al, 1995). This assay follows the autophagy-dependent proteolytic liberation of GFP from GFP-Atg8, which is indicative of autophagic flux. Free GFP was detected in the wild-type and *tsa1 tsa2* and *ppq1* mutant strains after spermidine treatment but not in the *atg1* mutant, which is defective in autophagy (Figure 2.5B). Of interest, low levels of free GFP were detected in the *tsa1 tsa2* and *ppq1* mutants in the absence of spermidine, suggesting that these mutants already have elevated basal levels of autophagy. Because *de novo* [*PIN*$^{+}$] formation occurs at a relatively high rate, we examined whether inducing autophagy with spermidine also protects against [*PIN*$^{+}$] formation. This analysis showed that spermidine reduces *de*

novo [*PIN*$^+$] formation from ~6% to <1% (Figure 2.5C). Spermidine treatment did not affect the elevated frequency of *de novo* [*PIN*$^+$] formation observed in an *atg1* mutant.

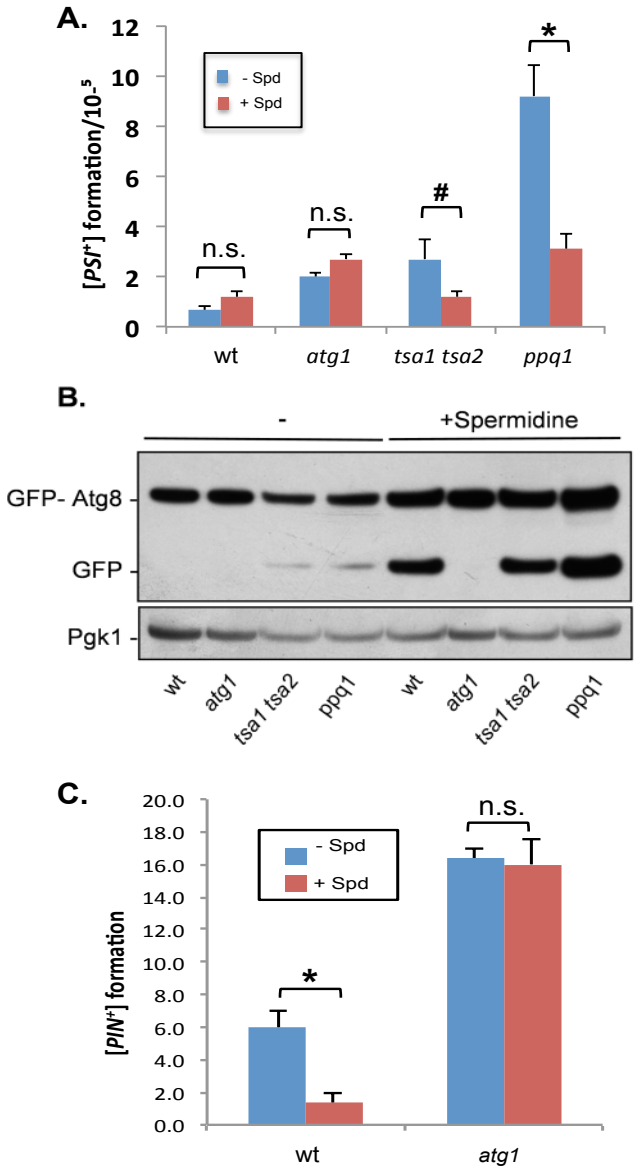

Figure 2.5: Inducing autophagy with spermidine protects against *de novo* [*PSI*$^+$] and [*PIN*$^+$] prion formation. (A) [*PSI*$^+$] prion formation was quantified in wild-type, *atg1, tsa1 tsa2* and *ppq1* mutant strains using an engineered *ura3-14* allele as described for Figure 2.3A. Autophagy was induced by growing cells in the presence of 4 mM spermidine (+ Spd). Data shown are the means of at least three independent biological repeat experiments. Error bars denote the standard deviation. Statistical analysis was performed by one-way ANOVA with pair-wise comparisons using Tukey HSD test comparing the [*PSI*$^+$] prion formation in the absence versus the presence of spermidine treatment in wild-type, *atg1, tsa1 tsa2* and *ppq1* mutant strains ($^{n.s.}$not statistically significant, *p<0.01, $^{\#}$p<0.05). **(B)** Autophagic flux was monitored in cells

expressing GFP-Atg8. Growth in the presence of spermidine induced autophagy in wild-type and *tsa1 tsa2* and *ppq1* mutant strains as detected by the appearance of free GFP indicative of autophagic flux. No free GFP was detected in an *atg1* mutant. **(C)** [*PIN*$^+$] prion formation was quantified in wild-type (Eisenberg et al, 2009) and *atg1* mutant cells as described for Figure 2.3C. Autophagy was induced by growing cells in the presence of 4 mM spermidine (+ Spd). Data shown are the means of at least three independent biological repeat experiments. Error bars denote the standard deviation. Statistical analysis was performed by one-way ANOVA with pair-wise comparisons using Tukey HSD test comparing the [*PIN*$^+$] prion formation in the absence versus the presence of spermidine treatment in wild-type strain and *atg1* mutant ($^{n.s.}$not statistically significant, *p<0.01).

2.2.5 Sup35 protein oxidation is increased in autophagy mutants.

To begin to address the mechanism by which prions form spontaneously in autophagy mutants, we examined whether the localization of [*PSI*$^+$] foci is altered in an autophagy mutant. Induced [*PSI*$^+$] prion formation is believed to proceed via targeted localization of misfolded Sup35 to the IPOD, which is formed adjacent to the vacuole (Tyedmers et al, 2010a; Sontag et al, 2014). The vacuolar dye FM4-64 was used to visualize vacuolar membranes in wild-type and *atg1* mutant strains (Figure 2.6A). This analysis revealed that similar vacuolar Sup35-GFP foci were detected in the wild-type and *atg1* mutant strains after copper induction of the Sup35NM-GFP (Figure 2.6A). We used CFP-ATG8 and CFP-ATG14 as markers of the preautophagosomal structure (PAS) in wild-type and *atg1* mutant strains (Figure 2.6B). Similar to previous reports (Tyedmers et al, 2010a), we observed that Sup35-GFP foci formed adjacent to these PAS markers. Similar Sup35-GFP foci were formed in the *atg1* mutant despite the absence of PAS formation. Thus, although an *atg1* mutant is deficient in macroautophagy and the recruitment of additional Atg proteins to the PAS (Parzych and Klionsky, 2014), Sup35 is still targeted to the vacuolar membrane.

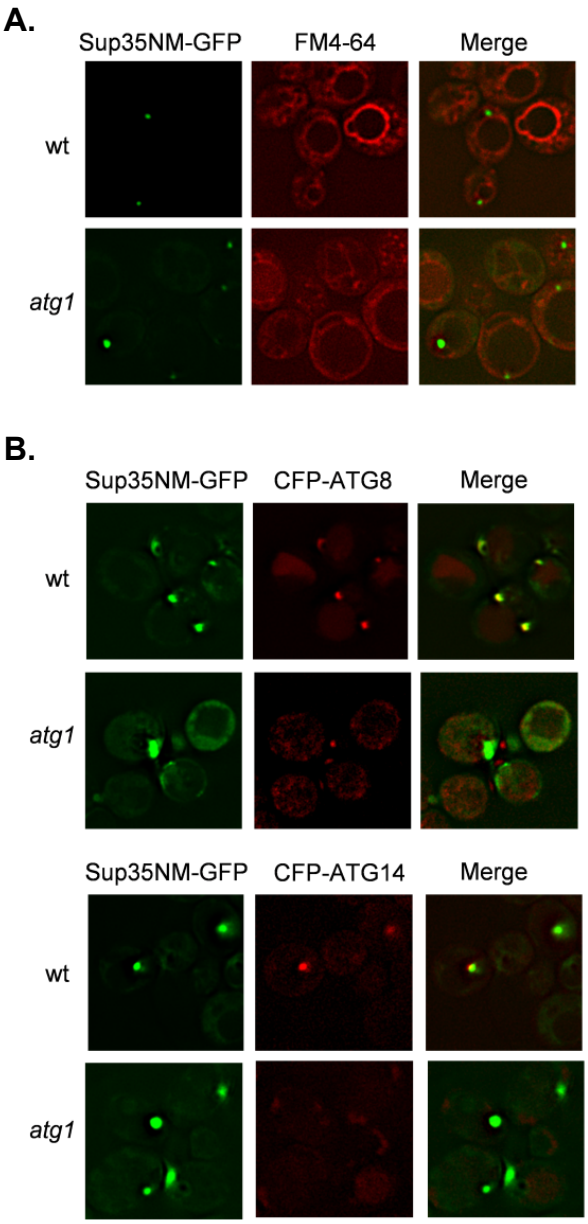

Figure 2.6: Sup35 aggregate formation occurs at similar intracellular sites in wild-type and *atg1* mutant strains. (A) The vacuolar dye FM4-64 was used to visualize vacuolar membranes in wild-type and *atg1* mutant strains. Similar vacuolar Sup35-GFP foci were detected in the wild-type and *atg1* mutant strains after copper induction of the *CUP1-SUP35NM-GFP* plasmid for 1 h. **(B)** CFP-ATG8 and CFP-ATG14 were used as markers of PAS in wild-type and *atg1* mutant strains. Strains were grown for 48 h in the presence of 4 mM spermidine to induce autophagy and Sup35NM-GFP induced with copper for 1 h. Sup35 aggregates form adjacent to PAS markers in the wild-type strain.

Given that vacuolar targeting of Sup35 appears to be unaffected in an *atg1* mutant, we next examined whether oxidatively damaged Sup35 accumulates in an autophagy mutant, which might trigger [*PSI*$^+$] prion formation. This is because oxidative damage to Sup35 is believed to be one possible cause of the initial misfolding event that triggers the formation of the [*PSI*$^+$] prion in yeast (Sideri et al, 2011). We previously showed that loss of antioxidants results in elevated levels of Sup35 methionine oxidation and [*PSI*$^+$] prion formation, suggesting that endogenous levels of reactive oxygen species (ROS) are sufficient to promote prion formation (Sideri et al, 2011). We reasoned that if autophagy acts to suppress prion formation by removing oxidatively damaged Sup35, we might detect oxidized Sup35 in an autophagy mutant. Sup35 oxidation was measured by immunoblot analysis using an antibody that recognizes methionine sulfoxide (MetO). No MetO was detected in a wild-type strain grown under nonstress conditions, but MetO was detected after exposure to 1 mM hydrogen peroxide for 1 h (Figure 2.7A). Formation of MetO was also detected in the *tsa1 tsa2* mutant, as previously reported (Sideri et al, 2011). In addition, MetO formation was detected in an *atg1* mutant in the absence of oxidative stress, suggesting that autophagy normally functions to remove oxidatively damaged Sup35 that forms during normal growth conditions and endogenous ROS exposure.

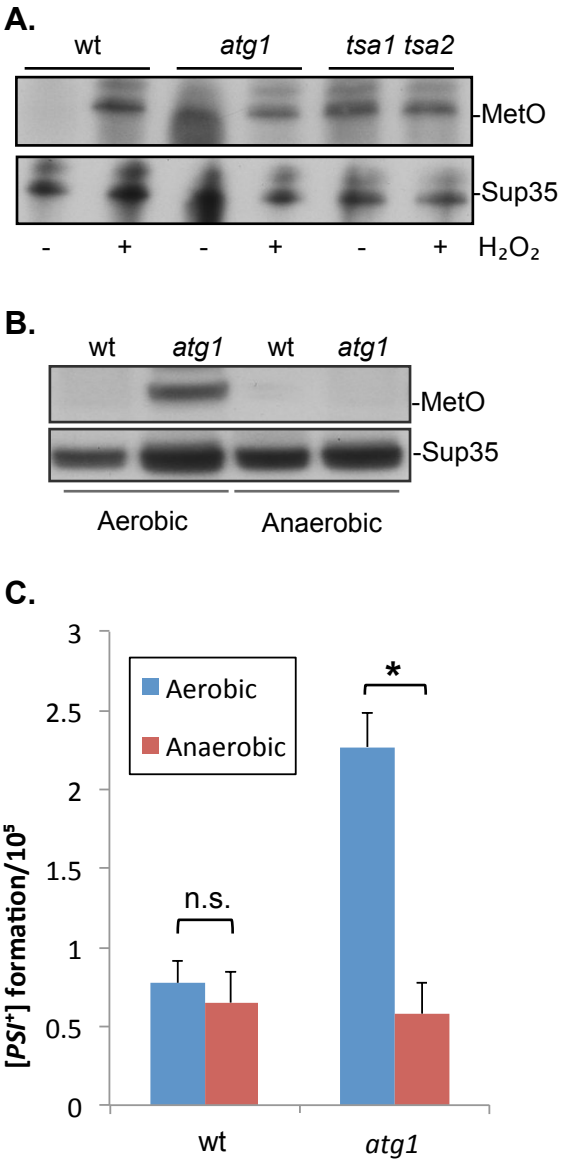

Figure 2.7: Oxidation of Sup35 in an *atg1* mutant causes [*PSI*$^+$] prion formation. **(A)** Sup35 was affinity purified using TAP chromatography from wild-type and *atg1* and *tsa1 tsa2* mutant strains. Western blots were probed with anti-PAP (peroxidase anti-peroxidase) to confirm that similar amounts of Sup35 were purified from each strain. Sup35 oxidation was detected using antibodies that recognize MetO. Strains were treated with 1 mM hydrogen peroxide where indicated. **(B)** Sup35 methionine oxidation was detected in wild-type and *atg1* mutant strains grown under aerobic versus anaerobic conditions. Western blots were probed with anti-Sup35 to confirm that similar amounts of Sup35 were purified from each strain. **(C)** [*PSI*$^+$] prion formation was quantified in wild-type and *atg1* mutant strains after growth under aerobic or anaerobic conditions. Data shown are the means of at least three independent biological repeat experiments. Error bars denote the standard deviation. Statistical analysis was performed by one-way ANOVA with pair-wise comparisons using Tukey HSD test comparing the [*PSI*$^+$] prion formation under aerobic versus anaerobic conditions in wild-type strain and *atg1* mutant ($^{n.s.}$not statistically significant, *p<0.01).

Given that oxidatively damaged Sup35 accumulates in an *atg1* mutant, we examined whether oxidative damage underlies the increased frequency of [*PSI*$^{+}$] prion formation in an autophagy mutant. The [*PIN*$^{+}$][*psi*$^{-}$] versions of the wild-type and *atg1* mutant strains were grown under aerobic or anaerobic conditions in the absence of molecular oxygen. Examination of Sup35 methionine oxidation revealed that no MetO was detected in the *atg1* mutant after growth under anaerobic conditions (Figure 2.7B). Under aerobic conditions, the frequency of [*PSI*$^{+}$] prion formation was elevated by approximately threefold, whereas no increased [*PSI*$^{+}$] prion formation was detected in the *atg1* mutant grown under anaerobic conditions (Figure 2.7C). These data indicate that oxidative growth conditions are required for the increased frequency of prion formation in an autophagy mutant.

2.3 DISCUSSION

Prions form spontaneously without any underlying genetic change. The emergence of disease correlates with the appearance of PrP^{Sc}, a novel conformational form of the cellular PrP^{C} protein. This prion form replicates through a cycle of seeded polymerization and fragmentation, and it is assumed that genetic or environmental factors can trigger the conformational change in the absence of any preexisting PrP^{Sc} “seeds” (Collinge and Clarke, 2007). However, the exact mechanisms underlying the switch from a normally soluble protein to the amyloid form are poorly understood. Prions cause many neurodegenerative diseases, including Alzheimer’s, Parkinson’s, and Creutzfeldt-Jakob diseases and amyotrophic lateral sclerosis. Most cases of these human diseases are sporadic (Prusiner 2013). It is therefore important to establish the conditions that trigger the switch to the prion or disease-causing

form. Our data indicate that autophagy is required to suppress *de novo* formation of the yeast [*PSI*$^+$] and [*PIN*$^+$] prions.

Mutants lacking several different core and associated autophagy components were found to elevate prion formation. In contrast, mutants lacking *ATG11* or *ATG32,* which are deficient in pexophagy and mitophagy, respectively, were unaffected in aggregate formation. Mutants lacking *ATG19* also displayed increased spontaneous aggregate formation. This was somewhat unexpected because Atg19 is believed to function as an essential component of the cytoplasm-to-vacuole targeting pathway (Cvt) rather than in nonselective autophagy (Xie and Klionsky, 2007). However, there is some evidence for a role for Atg19 in the degradation of an ER-associated degradation substrate (Mazon et al, 2007). Atg19 is required for the efficient degradation of Pma1 in a process that also requires the UPS. It is unclear whether Sup35 may act as a substrate of the Cvt pathway or whether Sup35 aggregation and [*PSI*$^+$] prion formation are indirect effects of loss of Atg19. This does not appear to arise specifically due to loss of the Cvt pathway, since Sup35 aggregation and [*PSI*$^+$] prion formation are unaffected in a mutant lacking Atg11, which functions as an adapter protein required for cargo loading in pexophagy and the Cvt pathway.

The frequency of *de novo* [*PSI*$^+$] formation is relatively low in a wild-type strain ($\sim 1 \times 10^{-5}$) and is elevated by approximately twofold to threefold in mutants lacking *ATG1*, *ATG8*, or *ATG19.* In contrast, Sup35NM-GFP aggregate formation was detected in ~4–5% of cells examined for the same autophagy mutants. This suggests that not all cells with fluorescent aggregates correspond

to true [*PSI*$^{+}$] formation. It has long been known that not all SUP35-GFP aggregates will give rise to prions. For example, previous studies suggested that about half of cells with fluorescent dots will die. Some of the rest contain nonproductive (e.g., nonamyloid) aggregates (Arslan et al, 2015). Thus, whereas overexpressing SUP35-GFP provides a way to look for the general propensity to promote aggregate formation, it does not distinguish among aggregates that will be dissolved/cleared by autophagy, the ones that will kill the cell, and the ones that will give rise to [*PSI*$^{+}$]. Our quantitative assay specifically quantifies "classical" PIN-dependent [*PSI*$^{+}$] formation, that is, prions that are capable of propagation and strong enough to give rise to viable colonies. [*PSI*$^{+}$] formation is strongly induced in response to copper addition, as expected. This induction is stronger in the *atg1* mutant than in the wild-type strain, confirming that autophagy suppresses induced [*PSI*$^{+}$] prion formation. Furthermore, taking the wild-type strain as an example, these experiments confirm that the frequency of true [*PSI*$^{+}$] formation (1.2×10^{-4}) is much lower than the number of cells containing visible Sup35-GFP aggregates (4.7×10^{-2}).

Sup35 containing oxidized methionine (MetO) was detected in the *atg1* mutant, which appears to underlie the increased frequency of [*PSI*$^{+}$] prion formation in this mutant. Increasing evidence suggests a causal link between protein oxidation and *de novo* prion formation (Grant, 2015). For example, oxidized methionine residues detected in misfolded PrP^{Sc} have been proposed to facilitate the structural conversion underlying the sporadic formation of PrP^{Sc} (DeMarco and Daggett, 2005; Wolschner et al, 2009; Elmallah et al, 2013).

Similarly, we showed that methionine oxidation of Sup35 in a range of yeast antioxidant mutants underlies the switch from a soluble form of the protein to the [*PSI*$^+$] prion (Sideri et al, 2011; Doronina et al, 2015). Abrogating methionine oxidation in antioxidant mutants prevents [*PSI*$^+$] formation, suggesting that protein oxidation may be a common mechanism underlying the aggregation of both mammalian and yeast amyloidogenic proteins (Sideri et al, 2011; Doronina et al, 2015). Similar increases in the levels of Met-SO formation were detected in *tsa1 tsa2* and *atg1* mutant strains and in a wild-type strain exposed to hydrogen peroxide. Note that the immunoblots used to detect Met-SO levels do not provide a quantitative measure of methionine oxidation, but the detection of oxidized methionine has been shown to correlate with elevated frequencies of [*PSI*$^+$] formation (Doronina et al, 2015). We do not know why MetO formation appears to decrease in *atg1* mutant cells after oxidative stress conditions. It is possible that the excess accumulation of oxidized proteins that might arise from the combination of oxidative stress and the loss of *atg1* is toxic to cells, or, alternatively, other protein degradation or aggregate-clearing systems may become active under these conditions. We suggest that autophagy normally functions to remove oxidized Sup35 from cells, but in the absence of autophagy, misfolded Sup35 undergoes structural transitions favoring its conversion to the propagatable [*PSI*$^+$] form. In agreement with this idea, growth under anaerobic conditions abrogated both methionine oxidation and the increased frequency of [*PSI*$^+$] formation in an *atg1* mutant.

Met-SO was detected in Sup35 in an *atg1* mutant grown under normal conditions in the absence of any added oxidant. This suggests that endogenous

ROS levels are sufficient to damage Sup35 but that autophagy normally functions to remove damaged Sup35, preventing [*PSI*$^+$] formation. The frequency of prion formation was lower in the *atg1* mutant than in antioxidant mutants under the same growth conditions. This presumably reflects the higher levels of endogenous ROS that are formed in the absence of antioxidants. A significant proportion of newly synthesized proteins are known to be misfolded, and this is exacerbated by conditions that promote further unfolding, such as oxidative stress (Hohn et al, 2014). Oxidized proteins are often nonfunctional and must be removed by degradation to prevent aggregate formation. The UPS and autophagy are the major routes of clearance for toxic proteins. The UPS is believed to mainly degrade short-lived proteins, whereas autophagy degrades high–molecular weight protein aggregates commonly seen in neurodegenerative disorders. Not surprisingly, therefore, dysregulation of autophagy has been implicated in the pathogenesis of neurodegenerative disorders, since aggregate-prone are eliminated more efficiently via the autophagy pathway than the UPS (Banerjee et al, 2010; Lynch-Day et al, 2012). Sup35 has been shown to be a proteasomal substrate, and proteasomal activity has been demonstrated to influence [*PSI*$^+$] propagation (Kabani et al, 2014). The proteasome was found to degrade highly ordered prion protein assemblies in a manner that does not require ubiquitination. It therefore seems likely that the UPS and autophagy provide overlapping defense systems to protect against prion formation and propagation.

It is difficult to model sporadic prion formation without overexpressing the corresponding protein. We used mutants that display an elevated frequency of [*PSI*$^+$] prion formation without any underlying effect on Sup35 protein levels to

test whether increasing autophagic flux could protect against prion formation. The elevated frequency of [*PSI*$^{+}$] prion formation was abrogated in a *tsa1 tsa2* mutant after induction of autophagy using spermidine. This does not simply reflect the role of autophagy in the turnover of oxidized proteins, since [*PSI*$^{+}$] prion formation was also reduced in a *ppq1* mutant that is not involved in the oxidative stress response. The nature of the misfolded intermediate in a *ppq1* mutant is unknown but is presumably normally removed via autophagy to prevent prion formation. Enhancing autophagy has also been shown to reduce toxicity in Huntington's disease models (Sarkar et al, 2007), suggesting that pharmacological agents that increase autophagic flux may represent a promising therapeutic route toward protecting against amyloid formation and toxicity

The role of autophagy in preventing prion formation and toxicity appears evolutionarily conserved. Previous studies established the importance of autophagy for delivery of PrP^{Sc} to lysosomes for degradation in chronically infected cells (Heiseke et al, 2010; Goold et al, 2013). Similarly, inhibitors of autophagy result in increased levels of PrP^{Sc}, and stimulating autophagy decreases PrP^{Sc} levels (Aguib et al, 2009; Heiseke et al, 2009; Goold et al, 2013; Homma et al, 2014; Joshi-Barr et al, 2014). Autophagy also appears to be stimulated in response to the *de novo* accumulation of prion aggregates, which may act to clear PrP^{Sc}. For example, PrP^{C} accumulates as ubiquitinated intracellular protein inclusions, which causes induction of endoplasmic reticulum chaperones, the unfolded protein response, and autophagy in a mouse model of prion disease (Joshi-Barr et al, 2014). It is interesting, therefore, that the

basal levels of autophagy were also somewhat elevated in the *ppq1* and *tsa1 tsa2* mutants, which show an elevated frequency of [*PSI*$^{+}$] prion formation. Yeast therefore provides a powerful genetic system to further establish and identify the protective systems that protect against the spontaneous formation of prions.

2.4 MATERIALS AND METHODS

2.4.1 Yeast strains and plasmids.

The wild-type yeast strain 74D-694 (*MATa ade1-14 ura3-52 leu2-3, 112 trp1-289 his3-200*) was used for all experiments. Strains deleted for autophagy genes were constructed in 74D-694 using standard yeast methodology. Sup35 was tagged at its C-terminus with a tandem affinity purification (TAP) tag and was described previously (Sideri et al, 2011). Sup35 was overexpressed using an inducible *GAL1-SUP35* plasmid (Josse et al, 2012). Plasmids expressing CFP-ATG8 and CFP-ATG14 were described previously (Tyedmers et al, 2010a).

2.4.2 Growth and stress conditions.

Strains were grown at 30°C with shaking at 180 rpm in rich YEPD medium (2% [weight/volume] glucose, 2% [weight/volume] bactopeptone, 1% [weight/volume] yeast extract) or minimal SD (0.67% [weight/volume] yeast nitrogen base without amino acids, 2% [weight/volume] glucose) supplemented with appropriate amino acids and bases. SGal media contained 2% (weight/volume) galactose, and SRaf media contained 2% (weight/volume) raffinose in place of glucose. Media were solidified by the addition of 2% (weight/volume) agar. Strains were cured by five rounds of growth on YEPD agar plates containing 4 mM GdnHCl. Anaerobic growth conditions were

established by degassing media with nitrogen gas as previously described (Beckhouse et al, 2008).

2.4.3 Analyses of prion formation.

A plasmid containing an engineered *ura3-14* allele, which contains the *ade1-14* nonsense mutation in the wild-type *URA3* gene (Manogaran et al, 2006), was used to score the frequency of *de novo* [*PSI*$^{+}$] prion formation as previously described. Alternatively, [*PSI*$^{+}$] prion formation was scored by growth in absence of adenine. *De novo* [*PIN*$^{+}$] formation was performed as previously described (Sideri et al, 2011). [*PSI*$^{+}$] and [*PIN*$^{+}$] formation was calculated based on the mean of at least three independent biological repeat experiments. *De novo* [*PSI*$^{+}$] prion formation was visualized as described previously using *CUP1-SUP35NM-GFP* (Sideri et al, 2011). The number of cells containing Sup35 puncta was quantified from ~300 cells counted.

2.4.4 Protein analysis.

The analysis of Sup35 amyloid polymers by SDD-AGE was performed as described previously (Alberti et al, 2010). Sup35-TAP affinity purification and detection of methionine oxidation were performed as described previously (Sideri et al, 2011).

2.4.5 Autophagy analysis and induction.

Autophagy was induced by growth in the presence of 4 mM spermidine (Eisenberg et al, 2009). The induction of autophagy was confirmed by examining the release of free GFP due to the proteolytic cleavage of GFP-Atg8 using a plasmid described previously (Noda et al, 1995).

2.4.6 Statistical analysis

Data are presented as mean values ± standard deviation (SD). Statistical analysis for multiple groups was performed using one-way ANOVA with pair-wise comparisons of sample means via the Tukey HSD test. Results were considered statistically significant with a p-value less than 0.05.

2.5 ACKNOWLEDGMENTS.

S.H.S. was supported by a Wellcome Trust funded studentship. V.A.D. was supported by Biotechnology and Biological Sciences Research Council Project Grant BB/J000183/1. We thank Susan Lindquist for the CFP-ATG8 and CFP-ATG14 plasmids. The Bioimaging Facility microscopes used in this study were purchased with grants from the Biotechnology and Biological Sciences Research Council, Wellcome Trust, and University of Manchester Strategic Fund.

Chapter 3: Spermidine cures yeast of prions.

Shaun H. Speldewinde and Chris M. Grant*

University of Manchester, Faculty of Life Sciences, The Michael Smith Building, Oxford Road, Manchester, M13 9PT, UK.

*Address correspondence to: Chris M. Grant, The University of Manchester, Faculty of Life Sciences, The Michael Smith Building, Oxford Road, Manchester, M13 9PT, UK. Phone: (0161) 306 4192; Email: chris.grant@manchester.ac.uk

With supervision from Prof Chris M. Grant, the author has designed the experiment, generated all the figures presented in this chapter, and wrote the manuscript.

3.1 Micro-review:

Prions are self-perpetuating amyloid protein aggregates which underlie various neurodegenerative diseases in mammals. The molecular basis underlying their conversion from a normally soluble protein into the prion form remains largely unknown. Studies aimed at uncovering these mechanism(s) are therefore essential if we are to develop effective therapeutic strategies to counteract these disease-causing entities. Autophagy is a cellular degradation system which has predominantly been considered as a non-selective bulk degradation process which recycles macromolecules in response to starvation conditions. We now know that autophagy also serves as a protein quality control mechanism which selectively degrades protein aggregates and damaged organelles. These are commonly accumulated in various neurodegenerative disorders including prion diseases. In our recent study [Speldewinde et al.,(2015)], we used the well-established yeast [*PSI*$^{+}$]/Sup35 and [*PIN*$^{+}$]/Rnq1 prion models to show that autophagy prevents sporadic prion formation. Importantly, we found that spermidine, a polyamine that has been used to increase autophagic flux, acts as a protective agent which prevents spontaneous prion formation.

The molecular basis by which prions arise spontaneously is poorly understood. Our data indicate that oxidative protein damage to Sup35, which is a known trigger for *de novo* prion formation, is normally suppressed by autophagy. Oxidatively damaged Sup35 was found to accumulate in mutants lacking core components of the autophagy pathway, and this was found to correlate with an increased frequency of *de novo* [*PSI*$^{+}$] prion formation. We showed that growth under anaerobic conditions in the absence of molecular

oxygen prevented the accumulation of oxidized Sup35 and abrogated the high frequency of [*PSI*$^+$] formation in an autophagy mutant. This suggests that autophagy normally functions to clear oxidatively damaged proteins prior to their conversion to the prion form. A protective role for autophagy in preventing *de novo* prion formation was further confirmed by showing that increasing autophagic flux by treatment with spermidine abrogates the formation of prions in mutants which normally show high rates of *de novo* prion formation. This important new finding strongly implicates autophagy as a defense system which protects against oxidative damage of the non-prion form of a protein. This is an important trigger for the formation of the heritable prion conformation, an event that has also been implicated in the formation of mammalian prions.

Our study highlights the potential use for autophagy-inducing agents such as spermidine in the prevention of the very early stages of spontaneous prion formation i.e. effectively acting as a prion prevention agent (Figure 3.1). By improving the clearance of damaged/misfolded proteins, there is less possibility for these abnormal proteins to accumulate and to act as nucleation sites catalyzing the aggregation of other damaged proteins. Polyamines such as spermidine are polycations which play multiple roles in cell growth, proliferation and longevity. Their beneficial effects in prolonging lifespan are thought to be mediated by increasing autophagic flux. Spermidine inhibits histone acetylases and the resulting alterations in the acetylproteome increases the transcription of different autophagy-related genes (Figure 3.1). More work will be required to determine whether the abrogation of prion formation by spermidine solely depends on increasing autophagic flux, or whether spermidine additionally promotes other stress protective pathways. For

example, spermidine supplementation has been linked with increased stress tolerance including heat and oxidative stress, which is not only mediated by increasing autophagic flux. Whether spermidine modulates the expression of other stress responsive genes, such as heat shock and antioxidant genes which are known to influence protein misfolding and prion formation, has not been fully established. Hence, spermidine may ameliorate prion formation via multiple mechanisms including the induction of autophagy and other stress-related pathways.

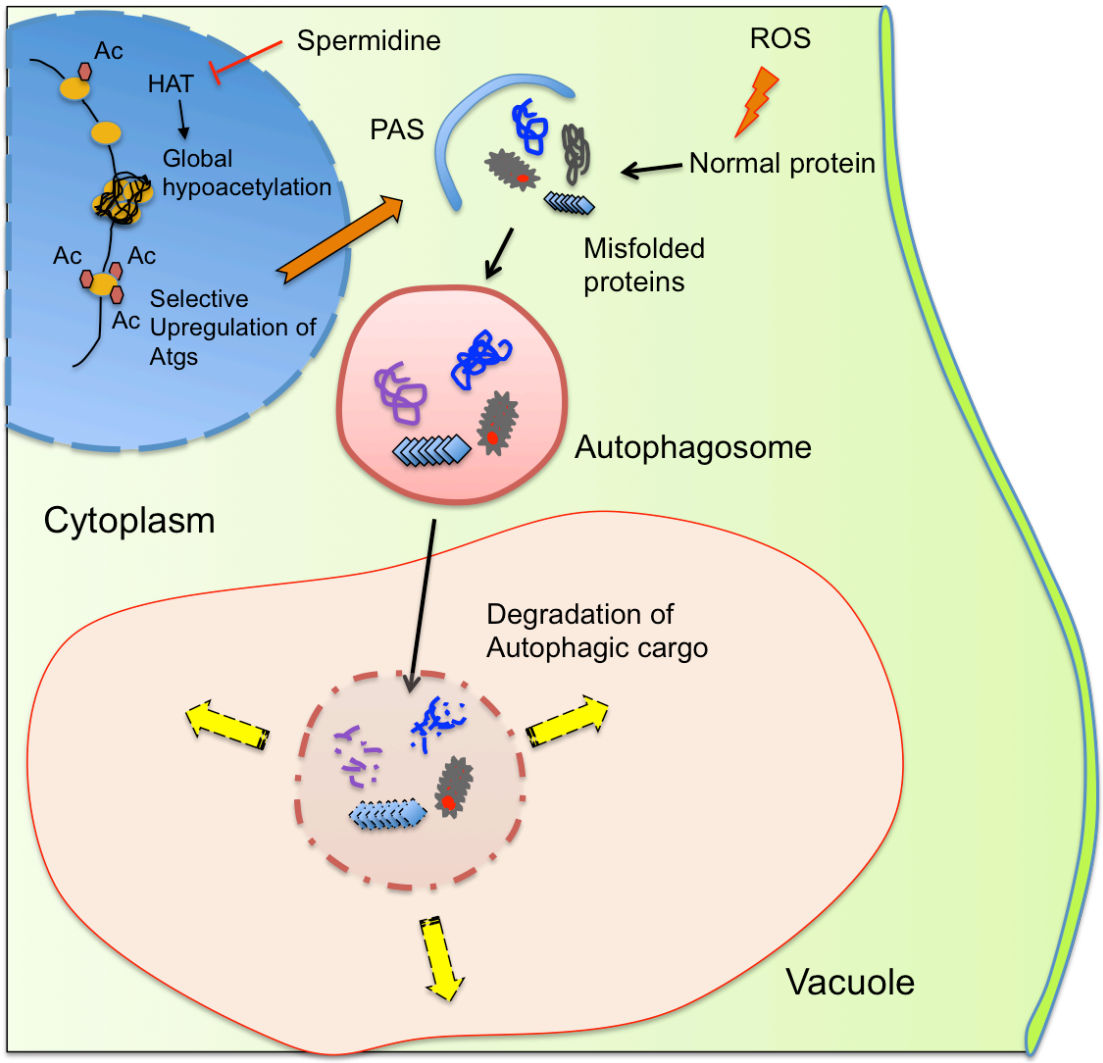

Figure 3.1: Model illustrating the cytoprotective action of spermidine in preventing spontaneous prion formation. Spermidine inhibits the activity of histone acetyl transferases (HATs) that function to insert acetyl (Ac) groups on histone H3. This causes global gene silencing, but certain genes including autophagy-related genes (Atgs) remain acetylated thus inducing autophagic activity. Reactive oxygen species (ROS), whether endogenous or exogenous, may damage soluble proteins leading to their misfolding/aggregation. These abnormal proteins can be encapsulated by the pre-autophagosomal structure (PAS), which then fully matures into an autophagosome. The autophagosome with its cargo fuses with the vacuole where resident hydrolases can degrade the cargo and the resultant products can be channelled for biosynthesis or for energy generation. Inducing autophagy by spermidine treatment prevents prion formation by removing misfolded/oxidized proteins prior to their conversion to the prion form.

Recent data from our lab, which was not included in the original publication, demonstrates that spermidine treatment can also promote the clearance of Sup35 aggregates from cells in an autophagy-dependent manner

(Figure 3.2). We used a Sup35NM-GFP fusion construct to visualize Sup35 aggregate formation in [*PSI*$^{+}$]-versions of wild-type and *atg1* mutant strains. Following short-term induction of the Sup35NM-GFP fusion construct, fluorescent foci can be detected due to the coalescence of newly made Sup35NM-GFP with pre-existing Sup35 aggregates. Fluorescent Sup35 aggregates are normally visible in approximately 70% of [*PSI*$^{+}$] cells examined (Figure 3.2). We found that spermidine treatment reduced this number such that visible Sup35 aggregates are only detected in approximately 25% of cells. This did not occur in an *atg1* mutant confirming the requirement for an active autophagy pathway to clear aggregates in response to spermidine treatment (Figure 3.2). This experiment suggests that increasing autophagic flux via spermidine treatment, not only promotes the removal of smaller misfolded/oxidized Sup35 proteins, but can also promote the removal of larger molecular weight Sup35 aggregates which are already formed within cells. It should be emphasized that visible Sup35-GFP aggregates do not necessarily correspond to the number of true heritable [*PSI*$^{+}$] aggregates in cells and more work will be required to examine whether spermidine treatment can really cure cells of the [*PSI*$^{+}$] prion. This may be unlikely though, since the presence of only a few low molecular weight Sup35 propagons will be inherited by daughter cells resulting in [*PSI*$^{+}$] prion transmission. However spermidine may well be beneficial in the treatment of other non-heritable and amorphous protein aggregate diseases.

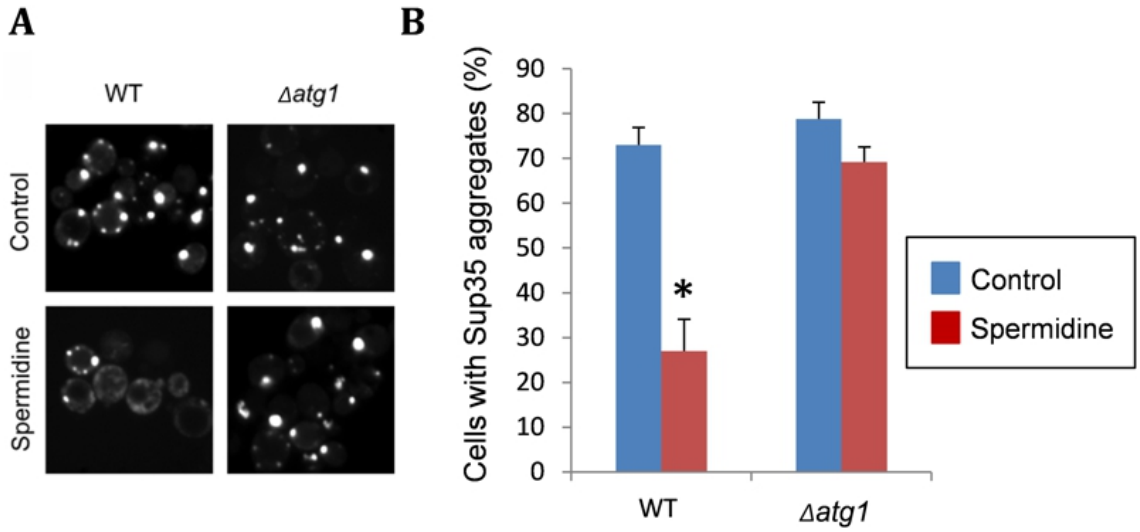

Figure 3.2: Spermidine treatment decreases the number of cells with visible Sup35 fluorescent aggregates. (A) Representative fluorescence micrographs are shown for [*PIN*$^+$][*PSI*$^+$] versions of the wild-type yeast strain 74D-694 (*MATa ade1-14 ura3-52 leu2-3,112 trp1-289 his3-200)* and an isogenic *atg1* mutant containing the *CUP1-SUP35NM-GFP* plasmid. Strains were grown in minimal media in the presence or absence of 4 mM spermidine for 48 hours to induce autophagy. Sup35NM-GFP was induced with copper for one hour. Following copper induction, fluorescent foci can be detected due to the coalescence of newly made Sup35NM-GFP with pre-existing Sup35 aggregates. **(B)** The percentage of cells containing visible puncta is shown for each strain from an average of 300 cells counted. Data shown are the means of three independent biological repeat experiments ± standard deviation. The number of visible aggregates in the wild-type strain treated with spermidine is significantly different to the number of aggregates detected in the same strain in the absence of spermidine (*p = <0.001).

Polyamines, such as spermidine, are present in millimolar quantities within all eukaryotic cells. They play essential roles in a multitude of cellular processes related to cell growth, proliferation and metabolism. Spermidine is a naturally occurring polyamine and rich dietary sources include soy products, legumes, corn, and whole grain cereals. The cellular levels of polyamines, such as spermidine, decline with age and have been linked to lifespan and age-

related disorders. Supplementation of spermidine into dietary regimes may therefore have added benefits for cellular health and healthy ageing. Relative to other established pharmacological inducers of autophagy, such as rapamycin and resveratrol, spermidine can be readily obtained from dietary sources and does not exhibit deleterious side effects. This places spermidine as a promising therapeutic agent for the prevention and amelioration of protein homeostasis and related aggregation diseases.

3.2 ACKNOWLEDGEMENTS

S.H.S. was supported by a Wellcome Trust funded studentship.

Chapter 4: The yeast [*PSI*$^{+}$] prion improves chronological ageing in autophagy competent cells.

Shaun H. Speldewinde and Chris M. Grant*

University of Manchester, Faculty of Life Sciences, The Michael Smith Building, Oxford Road, Manchester, M13 9PT, UK.

*Address correspondence to: Chris M. Grant, The University of Manchester, Faculty of Life Sciences, The Michael Smith Building, Oxford Road, Manchester, M13 9PT, UK. Phone: (0161) 306 4192; Email: chris.grant@manchester.ac.uk

With supervision from Prof Chris M. Grant, the author has designed the experiments, generated all the figures presented in this chapter, and wrote the manuscript.

Abstract:

Ageing is the time-dependent decline of a variety of intracellular mechanisms, and is associated with an increased sensitivity to environmental stresses and cellular senescence. Yeast has emerged as a powerful model organism to study ageing via the replicative lifespan model and the chronological ageing model. Prions are infectious, self-templating abnormal proteins responsible for several neurodegenerative diseases in mammals and several prion-forming proteins have been found in yeast. One such protein is the yeast [*PSI*$^{+}$], the prion form of the Sup35 translation termination factor. Our study focused on the effect of different prion status on chronological ageing in wild-type cells and in an autophagy-defective *atg1* mutant. We found an age-dependent increase in the *de novo* formation of [*PSI*$^{+}$] during chronological ageing, which is exacerbated in the *atg1* mutant. Relative to cells without [*PSI*$^{+}$], wild-type cells carrying [*PSI*$^{+}$] in normal media had improved chronological lifespan through an enhancement in autophagic flux. Cells with [*PSI*$^{+}$] also had a modest increase in protein aggregation that may also serve to facilitate autophagy. Thus the [*PSI*$^{+}$] prion may exert potentially beneficial effects on chronological lifespan via the promotion of autophagic activity.

4.1 INTRODUCTION

Biological ageing involves a progressive decline in the ability of an organism to survive stress and disease. It is a complex process which is influenced by both genetic and environmental factors (Kenyon, 2010). Common features of ageing include decreased resistance to stress, increased rates of apoptosis, a decline in autophagy and an elevated accumulation of protein aggregates (Levine and Kroemer, 2008; Lopez-Otin et al, 2013). In humans, ageing correlates with an increased frequency of age-related diseases including heart disease, metabolic syndromes and neurodegenerative diseases such as Alzheimer's, Parkinson's and dementia (Cherra and Chu, 2008; Rubinsztein et al, 2011)

Prions are aberrant infectious proteins which can self-replicate (Prusiner, 1998). They are causally responsible for transmissible spongiform encephalopathies that cause several incurable neurodegenerative diseases in mammals (Aguzzi and O'Connor, 2010). The underlying cause of TSEs is the structural conversion of a soluble prion protein (PrP^{C}) into a prion form (PrP^{Sc}) that is amylodogenic. The amyloid form of the prion protein can subsequently convert other soluble molecules into the prion form thus resulting in the accumulation of the aberrant protein specifically in neuronal cells (Collinge and Clarke, 2007; Prusiner, 2013). Human prion diseases are predominantly sporadic constituting approximately 70% of all cases with higher frequencies occurring during advanced age (Appleby and Lyketsos, 2011). There are several prion-forming proteins in yeast with the best-characterized being [*PSI*$^{+}$] and [*PIN*$^{+}$], which are formed from the Sup35 and Rnq1 proteins, respectively (Wickner, 1994; Derkatch et al, 1997). [*PSI*$^{+}$] is the altered conformation of the Sup35 protein, which normally functions as a translation termination factor

during protein synthesis. The *de novo* formation of [*PSI*$^{+}$] is enhanced by the presence of the [*PIN*$^{+}$] prion, which is the altered form of the Rnq1 protein whose native protein function is unknown (Treusch and Lindquist, 2012).

We have previously shown that autophagy protects against Sup35 aggregation and *de novo* [*PSI*$^{+}$] prion formation (Speldewinde et al, 2015). Autophagy is an intracellular quality control pathway that degrades damaged organelles and protein aggregates via vacuolar/lysosomal degradation (Parzych and Klionsky, 2014). It proceeds in a highly sequential manner leading to the formation of a double-membrane-bound vesicle called the 'autophagosome'. Fusion of the autophagosome with vacuoles/lysosomes introduces acidic hydrolases that degrade the contained proteins and organelles. Autophagy has been implicated in the ageing process and for example, autophagy is essential for calorie-restriction dependent chronological lifespan in yeast (Alvers et al, 2009a). Additionally, pharmacological interventions which induce autophagy result in lifespan extension during yeast chronological ageing (Alvers et al, 2009b; Eisenberg et al, 2009). Autophagy appears to play a protective role in the ageing process since dysregulated autophagy is implicated in the accumulation of abnormal proteins associated with several age-related diseases including Alzheimer's, Parkinson's and Huntington's diseases (Hara et al, 2006; Komatsu et al, 2006; Rubinsztein et al, 2011).

Yeast cells have been increasingly used as a model of ageing and have significantly contributed to our understanding of numerous conserved ageing genes and signalling pathways (Ocampo and Barrientos, 2011). Yeast cells can survive for prolonged periods of time in culture and have been used as a model of the chronological life span (CLS) of mammals, particularly for tissues composed of non-dividing populations (Kaeberlein, 2010; Longo et al, 2012).

Studies using this model have identified many key conserved ageing factors that modulate ageing. Additionally, ageing is followed by replicative lifespan, which is defined as the number of budding daughter cells that originates from a particular mother yeast cell before it reaches senescence (Mortimer and Johnston, 1959; Wasko and Kaeberlein, 2014). Given that amyloidoses are typically diseases of old-age, yeast prions might be expected to form at a higher frequency in ageing yeast cells. However, one study using the yeast replicative ageing model found that ageing does not increase the frequency of prion formation (Shewmaker and Wickner, 2006). In this current study we have examined [*PSI*$^{+}$] prion formation using the yeast CLS model and found that the frequency of prion formation is increased during ageing. Furthermore, this frequency is elevated in an autophagy mutant suggesting that autophagy normally acts to suppress age-dependent prion formation. We show that the prion-status of cells influences CLS in an autophagy-dependent manner suggesting that prions can be beneficial in aged populations of yeast cells.

4.2 RESULTS

4.2.1 The frequency of *de novo* [*PSI*$^+$] formation increases during chronological ageing.

In the yeast CLS model, populations of stationary phase cells are maintained in liquid culture and various physiological parameters, such as viability, replication ability and metabolism, measured over time. We examined CLS to determine whether there is an increased frequency of [*PSI*$^+$] appearance during ageing. Cultures were grown to stationary phase in liquid SCD (synthetic complete dextrose) media and prion formation measured over time. [*PSI*$^+$] prion formation was quantified using the *ade1-14* mutant allele which confers adenine auxotrophy and prions differentiated from nuclear *SUPX* gene mutations by their irreversible elimination in guanidine hydrochloride (GdnHCl). The frequency of *de novo* [*PSI*$^+$] prion formation in a control [*PIN*$^+$][*psi*$^-$] strain was estimated to be approximately 1.1 x 10^{-5} (Figure 4.1) comparable to previously reported frequencies (Lund and Cox, 1981; Lancaster et al, 2010; Speldewinde et al, 2015). This frequency increased during CLS and a 39-fold increase was observed by day 12. Atg1 is the only identified serine/threonine kinase in the autophagy pathway and is responsible for the initiation of autophagy (Matsuura et al, 1997; Parzych and Klionsky, 2014). The frequency of [*PSI*$^+$] prion formation was further elevated during CLS suggesting that autophagy normally acts to suppress [*PSI*$^+$] prion formation during ageing (Figure 4.1).

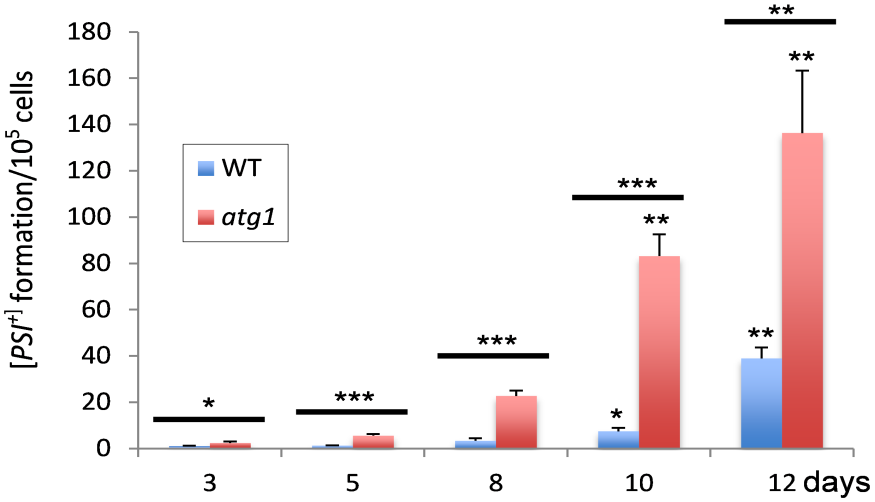

Figure 4.1: Increasing *de novo* [*PSI*$^+$] frequency during chronological lifespan. Wild-type and *atg1* stains in the [*PIN*$^+$][*psi*$^-$] background were grown to stationary phase in liquid complete media up to day 12 as indicated above to assess for *de novo* [*PSI*$^+$] frequency. [*PSI*$^+$] formation was quantified using the *ade1-14* mutant allele by growth on media lacking adenine and differentiated from nuclear *SUPX* gene mutations by their irreversible elimination in GdnHCl. Data shown are the means of at least three independent biological repeat experiments expressed as the number of colonies per 10^5 viable cells. Error bars denote standard deviation. The asterisk(s) directly above the columns denote statistical analysis as performed by one-way ANOVA with pair-wise comparisons using Tukey HSD (honest significant difference) test comparing the [*PSI*$^+$] prion formation at day 3 to the [*PSI*$^+$] prion formation at days 10 and 12 in wild-type and *atg1* strains (*p<0.01, **p<0.001). The bars with asterisk(s) above the columns denote the statistical analysis as performed by one-way ANOVA with pair-wise comparisons using Tukey HSD test comparing the [*PSI*$^+$] prion formation between wild-type and *atg1* strains at each time point [days 3, 5, 8, 10, and 12] (*p< 0.01, **p< 0.001, ***p< 0.0001).

4.2.2 The [*PSI*$^+$] prion increases longevity in a yeast CLS model.

We next examined viability to determine whether the [*PSI*$^+$] prion status of cells influences longevity. [*PIN*$^+$][*PSI*$^+$] and [*PIN*$^+$][*psi*$^-$] cells had a similar maximal lifespan with most cells dead by day 30 (Figure 4.2A). However, viability in the [*PIN*$^+$][*PSI*$^+$] strain remained higher than the [*PIN*$^+$][*psi*$^-$] strain over this time-course suggesting that [*PSI*$^+$] improves viability during ageing. Treating cells with GdnHCl blocks the propagation of yeast prions by inhibiting the key ATPase activity of Hsp104, a molecular chaperone that is absolutely

required for yeast prion propagation (Ferreira et al, 2001; Jung and Masison, 2001). GdnHCl cures yeast cells of [*PSI*$^+$] and all known prions (Tuite et al, 1981; Liebman and Chernoff, 2012). Curing the [*PIN*$^+$][*PSI*$^+$] strain with GdnHCl decreased viability during CLS and maximal lifespan was reduced to 10 days suggesting that prions are beneficial during CLS (Figure 4.2A). Autophagy is known to be required for chronological longevity and for example loss of *ATG1* reduces CLS (Alvers et al, 2009a). Similarly, we found that loss of *ATG1* reduced CLS in the 74D-694 yeast strain used for our studies (Figure 4.2B). Interestingly, longevity was comparable in the [*PIN*$^+$][*PSI*$^+$], [*PIN*$^+$][*psi*$^-$] and cured strains indicating that autophagy is required for prion dependent effects on longevity.

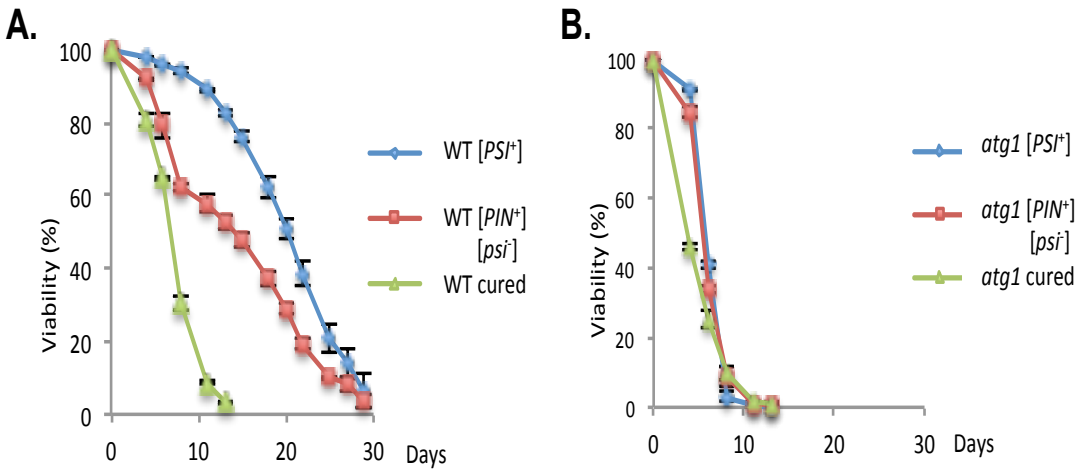

Figure 4.2: Cells carrying the [*PSI*$^+$] prion have improved chronological lifespan. Chronological lifespan analysis for **(A)** the wild-type strain and **(B)** *atg1* mutant strain in the [*PSI*$^+$], [*PIN*$^+$][*psi*$^-$] and cured background respectively. Cells were cultured in SCD media for 3 days to reach stationary phase and then aliquots taken every 2-3 days for flow cytometry analysis based on propidium iodide uptake by non-viable cells as assayed through flow cytometry. Data shown are the means of at least three independent biological repeat experiments expressed as the percentage of viable cells out of 10000 cells analysed. Error bars denote standard deviation.

4.2.3 [*PSI*$^{+}$] cells have an increased rate of autophagy and decreased concentrations of amorphous protein aggregates.

Given that the [*PSI*$^{+}$]-prion status of cells affect CLS in an autophagy-dependent manner, we examined whether autophagy is altered in [*PSI*$^{+}$] cells. We utilized a GFP-Atg8 fusion construct to follow the autophagy-dependent proteolytic liberation of GFP from GFP-Atg8, which is indicative of autophagic flux (Noda et al, 1995). More free GFP was detected in the [*PIN*$^{+}$][*PSI*$^{+}$] strain compared with the [*PIN*$^{+}$][*psi*$^{-}$] strain as well as the cured strain (Figure 4.3A). As expected, an absence of autophagic activity was observed for the *atg1* knockout mutants. This suggests that cells carrying the [*PSI*$^{+}$] prion may play a role in promoting autophagic activity that may have beneficial effects in improving the CLS of autophagy competent cells.

We next examined whether the increased autophagic activity in the [*PIN*$^{+}$][*PSI*$^{+}$] strain affects amorphous protein aggregation. This seemed likely given the previous studies which have suggested that autophagy plays a role in the clearance of misfolded and aggregated proteins (Hara et al, 2006; Komatsu et al, 2006). For this analysis, we used a biochemical approach where we separated insoluble proteins from soluble proteins by differential centrifugation, and removed any contaminating membrane proteins using detergent washes (Tomoyasu et al, 2001; Jang et al, 2004; Rand and Grant, 2006; Koplin et al, 2010). Interestingly, protein aggregation was decreased in the [*PIN*$^{+}$][*PSI*$^{+}$] strain compared with the [*PIN*$^{+}$][*psi*$^{-}$] strain (Figure 4.3B). This reduction in protein aggregation required autophagy since the levels of protein aggregation were comparable in the *atg1*-mutant versions of the [*PIN*$^{+}$][*PSI*$^{+}$] and [*PIN*$^{+}$][*psi*$^{-}$] strains.

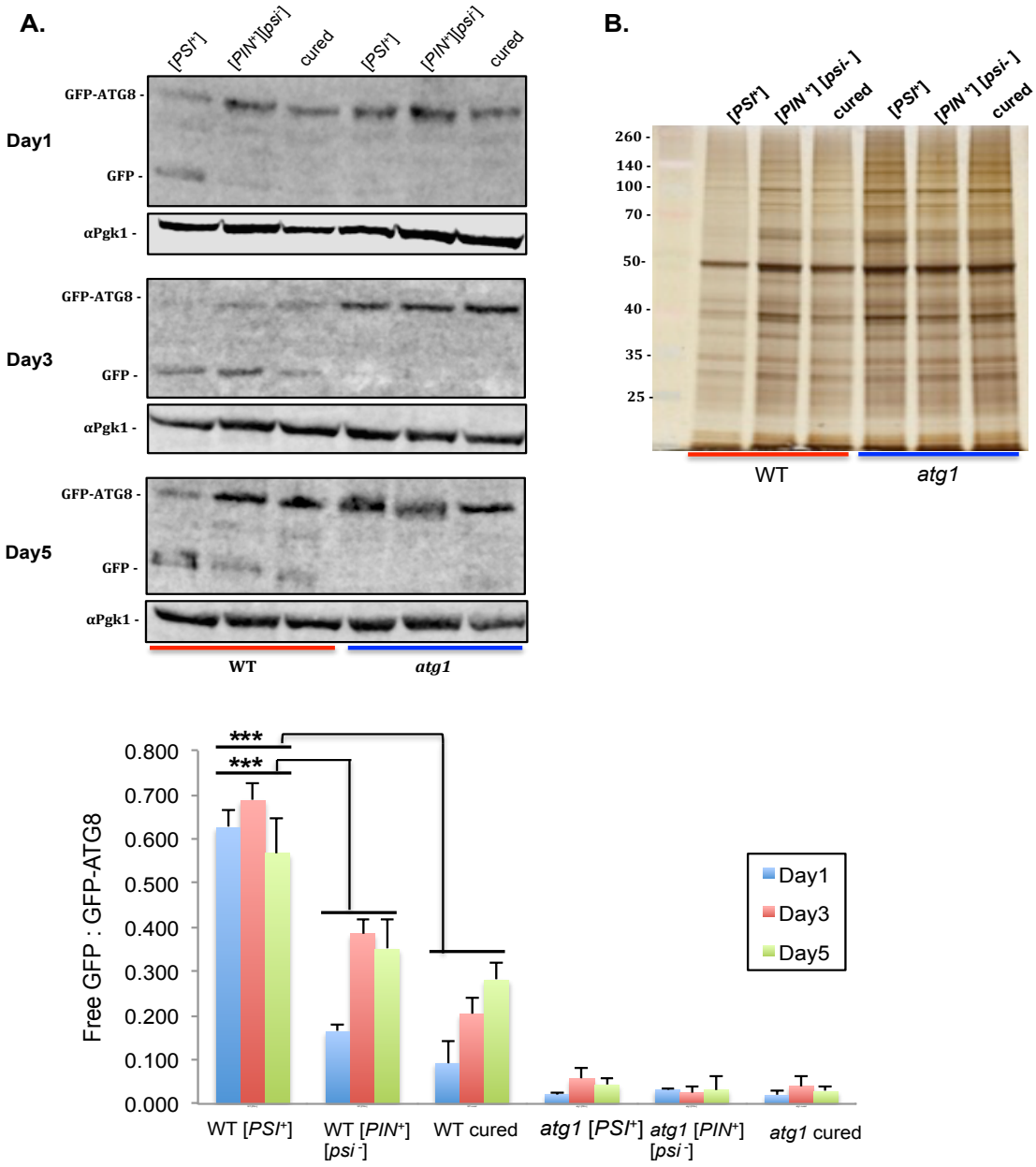

Figure 4.3: Increased autophagic flux and reduced protein aggregates in wild-type [*PSI*$^+$] cells. (A) Autophagic flux was monitored in cells expressing GFP-Atg8. Immunoblots of the GFP showing increased autophagy activity for wild-type [*PSI*$^+$] strains as detected by the appearance of free GFP indicative of autophagic flux at days 1, 3, and 5 of chronological growth. No free GFP was detected in the *atg1* mutants. Blots were probed with α-GFP or α-Pgk1 as a loading control. Quantification is shown for the three independent biological repeats comparing the ratio of free GFP with GFP-Atg8. Error bars denote standard deviation. Statistical analysis as performed by two-way ANOVA with multiple comparisons using Tukey HSD test comparing the ratio of free GPF with GFP-ATG8 at days 1, 3, and 5 in the wild-type [*PIN*$^+$][*psi*$^-$] and wild-type cured backgrounds to the ratio of free GPF with GFP-ATG8 at days 1, 3, and 5 in the wild-type [*PSI*$^+$] background (***p<0.0001). **(B)** Insoluble protein aggregates were isolated from the wild-type strain and the *atg1* mutant in the [*PSI*$^+$], [*PIN*$^+$][*psi*$^-$] and cured backgrounds after day 5 of chronological growth. The protein aggregates were analyzed using SDS-PAGE and silver staining.

4.3 Discussion

Ageing is associated with declining quality control mechanisms including autophagy and an increased susceptibility to environmental challenges. Autophagy is a generic degradation pathway for the clearance of damaged and aggregated proteins during basal growth conditions (Parzych and Klionsky, 2014) and is widely implicated in the ageing process (Rubinsztein et al, 2011). A role for autophagy in protecting against prion formation and prion-induced toxicity has previously been established in mouse models of prion formation. Autophagy was shown to be essential in enhancing the clearance of PrP^{Sc} and protecting cells against its accumulation (Aguib et al, 2009; Heiseke et al, 2010; Goold et al, 2013). Similarly, our data using the yeast CLS model suggests an age-dependent increase in the frequency of *de novo* [*PSI*$^{+}$] prion formation, that is further exacerbated when autophagy is absent, supporting a role for autophagy in the clearance of aggregated prion proteins.

We found that the presence of the [*PSI*$^{+}$] prion may confer a beneficial advantage during yeast chronological lifespan, possibly through an enhanced autophagic flux. There is evidence to suggest that increased *de novo* formation and accumulation of protein aggregates may exert a stimulatory effect on the autophagy pathway, which may further extend to prions as well. For instance, there is a correlation between the accumulation of PrP^{Sc} and the enhanced activity of quality control pathways including endoplasmic reticulum chaperones, the unfolded protein response and autophagy (Joshi-Barr et al, 2014). Furthermore, ablation of autophagy was found to cause neurodegenerative diseases in mice supporting a protective role for autophagy against abnormal protein accumulation (Hara et al, 2006; Komatsu et al, 2006). A modest level of protein aggregation in the [*PSI*$^{+}$] wild-type may similarly stimulate protective

mechanisms such as increased chaperone activity and autophagy leading to improved ageing.

The [*PSI*$^{+}$] prion causes a loss of function phenotype where translation termination activity is reduced due to aggregation of the normally soluble Sup35 (Wickner, 1994). A loss of translational fidelity may indeed translate into the production of novel peptides with new possible functions. The theory of prions being an epigenetic mechanism in uncovering hidden genetic variability has also been previously proposed (True et al, 2004; Tyedmers et al, 2008). Expanding the protein repertoire of cells and their regulation may facilitate additional pro-survival pathways or improve stress response in cells. In this case, the epigenetic diversity uncovered by the [*PSI*$^{+}$] prion may directly or indirectly contribute to lifespan extension during chronological ageing. Prions are known to be toxic particularly under conditions where the soluble protein form is over-expressed (Chernoff et al, 1992; Derkatch et al, 1997). Conversely, prions have also been found in wild yeast isolates albeit rarely and could represent a transient switching mechanism to ensure higher survival during environmental insults while switching back into the soluble form when the non-stress conditions are restored (Halfmann et al, 2012; Newby and Lindquist, 2013). Furthermore, it is likely that cells that are [*PIN*$^{+}$][*psi*$^{-}$] initially, become increasingly [*PSI*$^{+}$] during chronological ageing but still demonstrate extended lifespan. Conversely, curing cells of prions may have a negative impact on lifespan at least in the case of chronological ageing in agreement with the idea that prion formation may represent a protective mechanism against the toxic accumulation of aberrant protein monomers/oligomers that sequester/alter proteins essential for cell survival as has been suggested previously (Ganusova et al, 2006). Thus, having a [*PSI*$^{+}$] prion under non-induced and at tolerable

levels that does not impair cell viability may actually provide an added advantage to an autophagy competent cell.

It is unclear what triggers the increased frequency of [*PSI*$^{+}$] prion formation during ageing. One possibility is oxidative stress, since ROS-induced protein aggregation and mitochondrial dysfunction is a common feature in age-related diseases (Shacka et al, 2008; Lee et al, 2012). In addition, ROS and oxidative stress are known to induce autophagy (Scherz-Shouval et al, 2007; Chen et al, 2009; Filomeni et al, 2010). Thus, a defective autophagy pathway may result in the ineffective clearance of damaged or leaky mitochondria that may contribute to increased ROS production during chronological ageing. Further research will be required to elucidate the exact signaling pathways and the range of quality control mechanisms that may be modulated through the direct and indirect action of the [*PSI*$^{+}$] prion during yeast ageing. Indeed, in mammalian models, the soluble prion protein may exert certain protective functions in nerve cells, but this is dysregulated when it is converted into the prion form (Lee et al, 2007). For instance, neuronal cells derived from a PrP^{C} knockout mouse were found to have reduced viability and were more sensitive towards oxidative stress-induced damage and toxicity (Brown et al, 1997; Kuwahara et al, 1999). Although yeast fungal prions have been widely studied for more than 20 years, the full extent of the properties and effects of their presence still remain enigmatic with more to be discovered.

4.4 MATERIALS AND METHODS

4.4.1 Yeast Strains.

[*PIN*$^{+}$] [*PSI*$^{+}$], [*PIN*$^{+}$] [*psi*$^{-}$] and [*pin*$^{-}$] [*psi*$^{-}$] derivatives of the wild-type yeast strain 74D-694 (*MATa ade1-14 ura3-52 leu2-3, 112 trp1-289 his3-200)* were used for all experiments (Sideri et al, 2010). The strain deleted for *ATG1* (*atg1::HIS3*) has been described previously (Speldewinde et al, 2015).

4.4.2 Growth Conditions.

Yeast strains were grown at 30℃, 180 rpm in minimal SCD medium (2% w/v glucose, 0.17% yeast nitrogen base without amino acids, supplemented with Kaiser amino acid mixes, Formedium, Hunstanton, England). Chronological life span experiments were performed in liquid SCD media supplemented with a four-fold excess of uracil, leucine, tryptophan, adenine and histidine to avoid any possible artefacts arising from the auxotrophic deficiencies of the strains. Strains were cured by five rounds of growth on YEPD agar plates containing 4 mM GdnHCl.

4.4.3 *De novo* [*PSI*$^{+}$] Formation.

[*PSI*$^{+}$] prion formation was scored by growth in the absence of adenine as described previously (Speldewinde et al, 2015). [*PSI*$^{+}$] formation was calculated based on the mean of at least three independent biological repeat experiments.

4.4.4 Yeast Chronological Lifespan Determination.

CLS experiments were performed according to Ocampo and Barrientos (2011). Briefly, cells were cultured in liquid SCD media for 3 days to reach

stationary phase and then aliquots taken every 2-3 days for flow cytometry analysis. 50µl of 4 mM of propidium iodide (P.I.) were added to 950µl of culture and cell viability was measured based on propidium iodide uptake by non-viable cells as assayed through flow cytometry. Flow cytometry readings were performed using a Becton Dickinson (BD) LSRFortessa™ cell analyser, BD FACSDiva 8.0.1 software after staining with propidium iodide.

4.4.5 Protein Analysis.

Protein extracts were electrophoresed under reducing conditions on SDS-PAGE minigels and electroblotted onto PVDF membrane (Amersham Pharmacia Biotech). Bound antibody was visualised using WesternSure® Chemiluminescent Reagents (LI-COR) and a C-DiGit® Blot Scanner (LI-COR). Insoluble protein aggregates were isolated as previously described (Rand and Grant, 2006; Jacobson et al, 2012; Weids and Grant, 2014). Insoluble fractions were resuspended in reduced protein loading buffer, separated by reducing SDS/PAGE (12% gels) and visualized by silver staining with the Bio-Rad silver stain plus kit. The induction of autophagy was confirmed by examining the release of free GFP due to the proteolytic cleavage of GFP-Atg8 (Noda et al, 1995).

4.4.6 Statistical analysis.

Data are presented as mean values ± standard deviation (SD). Statistical analysis for multiple groups was performed using one-way ANOVA with pair-wise comparisons of sample means via the Tukey HSD test or two-way ANOVA with multiple comparisons of sample means via the Tukey HSD test. Results were considered statistically significant with a p-value less than 0.05.

4.5 Acknowledgements.

S.H.S. was supported by a Wellcome Trust funded studentship. The Bioimaging Facility microscopes used in this study were purchased with grants from BBSRC, Wellcome Trust and the University of Manchester Strategic Fund.

Chapter 5: The Abp1 actin-binding protein of the cortical actin cytoskeleton is required for the increased frequency of yeast [*PSI*$^+$] prion formation during oxidative stress conditions.

Shaun H. Speldewinde[1], Victoria A. Doronina[1], Mick F. Tuite[2] and Chris M. Grant[1]

[1]University of Manchester, Faculty of Life Sciences, The Michael Smith Building, Oxford Road, Manchester, M13 9PT, UK.
[2]Kent Fungal Group, School of Biosciences, University of Kent, Canterbury, Kent CT2 7NJ, UK

Address correspondence to: Chris M. Grant, The University of Manchester, Faculty of Biology, Medicine and Health, The Michael Smith Building, Oxford Road, Manchester, M13 9PT, UK. Phone: (0161) 306 4192; Email: chris.grant@manchester.ac.uk

This chapter follows the work done previously by Dr. Victoria A. Doronina who generated Figure 5.1A, parts of Figure 5.1B, and Supplementary Figure 5.2. The author generated the rest of the figures presented in this chapter namely parts of Figure 5.1B, Figure 5.2A and B, Figure 5.3A-C, Figure 5.4A-E, Figure 5.5A-D, Figure 5.6, and Supplementary Figure 5.1. The author designed the experiments and wrote the manuscript with the help of Prof. Chris M. Grant. Additionally, Prof. Mick F. Tuite reviewed the manuscript.

ABSTRACT

Prions can arise spontaneously but little is known regarding the mechanisms underlying their sporadic formation. The frequency of yeast [*PSI*$^{+}$] prion formation can be increased by overexpression of Sup35 or by exposure to oxidative stress conditions. We have used tandem affinity purification (TAP) and mass spectrometry to identify the proteins which associate with Sup35 in a *tsa1 tsa2* antioxidant mutant to address the mechanism by which Sup35 forms the [*PSI*$^{+}$] prion during oxidative stress conditions. This analysis identified several components of the cortical actin cytoskeleton including the Abp1 actin nucleation promoting factor and we show that loss of *ABP1* abrogates oxidant induced [*PSI*$^{+}$] prion formation. In contrast, loss of *ABP1* only modestly disrupted overexpression-induced Sup35 aggregation and [*PSI*$^{+}$] prion formation. Furthermore, treating yeast cells with latrunculin A to disrupt the formation of actin cables and patches abrogated oxidant-induced, but not overexpression-induced [*PSI*$^{+}$] prion formation suggesting a mechanistic difference in prion formation. The amyloidogenic [*RNQ*$^{+}$] prion form of Rnq1 localizes to the IPOD and is thought to influence the aggregation of other proteins. We show that oxidant-induced Sup35 aggregates are formed at a reduced frequency and do not colocalize with Rnq1 in an *abp1* mutant which may account for the reduced frequency of [*PSI*$^{+}$] prion formation in this mutant.

5.1 INTRODUCTION

Prions are infectious agents composed of misfolded proteins. They are associated with a group of neurodegenerative diseases in animals and humans that have common pathological hallmarks, typified by human Creutzfeldt-Jakob Disease (CJD). The presence of misfolded prion protein (PrP^{Sc}) underlies the development of prion diseases in a mechanism which involves conversion of the normal prion protein (PrP^{C}) into its infectious PrP^{Sc} conformation (Collinge and Clarke, 2007; Requena and Wille, 2014). Aggregated, protease-resistant PrP^{Sc} seeds are believed to act as templates which promote the conversion of normal PrP^{C} to the pathological PrP^{Sc} state, which is rich in β-sheets and resistant to degradation. PrP^{C} can adopt an alternative conformational state by spontaneous misfolding event(s) that might be triggered by mutation, mistranslation, environmental stresses and/or by disruption of the chaperone network (DeMarco and Daggett, 2005).

This 'protein-only' mechanism of infectivity can also explain the unusual genetic behaviour of several prions found in the yeast *Saccharomyces cerevisiae* (Wickner, 1994). At present, several proteins are known to form prions in yeast with many other proteins classified as potential prion candidates (Alberti et al, 2009). [*PIN*$^{+}$] and [*PSI*$^{+}$] are the best studied yeast prions, which are formed from the Rnq1 and Sup35 proteins, respectively (Wickner, 1994; Derkatch et al, 1997). [*PSI*$^{+}$] is the altered conformation of the Sup35 protein, which normally functions as a translation termination factor during protein synthesis. The *de novo* formation of [*PSI*$^{+}$] is enhanced by the presence of the [*PIN*$^{+}$] prion, which is the altered form of the Rnq1 protein whose native protein function is unknown (Treusch and Lindquist, 2012).

How prions form spontaneously without underlying infection or genetic change is poorly understood at the molecular level, yet if we are to develop effective preventative measures for human and animal amyloidoses, this mechanism must be established. Of particular importance is identifying what can trigger this event. One strong possibility is that oxidative damage to the non-prion form of a protein may be an important trigger influencing the formation of its heritable prion conformation (Grant, 2015). For example, methionine oxidation of mammalian PrP^{C} has been proposed to underlie the misfolding events which promote the conversion to PrP^{Sc} (Canello et al, 2008; Wolschner et al, 2009; Canello et al, 2010). Methionine oxidation has also been shown to destabilize native PrP^{C} facilitating misfolding and transition to the PrP^{Sc} conformation (Younan et al, 2012). Methionine oxidation is also a common factor in many protein misfolding diseases (Dong et al, 2003; Yamin et al, 2003; Oien et al, 2009) and an age-dependent increase in methionine oxidation is detected in various model systems (Stadtman et al, 2005). Several different environmental stress conditions, including oxidative stress, have been shown to increase the frequency of yeast [*PSI*$^{+}$] prion formation (Tyedmers et al, 2008). The *de novo* formation of the [*PSI*$^{+}$] prion is also significantly increased in yeast mutants lacking key antioxidants suggesting that endogenous reactive oxygen species (ROS) can trigger the *de novo* formation of the [*PSI*$^{+}$] prion (Sideri et al, 2010; Sideri et al, 2011; Doronina et al, 2015). Preventing methionine oxidation by overexpressing methionine sulfoxide reductase abrogates the shift to the prion form indicating that the direct oxidation of Sup35 may trigger structural transitions favouring its conversion to the transmissible amyloid-like form (Sideri et al, 2011; Doronina et al, 2015).

Hence, protein oxidation appears to be a common mechanism underlying the aggregation of both mammalian and yeast amyloidogenic proteins.

The frequency of *de novo* appearance of the [*PSI*$^+$] prion can be increased by overexpression of Sup35 in [*PIN*$^+$][*psi*$^-$] cells since the excess Sup35 increases the probability of forming prion seeds (Wickner, 1994). This is enhanced by components of the actin cytoskeleton which physically associate with Sup35 including various proteins of the cortical actin cytoskeleton (Sla1, Sla2, End3, Arp2, Arp3) that are involved in endocytosis (Ganusova et al, 2006). Loss of some of these proteins decreases the aggregation of overexpressed Sup35 and *de novo* [*PSI*$^+$] formation. This is particularly interesting given the increasing evidence suggesting that cytoskeletal structures provide a scaffold for the generation of protein aggregates. Insoluble aggregates of amyloid-forming proteins such as prions are targeted to the IPOD as part of the cells protein quality control, which is required for prion fragmentation and seeding (Kaganovich et al, 2008; Sontag et al, 2014). The IPOD is located at a perivacuolar site adjacent to the “preautophagosomal structure (PAS)” where cells initiate autophagy (Parzych and Klionsky, 2014). Prion conversion has been proposed to occur at the cell periphery in association with the actin cytoskeleton, prior to deposition at the IPOD (Mathur et al, 2010). The actin cytoskeleton has also been implicated in the asymmetric inheritance of oxidatively damaged proteins (Aguilaniu et al, 2003). Actin organization therefore appears to play an important role in the aggregation of damaged proteins, which in some cases results in prion formation.

Oxidative stress provides a powerful tool to examine the *de novo* formation of prions which does not require overexpression or mutation of the normally soluble version of the prion protein. In this current study, we have used

a mutant lacking the Tsa1 and Tsa2 antioxidants to isolate the proteins which aggregate with Sup35. We used the *tsa1 tsa2* antioxidant mutant in order to enrich for factors which associate with oxidized Sup35 and therefore might be important for the conversion of Sup35 to the [*PSI*$^{+}$] prion. Our data suggest a key role for the cortical actin cytoskeleton since we have identified a number of components of the Arp2/3 actin-nucleation complex which specifically associate with Sup35 in the antioxidant mutant. We show that loss of several of these factors abrogate the increased frequency of [*PSI*$^{+}$] prion formation which is normally observed in response to oxidative stress conditions. However, these mutants do not affect the increased frequency of [*PSI*$^{+}$] prion formation observed in response to Sup35 overexpression. We show that Sup35 aggregation occurs in actin-nucleation complex mutants in response to oxidative stress conditions, but the aggregates do not appear to form normally at the IPOD. Our data suggest that the cortical actin cytoskeleton is important for the formation of a propagating [*PSI*$^{+}$] conformer following oxidant-induced misfolding and aggregation of Sup35.

5.2 RESULTS

5.2.1 Identification of Sup35-interacting proteins in a *tsa1 tsa2* mutant.

To address the mechanism by which Sup35 forms the [*PSI*$^{+}$] prion during oxidative stress conditions, we used tandem affinity purification (TAP) and mass spectrometry to identify proteins which associate with Sup35 in a *tsa1 tsa2* mutant. For this analysis, we used wild-type and *tsa1 tsa2* mutant strains containing genomically-tagged Sup35. We have previously confirmed that TAP-tagging Sup35 does not affect reversible [*PSI*$^{+}$] prion formation (Sideri et al, 2011). Freshly inoculated [*PIN*$^{+}$][*psi*$^{-}$] strains were grown for 20 hours (approximately ten generations) and Sup35 affinity-purified from both strains using TAP chromatography. The associated proteins were identified from three repeat experiments and were considered significant if they were identified in at least two independent experiments. This resulted in the identification of 63 and 47 proteins which co-purify with Sup35 in the wild-type and *tsa1 tsa2* mutant strains, respectively (Supplementary Table 1).

We searched for functional categories that were enriched in the Sup35 co-purifying proteins using MIPS category classifications (Figure 5.1A). The overlap between these two datasets is 18 proteins and as might be expected this included functions related to protein fate (>3-fold enrichment; Fischer's exact test, $P<10^{-7}$) such as chaperones and stress-related proteins (Sti1, Sse1, Cdc48, Ssa2, Hsc82, Ssb2, Ssa1, Hsp60) which have well characterized roles in prion formation and propagation in yeast (Liebman and Chernoff, 2012). Similar proteins were identified as part the unfolded protein response (21-fold; $P=1.5\times10^{-8}$) and stress response categories (4-fold; $P=2\times10^{-5}$). Overrepresented functions in the wild-type strain included protein synthesis (2-fold; $P=2\times10^{-5}$) and protein folding and stabilization (9-fold; $P=2\times10^{-10}$). The

protein synthesis category included a number of ribosomal proteins and translation factors which might be expected to associate with the Sup35 translation termination factor. Interestingly, proteins associated with the actin cytoskeleton were overrepresented in the *tsa1 tsa2* mutant (8-fold; $P=4\times10^{-6}$), but not in the wild-type strain, and this is what we explore further in this study.

Our data suggest an important role for the cortical actin cytoskeleton based on the cytoskeleton-related proteins which co-purify with Sup35 in the *tsa1 tsa2* mutant strain (Act1, Sac6, Crn1, Abp1, Arc40, Arp2, Arp3 and Arc35). These data strongly implicate the Arp2/3 complex, which is a seven-protein complex containing two actin-related proteins (Arp2 and Arp3) and five non-actin related proteins including Arc35 and Arc40 (Galletta et al, 2010). Abp1 is an actin-binding protein of the cortical actin cytoskeleton which is important for activation of the Arp2/3 complex (Goode et al, 2001). Crn1 and Act1 were identified with purified Sup35 in both the wild-type and *tsa1 tsa2* mutant strains. Crn1 is an actin binding protein which regulates the actin filament nucleation and branching activity of the Arp2/3 complex through its interaction with the Arc35 subunit (Humphries et al, 2002). Act1 encodes the single essential gene for actin in yeast. We validated our Sup35-interacting proteins for a number of proteins. Sup35-TAP was immunoprecipitated from the wild-type and *tsa1 tsa2* mutant and possible interactions examined using Western blot analysis (Figure 5.1B). This analysis confirmed that Abp1, Arp3 and Sap190 co-purify with Sup35 in the *tsa1 tsa2* mutant strain and Act1 co-purifies with Sup35 in both the wild-type and *tsa1 tsa2* mutant strains.

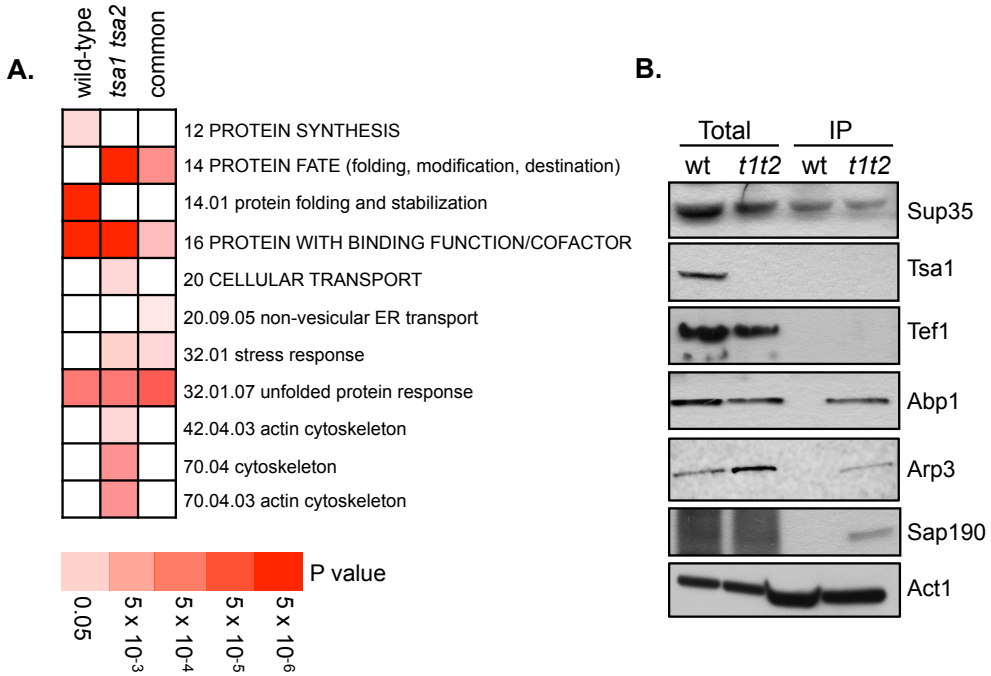

Figure 5.1: Identification of Sup35-interacting proteins in wild-type and *tsa1 tsa2* mutant strains. (A) Functional categorisation of Sup35-associated proteins. Results are ordered on MIPS category classification numbers and overarching categories are in capitals. Where an overarching category was enriched, sub-categories within the overarching category were omitted from the graph. Confidence of each classification category is shown as Bonferroni corrected *p*-values. **(B)** Sup35-TAP was immunoprecipitated from the wild-type and *tsa1 tsa2* mutant strains and possible interactions examined using Western blot analysis. Sup35-TAP co-immunoprecipitates Abp1, Arp3 and Sap190 in a *tsa1 tsa2* mutant. Sup35-TAP co-immunoprecipitates Act1 in both wild-type and *tsa1 tsa2* mutant strains. Total denotes whole cell extracts and IP denotes immunoprecipitates.

5.2.2 Mutations disrupting the cortical actin cytoskeleton abrogate oxidative stress induced [*PSI*$^+$] prion formation.

Mutant strains were constructed in a [*PIN*$^+$][*psi*$^-$] yeast strain (74D-694) which is commonly used to study yeast prion biology. We were unable to make *arp2* or *arp3* deletion mutants in this strain background in agreement with previous observations suggesting that Arp2 and Arp3 are essential for normal growth and viability in some strain backgrounds (Winter et al, 1999; Winzeler and *al.*, 1999; Ganusova et al, 2006). We therefore focused on Abp1 and Crn1 which were identified in our Sup35 immunopurification experiments. The induction of [*PSI*$^+$] prion formation was quantified using the *ade1-14* mutant

allele which confers adenine auxotrophy and prions differentiated from nuclear gene mutations by their irreversible elimination in guanidine hydrochloride (GdnHCl). The control [*PIN*$^+$][*psi*$^-$] strain was grown in the presence of 100 μM hydrogen peroxide for 20 hours prior to scoring [*PSI*$^+$] prion formation. This oxidative stress treatment increased the frequency of [*PSI*$^+$] prion formation by approximately ten-fold (Figure 5.2A), similar to our previous observations (Doronina et al, 2015). The basal frequency of spontaneous [*PSI*$^+$] prion formation was reduced by approximately 150-fold in the *abp1* mutant and 30-fold in the *crn1* mutant. Furthermore, loss of *ABP1* or *CRN1* abrogated the peroxide-induced increase in [*PSI*$^+$] prion formation (Figure 5.2A). The nucleation of actin patches by the Arp2/3 complex is enhanced by the activity of nucleation promoting factors such as Abp1 (Galletta et al, 2010; Mooren et al, 2012; Mishra et al, 2014; Goode et al, 2015). We therefore tested whether loss of another nucleation promoting factor, Pan1, similarly reduced the frequency of [*PSI*$^+$] prion formation. The frequency of spontaneous [*PSI*$^+$] prion formation was significantly reduced in the *pan1* mutant and no induction was observed in response to hydrogen peroxide stress (Figure 5.2A).

Since mutations which disrupt the cortical actin cytoskeleton reduce oxidative stress induced [*PSI*$^+$] formation, we examined whether the formation of another prion which is not related in sequence to the Sup35/[*PSI*$^+$] prion is similarly affected. Rnq1 can switch to the [*PIN*$^+$] prion, which is formed at relatively high frequencies compared with the *de novo* formation of [*PSI*$^+$] (Derkatch et al, 2002). The *de novo* formation of [*PIN*$^+$] prions was detected in approximately 6% of control [*pin*$^-$] cells, compared with 1.7% of *abp1* mutant cells (Figure 5.2B). Hydrogen peroxide treatment increased the frequency of

[*PIN*$^+$] prion formation in both strains but the frequency of [*PIN*$^+$] formation was significantly lower in the *abp1* mutant, compared with the wild-type strain.

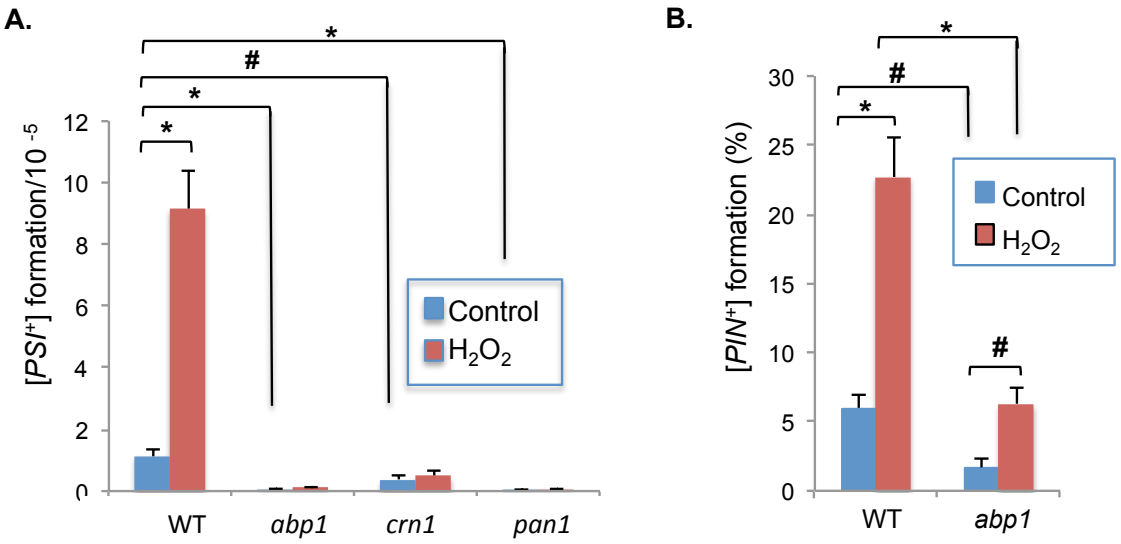

Figure 5.2: Reduced frequency of [*PSI*$^+$] formation in cortical actin cytoskeleton mutants. **(A)** The frequency of *de novo* [*PSI*$^+$] prion formation was quantified in the wild-type, *abp1, crn1*, and *pan1* mutant strains grown in the presence or absence of 100 μM hydrogen peroxide for 20 hours. [*PSI*$^+$] formation was quantified using the *ade1-14* mutant allele by growth on media lacking adenine and differentiated from nuclear *SUPX* gene mutations by their irreversible elimination in GdnHCl. Data shown are the means of at least three independent biological repeat experiments expressed as the number of colonies per 10^5 viable cells. Error bars denote standard deviation. Statistical analysis was performed by one-way ANOVA with pair-wise comparisons using Tukey HSD (honest significant difference) test comparing the [*PSI*$^+$] prion formation in the wild-type strain to the [*PSI*$^+$] prion formation in the *abp1*, *crn1*, and *pan1* mutant strains in the absence or presence of hydrogen peroxide treatment (*p<0.01, $^{\#}$p<0.05). **(B)** *De novo* [*PIN*$^+$] prion formation was quantified in the wild-type and *abp1* mutant strain grown in the presence or absence of 100 μM hydrogen peroxide for 20 hours. Data shown are the means of three independent biological repeats expressed as the percentage of viable cells forming [*PIN*$^+$] colonies. Error bars denote standard deviation. Statistical analysis was performed by one-way ANOVA with pair-wise comparisons using Tukey HSD test comparing the [*PIN*$^+$] prion formation in the absence versus the presence of hydrogen peroxide treatment between wild-type strain and *abp1* mutant (*p<0.01, $^{\#}$p<0.05).

5.2.3 Loss of *ABP1, CRN1* or *PAN1* modestly alter the frequency of induced [*PSI*$^+$] prion formation.

It has long been known that [*PSI*$^+$] prion formation can be induced by the overexpression of Sup35 in [*psi*$^-$] strains due to the increased possibility for

prion seed formation (Wickner, 1994). We therefore tested whether loss of *ABP1, CRN1* or *PAN1* similarly affected the frequency of induced [*PSI*$^{+}$] prion formation. Sup35NM-GFP was induced for 24 hours and visible fluorescent aggregates were observed in 6.1% of wild-type cells examined (Figure 5.3A). This included large fluorescent foci which arise due to decorating existing aggregates (3.7%), as well as rod- and ribbon-like aggregates (2.4%) characteristic of the *de novo* formation of [*PSI*$^{+}$] (Zhou et al, 2001; Ganusova et al, 2006; Mathur et al, 2010). Loss of *CRN1* or *PAN1* resulted in modest decreases in Sup35 aggregation including the formation of fewer visible puncta and rod and ribbon-like aggregates (Figure 5.3A). A stronger effect was seen with the *abp1* mutant, with no rod or ribbon-like aggregates detected, although 1% of *abp1* mutant cells still contained visible Sup35NM-GFP puncta (Figure 5.3A). Western blot analysis was used to rule out any differences in Sup35NM-GFP induction in the mutant strains compared with the wild-type strain (Figure 5.3B). This analysis showed a similar increase in Sup35NM-GFP expression in the *abp1, crn1* and *pan1* mutants compared with the wild-type strain.

Rhodamine-phalloidin staining was used to visualize the cortical actin cytoskeleton in the wild-type and mutant strains. Multiple bright rhodamine-phalloidin–stained puncta were detected in the wild-type strain (Supplementary Figure 5.1), typical of the cortical actin patches normally observed in wild-type yeast cells (Karpova et al, 1998; Yang and Pon, 2002). In comparison, fewer, fainter cortical actin patches were detected in the *abp1, crn1* and *pan1* mutant strains. In some cells, the formation of Sup35NM-GFP aggregates was coincident with actin patches but this was difficult to differentiate since rhodamine-phalloidin–stained puncta covered a large proportion of the cellular cortex (Supplementary Figure 5.1). This is similar to previous studies which

have shown that few Sup35-GFP puncta (Ganusova et al, 2006) or no Sup35-GFP puncta (Zhou et al, 2001) colocalize with actin patches. Similarly some examples of colocalized Sup35NM-GFP/rhodamine-phalloidin–stained puncta were observed in the *abp1, crn1* and *pan1* mutants. Although it is difficult to determine whether Sup35 aggregates are associated with the cortical actin cytoskeleton, our mutants which disrupt cortical actin patch formation appear to modestly affect induced Sup35 aggregate formation.

The presence of fluorescent Sup35-GFP aggregates is not necessarily indicative of [*PSI*$^{+}$] prion formation since some cells with fluorescent dots will die, and some contain non-productive or non-amyloid aggregates (Arslan et al, 2015). We therefore quantified [*PSI*$^{+}$] prion formation using the *ade1-14* mutant allele as described above. [*PSI*$^{+}$] formation was strongly induced by approximately 65-fold in the wild-type [*PIN*$^{+}$][*psi*$^{-}$] strain in response to Sup35 overexpression (Figure 5.3C). A similar induction of [*PSI*$^{+}$] prion formation was observed in the *crn1* and *pan1* mutants. This induction was reduced in the *abp1* mutant compared with the wild-type strain, although a 21-fold increase in the frequency of [*PSI*$^{+}$] prion formation was still observed in response to Sup35 induction (Figure 5.3C). Taken together, these data indicate that in contrast to oxidative stress-induced prion formation, mutations which disrupt cortical actin patch formation only modestly affect the induction of [*PSI*$^{+}$] prion formation in response to Sup35 overexpression.

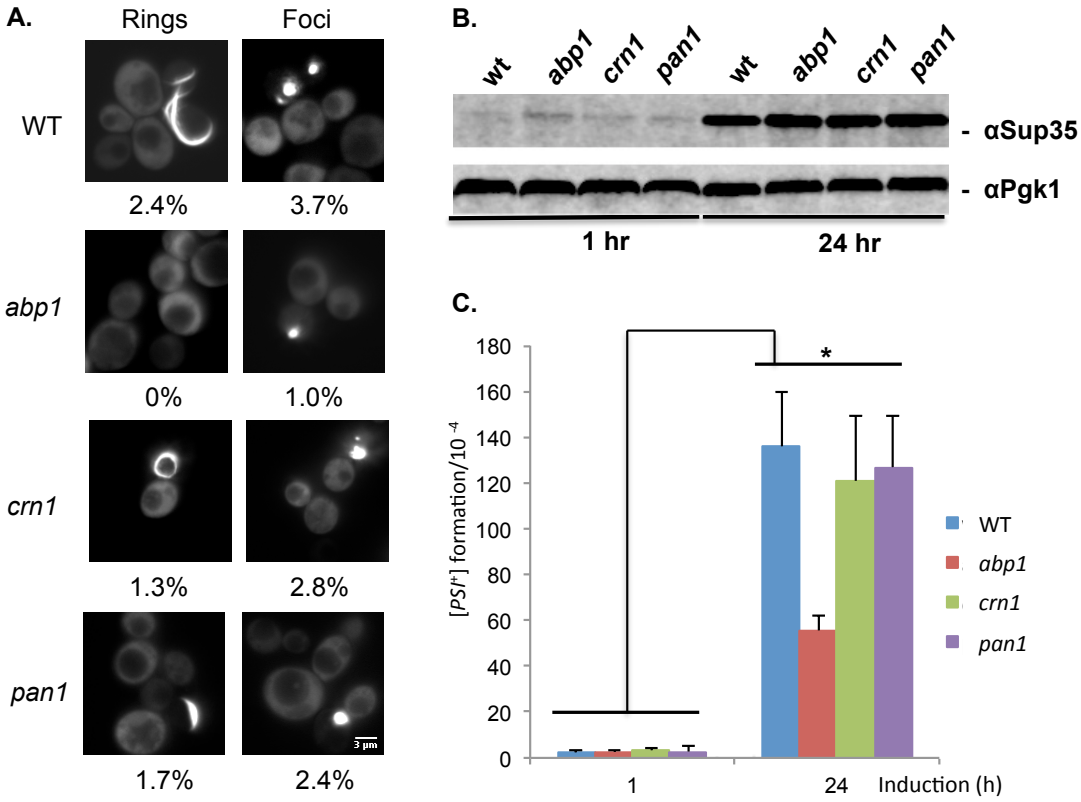

Figure 5.3: Induction of [*PSI*$^+$] prion formation by overexpression of Sup35. (A) Fluorescence micrographs are shown for [*PIN*$^+$][*psi*$^-$] versions of the wild-type, *abp1, crn1* and *pan1* mutant strains containing the *CUP1-SUP35NM-GFP* plasmid induced with copper for 24 hours. Representative images are shown for ring/ribbon-like and foci aggregate formation. The numbers indicate the percentage of cells containing each type of aggregate from an average of 300 cells counted. The scale bar is 3μm. **(B)** Western blot analysis of the wild-type and *abp1* mutant strain following induction of Sup35NM-GFP. Blots were probed with αSup35 or α-Pgk1 as a loading control. **(C)** [*PSI*$^+$] prion formation was quantified in the wild-type and *abp1* mutant strain containing the *CUP1-SUP35NM-GFP* plasmid following 24 h of copper induction. Data shown are the means of at least three independent biological repeat experiments expressed as the number of colonies per 10^4 viable cells. Error bars denote the standard deviation. Statistical analysis was performed by two-way ANOVA with multiple comparisons using Tukey HSD test comparing the [*PSI*$^+$] prion formation between 1h and 24 h of induction in the wild-type, *abp1, crn1* and *pan1* mutant strains (*p<0.01).

5.2.4 Latrunculin A treatment disrupts oxidative stress induced [*PSI*$^+$] prion formation.

Treatment of yeast cells with latrunculin A (LTA) disrupts the formation of actin cables and patches (Ayscough et al, 1997). This has been used to show that the actin cytoskeleton plays a role in [*PSI*$^+$] propagation since disrupting the

actin cytoskeleton by treatment with LTA causes the loss of [*PSI*$^+$] from yeast cells (Bailleul-Winslett et al, 2000). This effect was observed at relatively high concentrations of LTA (40-200 μM) and so we wanted to test whether a lower concentration of LTA which does not affect [*PSI*$^+$] propagation, might disrupt oxidative-stress induced prion formation. We first tested the effect of growing a [*PSI*$^+$] strain in the presence of 10 μM LTA for 20 hours. This concentration of LTA resulted in modest curing (~7%) of [*PSI*$^+$] and so we reasoned that we could use this concentration of LTA to test whether it affects the induction of [*PSI*$^+$]. Rhodamine-phalloidin staining was used to visualize the cortical actin cytoskeleton and to confirm that 10 μM LTA treatment disrupted the formation of actin patches (Figure 5.4A).

The wild-type [*PIN*$^+$][*psi*$^-$]-strain was grown in the presence of 10 μM LTA and prion formation induced by treatment with 100 μM hydrogen peroxide for 20 hours. We first examined Sup35 aggregation by expressing Sup35NM-GFP for the final two hours of the oxidant treatment. Approximately 8% of wild-type cells contained visible Sup35 aggregates following exposure to hydrogen peroxide. This frequency was somewhat reduced in cells treated with 10 μM of LTA, where 3.9% of cells examined contained visible Sup35 aggregates (Figure 5.4B). [*PSI*$^+$] prion formation was quantified under the same conditions, using the *ade1-14* mutant allele. LTA treatment decreased the basal frequency of [*PSI*$^+$] prion formation by 3-fold and also abrogated the oxidant-induction of [*PSI*$^+$] prion formation (Figure 5.4C). For comparison, we examined whether 10 μM LTA treatment affected overexpression-induced [*PSI*$^+$] prion formation. [*PSI*$^+$] formation was strongly induced in response to Sup35 overexpression and only a modest decrease in induction frequency was observed in the presence of

LTA (Figure 5.4D). Western blot analysis was used to confirm that LTA does not affect Sup35 overexpression (Figure 5.4E). Thus, LTA disrupts oxidant induced [*PSI*$^+$] prion formation but only modestly affects overexpression-induced [*PSI*$^+$] prion formation.

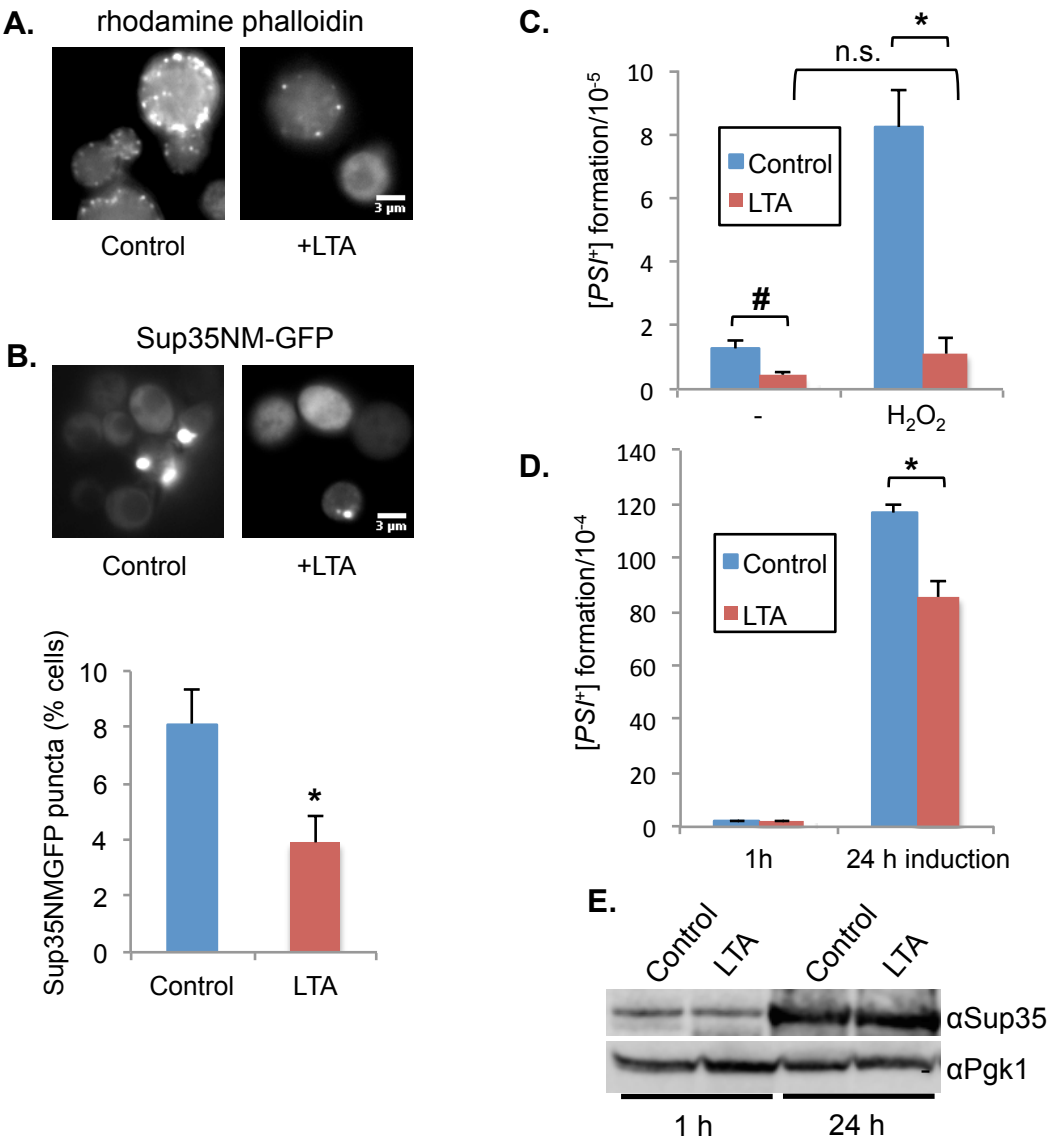

Figure 5.4: Latrunculin A treatment reduces oxidant-induced [*PSI*$^+$] formation. **(A)** Representative fluorescence micrographs are shown for a [*PIN*$^+$][*psi*$^-$] strain treated with 10 μM LTA for 20 hours. Cells were fixed, and stained with rhodamine phalloidin to visualize the cortical actin cytoskeleton. **(B)** Fluorescence micrographs are shown for a [*PIN*$^+$][*psi*$^-$] strain treated with 100 μM hydrogen peroxide for 20 hours in the presence or absence of 10 μM LTA. The aggregate frequency is expressed as the percentage of cells containing visible Sup35 foci from approximately 1000 cells counted. Data shown are the means of at least three independent biological repeats. Error bars denote standard deviation. Statistical analysis was performed by one-way ANOVA comparing

the Sup35 foci frequency with or without LTA treatment in the wild-type strain (*p<0.01). **(C)** [*PSI*$^+$] prion formation was quantified in a [*PIN*$^+$][*psi*$^-$] strain treated with 100μM hydrogen peroxide for 20 hours in the presence or absence of 10 μM LTA. Data shown are the means of three independent biological repeats expressed as the number of [*PSI*$^+$] colonies per 10^5 viable cells. Error bars denote the standard deviation. Statistical analysis was performed by one-way ANOVA with pair-wise comparisons using Tukey HSD test comparing the [*PSI*$^+$] prion formation in the absence versus the presence of hydrogen peroxide treatment in wild-type strain without LTA treatment and wild-type strain with LTA treatment ($^{n.s.}$not statistically significant, *p<0.01, $^{\#}$p<0.05). **(D)** [*PSI*$^+$] prion formation was quantified in a [*PIN*$^+$][*psi*$^-$] strain containing the *CUP1-SUP35NM-GFP* plasmid following 1 and 24 h of copper induction in the presence or absence of 10 μM LTA. Data shown are the means of three independent biological repeats expressed as the number of [*PSI*$^+$] colonies per 10^4 viable cells. Error bars represent the standard deviation. Statistical analysis was performed by one-way ANOVA with pair-wise comparisons using Tukey HSD test comparing the [*PSI*$^+$] prion formation in the absence versus the presence of LTA treatment in wild-type strain at 24 h of induction (*p<0.01). **(E)** Western blot analysis of cells grown under the same conditions as for panel D. Blots were probed with α-Sup35 and α-Pgk1 as a loading control.

5.2.5 Analysis of Sup35 oxidation and protein aggregation in *abp1* mutant cells.

We have previously shown that Sup35 oxidative protein damage is an important trigger for the formation of the heritable [*PSI*$^+$] prion in yeast (Sideri et al, 2011; Doronina et al, 2015). Cortical actin patch mutants may potentially decrease oxidative stress-induced [*PSI*$^+$] prion formation in a number of different ways including preventing Sup35 oxidative damage, altering the formation of Sup35 protein aggregates or by disrupting the formation of heritable [*PSI*$^+$] propagons. We therefore examined Sup35 oxidative damage in response to oxidative stress conditions, to determine whether disrupting the cortical actin cytoskeleton influences protein oxidative damage. Protein carbonylation is a commonly used measure of protein oxidative damage (Nystrom, 2005). Carbonyl groups on proteins can be detected by Western blot analysis using an antibody against the carbonyl-specific probe DNPH (2,4-dinitrophenyl-hydrazine). Using this assay we found that oxidative stress increased Sup35-carbonylation in response to oxidative stress as might be

expected (Figure 5.5A) for the wild-type strain as well as *abp1, crn1,* and *pan1* cortical actin mutants.

To address whether disrupting cortical actin patch formation influences Sup35 aggregate formation, a Sup35NM-GFP fusion construct was used to visualize aggregate formation. The wild-type and *abp1* mutant strains were treated with 100 μM hydrogen peroxide for 20 hours and Sup35NM-GFP expression induced for the final two hours by copper addition. Following hydrogen peroxide treatment, approximately 6% of wild-type cells contained visible Sup35 aggregates (Figure 5.5B). This was reduced in *abp1* mutant cells where 0.5% of cells examined contained visible Sup35 aggregates. Although the frequency of aggregate formation is reduced in the *abp1* mutant strain (frequency = 5×10^{-1}), it is still much higher than the frequency of [*PSI*$^{+}$] prion formation observed in the *abp1* mutant in response to the same oxidative stress conditions (frequency = 1.28×10^{-6}).

To further examine whether loss of *ABP1* affects Sup35 aggregation, the subcellular distribution of Sup35 was examined biochemically during oxidative stress conditions. Sup35-GFP puncta are not necessarily indicative of amyloidogenic-aggregation since GFP-puncta may arise due to amorphous aggregation or the formation of other granules such as stress granules. We therefore used a protocol which separates soluble fractions from SDS-insoluble high-molecular weight forms (Ness et al, 2002). Sup35 was predominantly detected in the soluble fraction in wild-type cells as expected. In response to oxidative stress conditions, a small fraction of Sup35 was present in an SDS-insoluble high-molecular weight form (Figure 5.5C). Surprisingly, a higher proportion of Sup35 was already present in this SDS-insoluble high-molecular

weight form in the *abp1* mutant in the absence of stress, and there was no further increase in response to hydrogen peroxide treatment (Figure 5.5C).

For comparison to Sup35 aggregation, we examined the aggregation of a non-amyloidogenic protein in the *abp1* mutant. We used a thermolabile allele of *UBC9* fused to GFP (GFP–Ubc9^{ts}) which was expressed under the control of the *GAL1* galactose-regulated promoter (Escusa-Toret et al, 2013). At permissive temperatures, GFP–Ubc9^{ts} is native and diffuse, whereas, shifting cells to 37 °C causes GFP–Ubc9^{ts} to misfold and to form puncta visible by fluorescence microscopy. These protein quality control structures are referred to as Q-bodies and do not contain amyloid aggregates (Escusa-Toret et al, 2013). Cells were grown in raffinose media prior to inducing GFP–Ubc9^{ts} expression for three hours following galactose addition. We found that approximately 90% of wild-type cells formed Q-bodies following a temperature shift to 37 °C for 30 minutes (Figure 5.5D). A similar number of cells containing Q-bodies were also detected in the *abp1* mutant suggesting that loss of *ABP1* does not affect non-amyloidogenic protein aggregation.

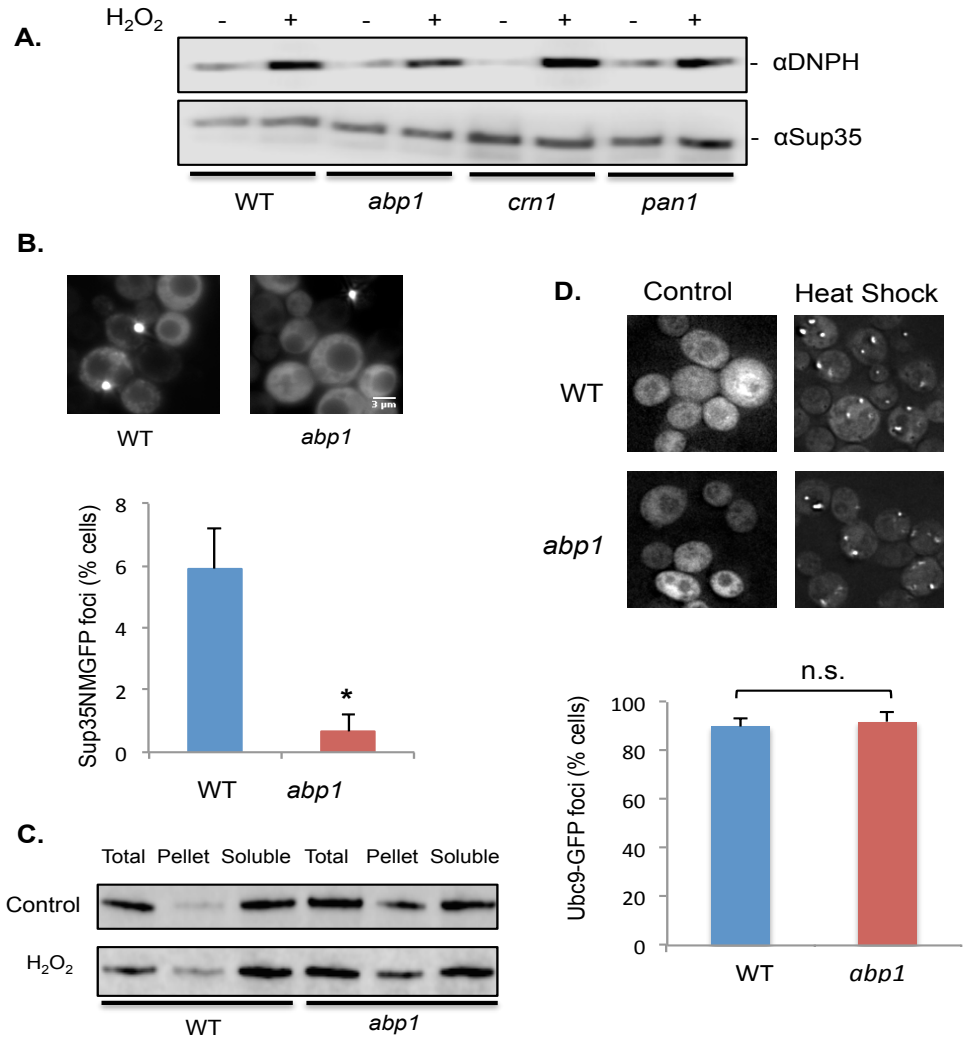

Figure 5.5: Loss of Abp1 does not affect Sup35 oxidation but reduces the frequency of Sup35 aggregate formation. (A) Mutants disrupting the cortical actin cytoskeleton do not affect Sup35 oxidative damage. The wild-type, *abp1, crn1* and *pan1* mutant strains were treated with 100 μM hydrogen peroxide for 20 hours and protein carbonylation used as a measure of protein oxidative damage. Protein extracts were treated with the carbonyl-specific probe, DNPH, and analyzed by Western blot analysis using an antibody against DNPH. Sup35 was used as a loading control detected using antibodies targeted against Sup35 (αSup35). **(B)** Loss of *ABP1* reduces the frequency of Sup35 aggregate formation. Fluorescence micrographs are shown for the wild-type and *abp1* mutant strain treated with 100 μM hydrogen peroxide for 20 hours. Sup35-NMGFP was induced with copper to visualize aggregate formation. The aggregate frequency is expressed as the percentage of cells containing visible Sup35 foci from approximately 1000 cells counted. Data shown are the means of at least three independent biological repeats. Error bars denote standard deviation. Statistical analysis was performed by one-way ANOVA comparing the Sup35 foci frequency between wild-type strain and *abp1* mutant (*$p<0.01$). **(C)** Subcellular distribution of Sup35 in wild-type and *abp1* mutant cells grown in the presence or absence of 100 μM hydrogen peroxide for 20 hours. Total, total crude extract; Soluble, soluble fraction; Pellet, SDS-resistant high molecular weight fraction. **(D)** Representative fluorescent micrographs are shown for the wild-type and *abp1* mutant cells expressing GFP–$Ubc9^{ts}$. Strains were grown in SRaf media before switching to SGal media to induce GFP–$Ubc9^{ts}$ expression for 3 hours. This was followed by a 37°C heat shock for 30 minutes to trigger the misfolding and aggregation of Ubc9. Quantification of the

frequency of GFP–Ubc9 foci is expressed as a percentage of cells containing fluorescence foci out of approximately 300 cells counted. Data shown are the means at least three independent biological repeats. Error bars denote standard deviation. Statistical analysis was performed by one-way ANOVA comparing the GFP–Ubc9 frequency between wild-type strain and *abp1* mutant ($^{n.s.}$not statistically significant).

5.2.6 Loss of *ABP1* reduces the colocalization of Sup35 with Rnq1 puncta.

The amyloidogenic [*RNQ*$^{+}$] prion form of Rnq1 localizes to the IPOD and is thought to influence the aggregation of other proteins (Kaganovich et al, 2008; Tyedmers et al, 2010b). This is further supported by the observation that during overexpression induced [*PSI*$^{+}$] prion formation, approximately 60% of Sup35-RFP puncta colocalize with Rnq1-GFP puncta (Arslan et al, 2015). Newly formed Sup35-RFP puncta were found to perfectly colocalize with Rnq1-GFP puncta, whereas, mature Rnq1-GFP and Sup35-RFP puncta were found that did not colocalize. We therefore visualized the relationship of Sup35 and Rnq1 during oxidant induced [*PSI*$^{+}$] prion formation. [*PIN*$^{+}$][*psi*$^{-}$]-versions of the wild-type and *abp1* mutant strains were grown in the absence or presence of 100 μM hydrogen peroxide for 20 hours to induce prion formation. Sup35NM-RFP and Rnq1-GFP were expressed under the control of the *GAL1* promoter and were induced for three hours to visualize Sup35 and Rnq1 aggregate formation. Similar to overexpression-induced [*PSI*$^{+}$] prion formation, 81% of Sup35 puncta colocalized with Rnq1 puncta following oxidant treatment of the wild-type strain (Figure 5.6). This was comparable to the 71% of Sup35 puncta which colocalized with Rnq1 puncta during control conditions in the absence of stress. In contrast, 14% (stressed) and 10% (unstressed) of Sup35 puncta colocalized with Rnq1 puncta in the *abp1* mutant strain. Oxidant induced Sup35 aggregates are therefore formed at a somewhat reduced frequency and do not

colocalize with the IPOD in an *abp1* mutant which may account for the reduced frequency of [*PSI*$^{+}$] prion formation in this mutant.

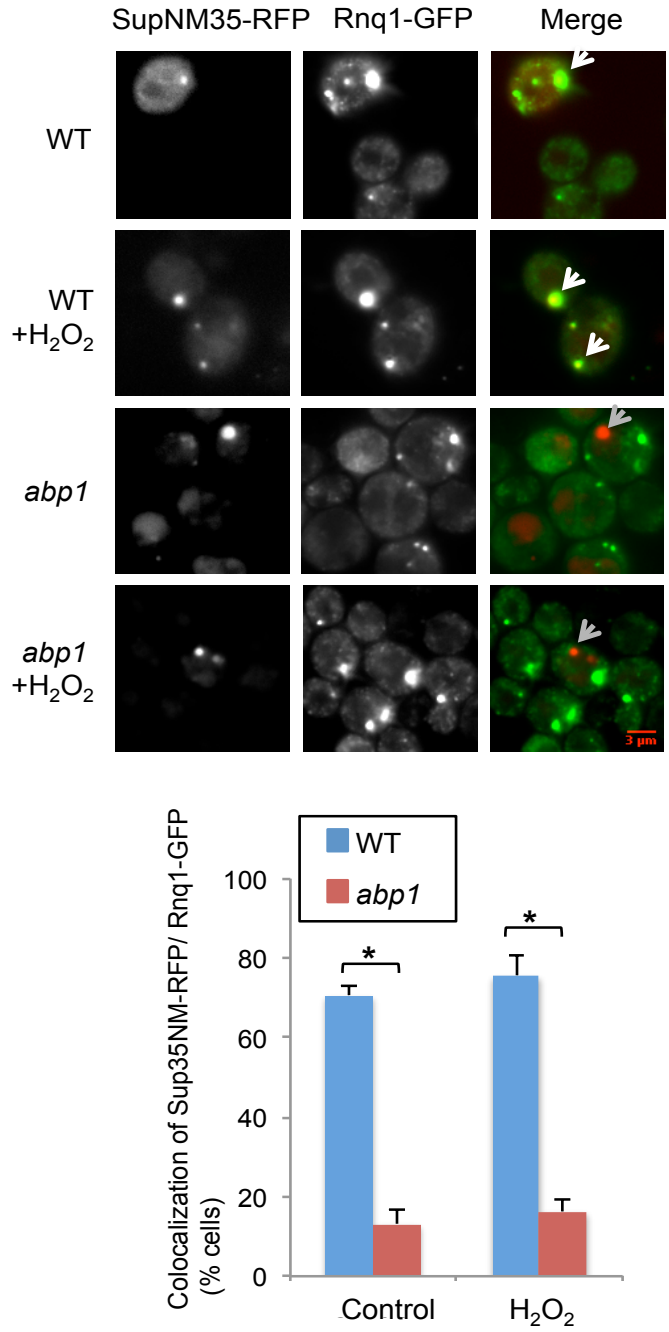

Figure 5.6: Loss of *ABP1* reduces the colocalization of Sup35 with Rnq1 aggregates. The wild-type and *abp1* mutant strains containing *GAL1-SUP35NM-RFP* and *GAL1-RNQ1-GFP* plasmids were grown for 20 hours in SRaff media in the absence or presence of 100 μM hydrogen peroxide before switching to SGal media for three hours to induce the expression of Sup35NM-RFP and Rnq1-GFP respectively. White arrows show examples where Sup35NM-RFP and Rnq1-GFP colocalize, whereas, grey arrows show examples where Sup35NM-RFP does not localize with Rnq1-GFP. The frequency of colocalization of Sup35NM-RFP and Rnq1-GFP is shown as a percentage of cells examined from at least 17 Sup35NM-RFP aggregates counted. Data shown are the means at least three independent biological repeats.

Error bars denote standard deviation. Statistical analysis was performed by one-way ANOVA with pair-wise comparisons using Tukey HSD test comparing the frequency of colocalization of Sup35NM-RFP and Rnq1-GFP between the wild-type strain and the *abp1* mutant in the absence or presence hydrogen peroxide treatment (*p<0.01).

5.3 DISCUSSION

Our data suggest an important role for the Arp2/3 complex in prion formation since loss of *ABP1, CRN1* or *PAN1* all abrogate oxidant-induced [*PSI*$^{+}$] prion formation. The Arp2/3 complex is a seven-protein complex containing two actin-related proteins (Arp2 and Arp3) and five non-actin related proteins (Galletta et al, 2010). It is required for the motility and integrity of actin cortical patches, and for actin-dependent processes such as endocytosis and organelle inheritance. For example, conditional Arp2/3 mutants are deficient in actin patch formation suggesting that Arp2/3 is required for the assembly and organization of cortical actin filaments (Winter et al, 1997). Nucleation promoting factors such as Abp1 and Pan1 associate with the Arp2/3 complex and stimulate actin nucleation (Mishra et al, 2014; Goode et al, 2015). Crn1 regulates actin filament nucleation and the branching activity of the Arp2/3 complex through its interaction with the Arc35 subunit (Humphries et al, 2002). Disrupting the actin cytoskeleton by deletion of *ABP1,* or treating cells with LTA, decreased the frequency of Sup35 aggregate formation and [*PSI*$^{+}$] prion formation suggesting that the cortical actin cytoskeleton is required for the conversion of soluble Sup35 into its heritable prion form.

Previous studies have implicated the Arp2/3 complex in prion formation and shown that Sup35 physically interacts with various proteins of the cortical actin cytoskeleton (Ganusova et al, 2006). This includes Arp2 and Arp3 which were shown to interact with the N-terminal prion forming domain of Sup35 using a two-hybrid assay. We found that Arp2 and Arp3 preferentially associate with

Sup35 under oxidative stress conditions. This difference might arise since we have used native Sup35 expressed under the control of its own promoter, rather than a fragment of Sup35 fused to the DNA domain of Gal4 in a two-hybrid assay. Additionally, Gal4-activation domain fusion proteins are unlikely to assemble into normal actin complex structures in the nuclear two-hybrid assay (Ganusova et al, 2006). An interaction between actin and overexpressed Sup35 was also shown using immunoprecipitation experiments (Ganusova et al, 2006) similar to our finding that Sup35 interacts with actin in wild-type and *tsa1 tsa2* mutant cells. This is in agreement with the idea that actin organization at the cell periphery is important for the initial formation of the [*PSI*$^+$] ring, which is thought to be an initial stage in prion formation (Mathur et al, 2010).

We found that loss of *ABP1, CRN1* or *PAN1*, or disrupting the cortical actin cytoskeleton by LTA treatment, prevented oxidative stress-induced [*PSI*$^+$] prion formation but only modestly disrupted Sup35-overexpression-induced aggregation and [*PSI*$^+$] prion formation. This suggests that the mechanism underlying the conversion of the soluble protein to its amyloid form is different for overexpression-induced versus oxidative stress promoted formation. The strongest effect on induced [*PSI*$^+$] prion formation was seen with an *abp1* mutant, which abrogated Sup35 ring formation, although the frequency of [*PSI*$^+$] prion formation was still strongly induced in this mutant. In comparison, loss of *PAN1* or *CRN1* did not affect the frequency of Sup35 overexpression-induced [*PSI*$^+$] prion formation and only modestly decreased Sup35 aggregate formation. Other studies have linked cortical actin patch formation with overexpression-induced [*PSI*$^+$] prion formation. For example, loss of *LAS17* or *SAC6* inhibited both induced [*PSI*$^+$] prion and ring formation (Manogaran et al, 2011). Las17 is a nucleation promoting factor similar to Pan1 and Abp1,

although Las17 is a stronger nucleation promoting factor compared with Pan1 and Abp1 (Sun et al, 2006). Lsb2 is a stress-induced Las17-interacting protein which promotes induced [*PSI*$^{+}$] prion formation via the association of Las17 with cortical actin patches (Chernova et al, 2011). Sac6, an actin-bundling protein is the major F-actin crosslinking protein in budding yeast (Adams et al, 1995). Additionally, loss of other genes affecting actin patch formation including *SLA1, SLA2* and *END3* has been shown to decrease the frequency of Sup35 overexpression-induced [*PSI*$^{+}$] formation (Ganusova et al, 2006; Mathur et al, 2010). Taken together, these data strongly implicate actin cytoskeletal networks in [*PSI*$^{+}$] prion formation, although there appear to be mechanistic differences between overexpression and oxidative stress-induced prion formation.

Accumulating evidence suggests that eukaryotic cells defend themselves against protein aggregation by sequestering misfolded proteins into defined quality control compartments. Studies in yeast cells have revealed intricate protein quality control systems where insoluble proteins are partitioned into defined sites in the cell; amyloid and amorphous aggregates are believed to be processed via distinct cytosolic protein inclusion bodies (Kaganovich et al, 2008; Sontag et al, 2014). Upon proteasome inhibition, JUNQ (JUxta Nuclear Quality control compartment) serves as a sequestration site for ubiquitinated proteins, whereas, the IPOD sequesters terminally misfolded and amyloidogenic proteins. Additionally, when proteasomes are active, misfolded proteins aggregate into Q-bodies (Spokoini et al, 2012; Escusa-Toret et al, 2013; Roth and Balch, 2013). Asymmetric inheritance means that aggregated proteins are retained in the mother cell which protects daughter cells from the inheritance of aberrant protein aggregates (Liu et al, 2010; Zhou et al, 2011). Despite these PQC (Protein Quality Control) systems excessive widespread protein aggregation is toxic to

cells, especially during aggregation-promoting-stress conditions or when the proteostasis network is compromised (Koplin et al, 2010; Weids and Grant, 2014). Additionally, the build-up and aggregation of misfolded proteins is thought to impair ubiquitin-proteasome degradation in eukaryotic cells and may play a critical role in ageing and neurodegenerative diseases (Bence et al, 2001; Verhoef et al, 2002; Haynes et al, 2004; Andersson et al, 2013).

Extensive research has made use of Sup35NM-GFP fusion proteins that can be switched to a heritable prion form by wild-type [*PSI*$^{+}$] prions. As with wild-type Sup35, the Sup35NM-GFP fusion protein retains the unstructured PrD that has a high propensity to misfold (Scheibel and Lindquist, 2001). Overexpression of Sup35NM-GFP results in the detection of fluorescent puncta as well as ribbon and ring-like aggregates (Zhou et al, 2001; Ganusova et al, 2006). The ribbon and ring-like aggregates are characteristic of the *de novo* formation of [*PSI*$^{+}$]. Careful analysis of the temporal formation of aggregate structures has revealed the initial formation of cytoplasmic dots (Arslan et al, 2015). One of the dots located near the vacuole gives rise to lines which extend towards the cell periphery followed by peripheral and internal ring-like forms. Overexpressed Sup35NM-GFP is initially soluble, but the PrD has a high propensity to misfold and the misfolded protein is thought to be targeted to the IPOD (Tyedmers et al, 2010b). Other prion proteins including Ure2 and Rnq1 localize to the IPOD which facilitates nucleation and [*PSI*$^{+}$] induction (Kaganovich et al, 2008; Tyedmers et al, 2010b). All Rnq1 dots have been shown to overlap with newly induced Sup35 dots (Arslan et al, 2015). Similarly we found that all oxidant-induced Sup35 dots colocalized with Rnq1 dots in a wild-type strain. However, in contrast, relatively few oxidant-induced Sup35 dots were seen to colocalize with Rnq1 dots. This may explain the reduced

frequency of [*PSI*$^{+}$] prion formation since Sup35 may form aggregates in response to oxidative stress conditions, but these aggregates do not efficiently localize to the IPOD in an *abp1* mutant and hence do not form heritable propagons.

5.4 MATERIALS AND METHODS

5.4.1 Yeast strains and plasmids.

The wild-type yeast strain 74D-694 (*MATa ade1-14 ura3-52 leu2-3,112 trp1-289 his3-200)* was used for all experiments. Strains deleted for *TSA1* (*tsa1*::*LEU2*) and *TSA2* (*tsa2*::*KanMX*) and containing Sup35 tagged at its C-terminus with a tandem affinity purification (TAP) tag have been described previously (Sideri et al, 2011). Strains deleted for *ABP1, CRN1* and *PAN1* were constructed in 74D-694 using standard yeast methodology.

The yeast plasmid *CUP1-SUP35NM-GFP* [*URA3*] expressing the Sup35NM domain conjugated to GFP under the control of the *CUP1* promoter has been described previously (Patino et al, 1995) as has the yeast plasmid p2018 containing *GAL1-SUP35NM-RFP* [*LEU2*] (Arslan et al, 2015). Rnq1 was visualized using a yeast plasmid containing *GAL1-RNQ1-EGFP* [*URA3*] which expresses Rnq1-GFP under the control of the *GAL1* promoter (Meriin et al, 2002). A thermo-labile allele of *UBC9* fused to GFP (*GFP–Ubc9*^{ts}) was expressed under the control of the *GAL1* galactose-regulated promoter (Escusa-Toret et al, 2013).

5.4.2 Growth and stress conditions.

Strains were grown at 30°C with shaking at 180 rpm in rich YEPD medium (2% [weight/volume] glucose, 2% [weight/volume] bactopeptone, 1%

[weight/volume] yeast extract) or minimal SD (0.67% [weight/volume] yeast nitrogen base without amino acids, 2% [weight/volume] glucose) supplemented with appropriate amino acids and bases. SRaf media contained 2% (weight/volume) raffinose and SGal media contained 2% (weight/volume) galactose. Media were solidified by the addition of 2% (weight/volume) agar. Strains were cured by five rounds of growth on YEPD agar plates containing 4 mM guanidine hydrochloride (GdnHCl). Where indicated, strains were grown in the presence of 100μM hydrogen peroxide for 20 hours prior to analysing [*PSI*$^{+}$] prion formation. Cells were treated with 10μM latrunculin to disrupt the actin cytoskeleton.

5.4.3 Analyses of prion formation.

The frequency of spontaneous [*PSI*$^{+}$] prion formation was scored by growth in the absence of adenine. Diluted cell cultures were plated onto SD plates lacking adenine (SD-Ade) and incubated for 7-10 days. Colonies which grew on SD-Ade plates were counted and then picked onto new SD-Ade plates before replica-printing onto SD-Ade and SD-Ade containing 4mM GdnHCl. Colonies that grew on SD-Ade, but not on SD-Ade with GdnHCl were scored as [*PSI*$^{+}$]. [*PSI*$^{+}$] colonies were also scored by visual differentiation of red/white colony formation on YEPD plates and by the conversion of pink/white [*PSI*$^{+}$] colonies to red [*psi*$^{-}$] colonies on YEPD plates containing GdnHCl. For oxidant induced prion assays, cultures were grown in the presence of 100μM hydrogen peroxide for 20 hours prior to scoring [*PSI*$^{+}$] formation. For Sup35 overexpression-induced prion assays, cultures were grown in the presence of 50μM copper sulphate for 20 hours to induce *CUP1-SUP35NM-GFP* expression prior to scoring [*PSI*$^{+}$] formation (Speldewinde et al, 2015). *De novo* [*PIN*$^{+}$]

formation was performed as previously described (Sideri et al, 2011). [*PSI*$^{+}$] and [*PIN*$^{+}$] formation was calculated based on the means of at least three independent biological repeat experiments.

5.4.4 Microscopy analysis.

Rhodamine phalloidin staining of actin was performed as described previously (Amberg, 1998). Sup35 aggregate-formation was visualized using *CUP1-SUP35NM-GFP* following 50μM copper sulphate addition to induce the *CUP1* promoter (Sideri et al, 2011). Sup35 and Rnq1 colocalization experiments were conducted using plasmids containing *GAL1-SUP35NM-RFP* and *GAL1-RNQ1-EGFP.* Strains were grown in the presence or absence of 100mM hydrogen peroxide for 20 hours in SRaf media before switching to SGal media for three hours to induce the expression of *GAL1-SUP35NM-RFP* and *GAL1-RNQ1-EGFP.* Visualization of the aggregation of a non-amyloidogenic protein Ubc9 was performed using *GAL1-GFP–Ubc9*^{ts}. Strains were grown in SRaf media before switching to SGal media for 3 hours to induce the expression of *GAL1-GFP–Ubc9*^{ts}. The temperature was shifted to 37 °C for the final 30 minutes to trigger Ubc9 misfolding.

Cells were washed and immobilised on 10% (volume/volume) poly-L-lysine-coated slides. All images were acquired on a Delta Vision (Applied Precision) restoration microscope using a 100x/NA 1.42 Plan Apo objective and fluorescein isothiocyanate (FITC) and Texas Red band pass filters from the Sedat filter set (Chroma). The images were collected using a Coolsnap HQ (Photometrics) camera with a Z optical spacing of 0.2μm. Raw images were then deconvolved using the Softworx software and maximum intensity projections of these deconvolved images are shown in the results.

5.4.5 Sup35-TAP affinity purification and mass spectrometry.

Sup35-TAP affinity purification was performed as described previously (Sideri et al, 2011). Sup35-interacting proteins were identified in the wild-type and *tsa1 tsa2* mutant strains by mass spectrometry in triplicate for each strain. For protein identification, protein samples were run a short distance into SDS-PAGE gels and stained using colloidal Coomassie blue (Sigma). Total proteins were excised, trypsin digested, and identified using liquid chromatography-mass spectrometry (LC-MS) performed by the Biomolecular Analysis Core Facility, Faculty of Life Sciences, The University of Manchester. Proteins were identified using the Mascot mass fingerprinting programme (www.matrixscience.com) to search the NCBInr and Swissprot databases. Final datasets for each condition were determined by selecting proteins that were identified in at least two of the three replicates.

5.4.6 Protein analysis.

Protein extracts were electrophoresed under reducing conditions on SDS-PAGE minigels and electroblotted onto PVDF membrane (Amersham Pharmacia Biotech). Bound antibody was visualised by chemiluminescence (ECL, Amersham Pharmacia Biotech). Primary antibodies used were Sup35 (Ness et al, 2002), Tsa1 (Trotter et al, 2008), Tef1 (Sundaram and Grant, 2014), Abp1 (Abcam), Arp3 (Santa Cruz Biotechnology), Sap190 (affinity-purified polyclonal antibody raised against Sap190 peptides), Act1 (ThermoFisher Scientific) and Pgk1 (ThermoFisher Scientific).

The analysis of Sup35 aggregates by subcellular fractionation was performed essentially as described previously (Ness et al, 2002). Briefly, exponential phase cells (A_{600} ~0.5) were collected by centrifugation, washed

once with distilled water, and resuspended in buffer ST [10mM sodium phosphate buffer, pH7.5, 250mM NaCl, 2% (weight/volume) SDS, 1% (weight/volume) Triton X-100, 2mM PMSF]. Cells were broken with glass beads using a Minibead beater (Biospec Scientific, Bartlesville) for 30 s at 4°C and centrifuged at 3000g for 3 minutes at 4°C. The supernatant (total) was centrifuged at 13000g for 45 minutes at 4°C to separate the soluble (supernatant) and insoluble (pellet) fractions. The soluble and insoluble fractions were resuspended in an equal volume of ST buffer prior to western blot analysis.

Protein carbonylation was measured by reacting carbonyl groups with 2,4-dinitrophenyl-hydrazine (DNPH) based on previously described methods (Shacter et al, 1994; Trotter et al, 2006). Briefly, exponential phase cells (A_{600} ~0.5) were broken with glass beads in 10% (weight/volume) trichloroacetic acid (TCA) using a Minibead beater. The supernatant was centrifuged at 13000g for 15 mins at 4°C and the protein pellet washed with acetone to remove residual TCA. The pellet was dried and resuspended in 70 µl of 6% (weight/volume) SDS. 70 µl of 10mM 2,4-dinitrophenyl hydrazine (DNPH) in 10% (volume/volume) trifluoroacetic acid were added and incubated at room temperature for 20 minutes. 45 µl of 2M Tris/30% (volume/volume) glycerol were added to the suspension and mixed to neutralize the DNPH reaction. SDS-PAGE sample buffer was added prior to western blot analysis using rabbit anti::DNPH (Dako) antibodies to detect carbonylation.

5.4.7 Statistical analysis.

Data are presented as mean values ± standard deviation (SD). Statistical analysis for multiple groups was performed using one-way ANOVA with pair-

wise comparisons of sample means via the Tukey HSD test or two-way ANOVA with multiple comparisons of sample means via the Tukey HSD test. Results were considered statistically significant with a p-value less than 0.05.

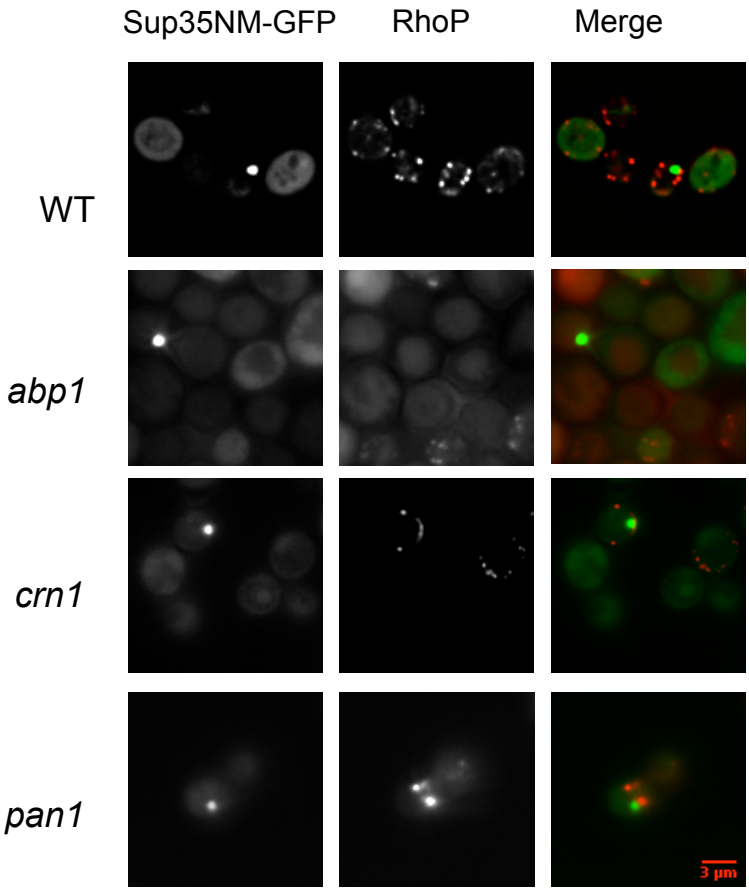

Supplementary Figure 5.1: Visualization of overexpression-induced Sup35 aggregates and the cortical actin cytoskeleton. Fluorescence micrographs are shown for [*PIN*$^+$][*psi*$^-$] versions of the wild-type, *abp1, crn1* and *pan1* mutant strains containing the *CUP1-SUP35NM-GFP* plasmid induced with copper for 24 hours. Rhodamine-phalloidin (RhoP) staining was used to visualize the cortical actin cytoskeleton.

Supplementary Table 5.1: Proteins co-purifying with Sup35 in wild-type and *tsa1 tsa2* mutant strain.

Strain	Protein
Wild-type (63)	Vma2, Tdh1, Ura7, Adh1, Gfa1, Faa4, Ssc1, Ura1, Atp1, Rpl3, Nop58, Prp43, Cct8, Rpl6B, Nan1, Ddr48, Mss116, Rps20, Gcd6, Faa1, Eno2, Tdh2, Cdc19, Puf6, Tub2, Nop56, Rps6B, Mcm6, Utp4, Sam1, Rvb2, Rpl13B, Gcn1, Utp8, Rrp5, Pfk1, Ilv2, Rpl4A, Sec23, Rpl21A, Pet9, Kar2, Vma1, Fpr3, Eft1, Sst1, Act1, Sse1, Ccd48, Sec26, Kap123, Ssa2, Hsc82, Tef2, Pdi1, Rpn2, Acc1, Pma1, Crn1, Ssb2, Ssa1, Hsp60, YHR020W
tsa1 tsa2 (47)	Cop1, Abp1, Arc40, Ufd4, Ura2, Sec21, Vps13, Sap190, Sec27, Ufo1, Asc1, Yef3, Spt5, Fas1, Fas2, Lpd1, Arc35, Ssa4, Prc1, Rpb2, Noc3, Arp2, Sac6, Hsp78, Arp3, Pim1, Hsp104, Sap185, Aif1, Eft1, Sti1, Act1, Sse1, Cdc48, Sec26, Kap123, Ssa2, Hsc82, Tef2, Pdi1, Rpn2, Acc1, Pma1, Crn1, Ssb2, Ssa1, Hsp60
Common (18)	Eft1, Sti1, Act1, Sse1, Cdc48, Sec26, Kap123, Ssa2, Hsc82, Tef2, Pdi1, Rpn2, Acc1, Pma1, Crn1, Ssb2, Ssa1, Hsp60

5.5 Acknowledgements.

S.H.S. was supported by a Wellcome Trust funded studentship. This work was funded by BBSRC grants BB/J000183/1 (to CMG) and BB/J000191/1 (to MFT). We thank Susan Lindquist, Susan Liebman and Judith Frydmen for generously providing plasmids used in the study. The Bioimaging Facility microscopes used in this study were purchased with grants from BBSRC, Wellcome and the University of Manchester Strategic Fund. Special thanks goes to Peter March and Steve Mardsen for their help with the microscopy. We are grateful to David Knight and Emma-Jane Keevil in the Biomolecular Analysis Core Facility, The University of Manchester for their help with mass spectrometry analysis.

Chapter 6: General Discussion

6.1 Summary.

Prions are enigmatic proteinaceous entities capable of self-perpetuation and transmission from one species to another. Prions are the causal agent behind a group of infectious diseases collectively known as the transmissible spongiform encephalopathies. These diseases include scrapie in sheep, Creutzfeldt-Jakob disease and Kuru in humans and bovine spongiform encephalopathy in cattle (Prusiner, 1998). The self-replicating feature of prions occurs by the repeated seeding of the misfolded PrP^{Sc} prion form onto native PrP^{C} molecules and their conversion to the prion form that underlies the pathogenicity of these diseases (Aguzzi, 2008). As yet, no effective therapies have been developed against prion diseases. In addition, many other neurodegenerative diseases caused by abnormal protein aggregation including Alzheimer's, Parkinson's and Huntington's have been considered to share prion-like properties in terms of their formation, propagation and disease manifestation. As such, studies that focus upon uncovering the mechanistic basis and factors affecting prion formation as well as their propagation/infection have become increasingly relevant in the discovery of new therapeutic intervention strategies against these debilitating protein aggregation diseases.

6.2 Autophagy serves a protective role against prion formation.

Autophagy is an intracellular quality control process functioning in the degradation of toxic and aberrant proteins as well as the disposal of dysfunctional organelles. Autophagy proceeds in a highly sequential manner that is regulated by autophagy related genes (*ATG*s), of which 41 genes have been identified in yeast thus far. Impaired activity of autophagy has been

implicated in a variety of neurodegenerative diseases caused by the abnormal aggregation of specific proteins including prions in prion diseases (Wirawan et al., 2012). However, the mechanistic basis of the role for autophagy in *de novo* prion formation is not comprehensively understood which was the primary aim of our study. Previous studies have linked prions and autophagy where large autophagic bodies were often observed in neuronal cells of prion-infected mice models (Boellard et al., 1991; Liberski et al, 2004). In our study, we demonstrated that the knockdown of core *ATG*s required for non-selective autophagy to function corresponds with an increase in the *de novo* frequency of both [*PSI*$^{+}$] and [*PIN*$^{+}$] prion formation. Similarly, the rise in [*PSI*$^{+}$] formation is also consistent with an elevated frequency of Sup35 aggregates observed in these core autophagy knockout mutants. This data agrees with other studies in mammalian systems which have shown downregulation of autophagy activity via application of autophagy inhibitors such as wortmannin, or siRNA knockdown on *Atg5,* results in elevated prion formation (Heiseke et al, 2009; Aguib et al, 2009). Conversely, Atgs which are essential for selective autophagy to occur, such as Atg11 and Atg33*,* do not appear to influence *de novo* prion formation or Sup35 aggregation. This is in agreement with the idea that autophagy normally acts to suppress the *de novo* formation of prions.

Several studies using mammalian prion models have also shown that the supplementation of pharmacological compounds that elicit the promotion of autophagic flux such as lithium, rapamycin and trehalose, correlates with a clearing effect on prion aggregates (Heiseke et al, 2009; Aguib et al, 2009). The polyamine, spermidine, can be used as a pharmacological treatment to upregulate autophagic flux in yeast, flies, worms and mammalian cell lines (Eisenberg et al 2009). In our study, spermidine treatment was found to

attenuate the elevated frequency of *de novo* prion formation observed in an antioxidant mutant (*tsa1 tsa2*), and in a protein phosphatase 1 mutant, *ppq1* that allows the detection of low levels of prion formation. Further development of pharmacological agents that modulate autophagic flux may therefore be a promising area for developing therapeutic agents to prevent prion diseases.

Prion studies performed in our lab have also established oxidative stress as a causal trigger for yeast prion formation (Sideri et al, 2011; Doronina et al, 2015). Interestingly, this current study found increased oxidation of Sup35 methionine residues in an *atg1* mutant correlates with an increased frequency of *de novo* prion formation. Indeed, growth of the *atg1* mutant in the absence of oxygen (anaerobic conditions) reduced the frequency of prion formation to wild-type levels. These results indicate that autophagy has a role at the initial stages of prion formation by facilitating the clearance of oxidatively damaged Sup35 that have a higher propensity towards misfolding and its subsequent conversion into the infectious [*PSI*$^{+}$] prion form. Furthermore, spermidine application was also found to reduce the frequency of aggregated Sup35 molecules in cells that are already [*PSI*$^{+}$] as well as abrogating *de novo* [*PIN*$^{+}$] formation. These data show that the autophagy machinery may also act to clear larger Sup35 aggregated polymers as well as misfolded Rnq1 molecules within cells. Taken together, our data provides further evidence that the core autophagy machinery serves a protective role in preventing against elevated *de novo* prion formation and aggregation of prion proteins in yeast.

6.3 Prions have a pro-chronological effect on yeast lifespan in autophagy proficient cells.

The majority of prion disease cases in humans occur in a sporadic manner, predominantly manifesting during later stages of life (Appleby et al, 2007). Neuronal cells are post-mitotic in nature and rely on proteostasis mechanisms such as autophagy to facilitate elimination of superfluous and damaged material. Yeast has emerged as a powerful model to investigate the stochasticity of the ageing process and its contributing factors (Kaeberlein, 2010; Longo et al, 2012). Yeast ageing is primarily studied in two ways: via replicative lifespan (the number of daughter cells produced by a particular mother cell) and chronological lifespan (the length of time required for the cells to remain viable).

Yeast prions when formed and stably propagated confer either a loss or gain of function phenotype in their host. For example, prions such as Sup35 and Swi2 are involved in translation regulation and chromatin remodeling respectively and consequently may manifest a series of differential phenotypes epigenetically when they are converted to their prion forms (Liebman and Chernoff, 2012). However, whether prions are beneficial or deleterious to their fungal host still remain a hotly debated topic. Additionally, the role of prions towards the yeast ageing process and *vice versa* has also not been comprehensively understood. Moreover, autophagy has also been identified as an important modulator towards the ageing process as its dysregulation is strongly implicated in several neurodegenerative diseases. We thus sought to investigate the connection between prions and autophagy in the context of chronological ageing in yeast.

Using the wild-type strain and an *atg1* deletion mutant in a [*PIN*$^+$][*psi*$^-$] background we assessed the levels of *de novo* [*PSI*$^+$] formation in relation to the chronological age of cells. We found a correlation between the chronological age of cells and the frequency of *de novo* [*PSI*$^+$] formation i.e. as cells advance further in age, there is a proportional increase in *de novo* [*PSI*$^+$] formation. Furthermore, the elevation of spontaneous [*PSI*$^+$] formation was more pronounced in an *atg1* mutant relative to the wild-type strain thus supporting a protective role for autophagy against prion formation during chronological ageing.

A novel and somewhat intriguing finding in our study was the enhanced longevity observed in wild-type cells carrying either the [*PSI*$^+$] or [*PIN*$^+$] prions during chronological lifespan analysis while, in comparison, cells that were cured of prions showed a much reduced lifespan. Additionally, this longevity promoting phenotype was not observed in *atg1* mutants during chronological ageing regardless of prion background. During chronological ageing, we found that autophagy competent cells carrying the [*PSI*$^+$] prion had increased autophagic flux compared to the [*PIN*$^+$][*psi*$^-$] cells and the cured versions of the same cells. Supplementation of the growth media with the polyamine spermidine was also found to improve chronological lifespan in wild-type cells carrying prions but this effect was minimal in the cured version (Figure 6.1A). It is unclear why there was no improvement of chronological lifespan in cured wild-type strains with spermidine application. This could be due to unforeseen effects on chronological lifespan resulting from the inactivation of Hsp104 by GdnHCl treatment as well as the loss of prion formation that is not rescued by spermidine addition. Chronological lifespan studies in the absence or presence of spermidine in strains deleted for *RNQ1* that cannot effectively form the [*PSI*$^+$]

prion could be further employed to examine the reason for this observation. Moreover, spermidine addition improved the CLS of the *atg1* strains, notably in cured *atg1* cells (Figure 6.1B). These results indicate that spermidine may facilitate improved CLS extension through additional mechanisms other than autophagy such as alteration of acetylation patterns of proteins as have been suggested previously (Eisenberg et al, 2009; Morselli et al, 2011; Morselli et al, 2015) that may directly or indirectly impinge upon longevity-associated pathways. Furthermore, our data show the [*PSI*$^{+}$] prion may be harmful to yeast viability during chronological ageing when autophagy is dysfunctional. In our previous study we found that basal autophagy levels were slightly elevated in mutants with a higher rate of *de novo* [*PSI*$^{+}$] formation (Speldewinde et al, 2015) thus postulating a role where increased protein aggregation albeit at non-toxic levels may directly or indirectly promote basal autophagy thereby leading to improved lifespan extension. Calorie restriction has been shown to facilitate lifespan improvement in most model organisms tested (Longo et al, 2012), as such, the role of calorie restriction during chronological ageing in cells carrying prions compared to prion free cells should be further investigated. Our study provides evidence for a potentially beneficial role of prions to their host as they may present additional adaptive mechanisms to their host in order to increase chances of survival in response to environmental fluctuations.

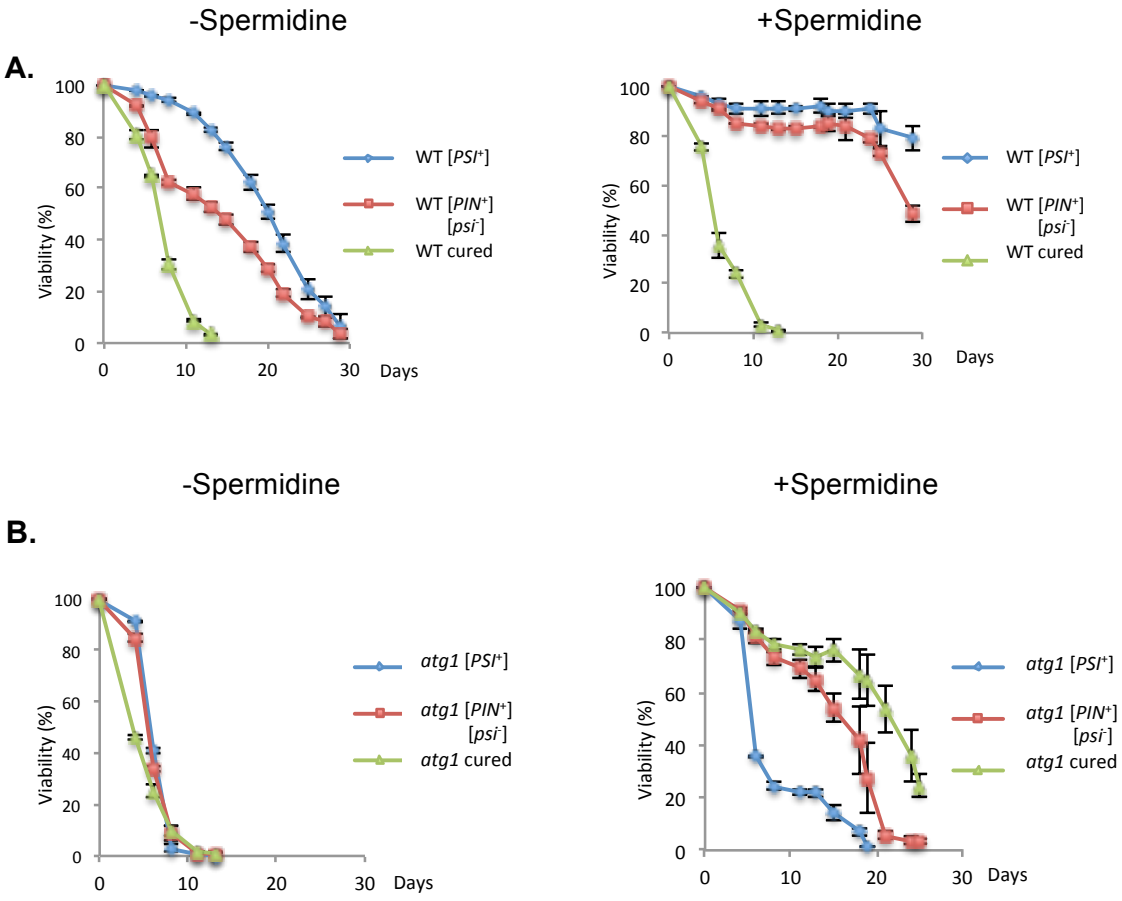

Figure 6.1: Spermidine improves the chronological lifespan of wild-type cells carrying prions but not for cured wild-type cells and extends the lifespan of *atg1* mutants regardless of prion status. Chronological lifespan analysis in liquid SCD media with or without 4mM spermidine supplementation in **(A)** the wild-type strain and **(B)** *atg1* mutant strain in the [*PSI*$^+$], [*PIN*$^+$][*psi*$^-$] and cured background respectively. Cells were cultured for 3 days to reach stationary phase and then aliquots taken every 2-3 days for flow cytometry analysis based on propidium iodide uptake by non-viable cells as assayed through flow cytometry as described in section 4.4.4 Yeast chronological lifespan determination. Data shown are the means of at least three independent biological repeat experiments expressed as the percentage of viable cells out of 10000 cells analysed. Error bars denote standard deviation.

6.4 The cortical actin cytoskeleton is involved in prion formation.

The actin cytoskeleton provides the structural framework for many essential functions of cells including cell division, intracellular transport, cell adhesion mechanosensation, and so on. Actin filament nucleation and branching occurs in a precisely regulated manner that involves the activity of over 100 different proteins including components of the Arp2/3 complex

(Moseley and Goode, 2006). The Arp2/3 complex drives actin filament branching and is comprised of Arp2, Arp3 and five subunits of the Arc1-40 protein family. The actin branching activity of the Arp2/3 complex is strongly facilitated by the nucleating promoting factors: Las17, Myo3/5, Abp1, and Pan1. Actin filament branching is essential in the formation of actin cortical patches and, in particular, the process of endocytosis. Previous studies have characterized the roles of several actin-related components in the formation of prions (Ganusova et al, 2006; Chernova et al, 2011; Manogaran et al, 2011). Additionally, actin monomer sequestration by the addition of the drug, latrunculin A, has been reported to destabilize prion formation in weak [*PSI*$^{+}$] strains (Bailleul-Winslett et al, 2000).

In our study, we further examined the role of the Arp2/3 complex and its nucleating promoting factors in *de novo* prion formation. We demonstrated that relative to the wild-type strain, knockout mutants of *abp1*, *crn1*, and *pan1* elicited reduced *de novo* [*PSI*$^{+}$] formation under basal conditions and, intriguingly, even after oxidative stress challenges which has not been shown in previous studies. Although these mutants abrogated oxidative-stress induced prion formation, they only modestly affect Sup35-overexpression–induced prion formation, suggesting that there may be mechanistic differences underlying the formation of prions during these two promoting conditions.

Given that extensive data has now shown that protein aggregates can be sequestered to distinct intracellular sites as part of the cells protein quality control systems, we examined whether the colocalization of Sup35 with the insoluble protein deposit (IPOD) was affected in an *abp1* mutant. The IPOD is an intracellular sequestration site for misfolded and oxidatively damaged proteins including [*PIN*$^{+}$] aggregates (Tyedmers et al, 2010a; Tyedmers et al,

2010b). [*PIN*$^+$] has been demonstrated to acts as nucleation sites for other prion forming proteins such as Sup35 and Ure2 to template upon thus further form larger prion aggregates (Derkatch et al, 2001; Derkatch et al, 2004). Colocalization studies of Sup35-RFP and Rnq1-GFP were performed under basal and oxidative stress conditions, and, revealed that both proteins do not colocalize in approximately 75% of *abp1* cells examined compared to approximately 20% of wild-type cells where Sup35-RFP and Rnq1-GFP do not colocalize. Furthermore, there was increased carbonylation of Sup35 after oxidant insults in the *abp1* and *pan1* mutants. These results indicate that the transport of oxidized or misfolded Sup35 to the IPOD is disrupted in the *abp1* mutant and possibly other deletion mutants of other components of the Arp2/3 complex such as *pan1* and *crn1* thus attenuating its propensity towards further [*PSI*$^+$] prion formation. Consistent with the phenotypes observed in the *abp1*, *crn1*, and *pan1* deletion mutants respectively, treatment with latrunculin A that inactivated actin nucleation and filament formation was also found to abrogate the frequency of [*PSI*$^+$] prion formation and Sup35 aggregation during oxidative challenges.

6.5 Concluding remarks and future perspectives.

Autophagy is a general protective cellular mechanism against damaged protein and dysfunctional organelles while the actin cytoskeleton provides the structural framework essential for an array of cellular activities, and both these processes are impacted by and/or impact upon cellular ageing. This is particularly true for post-mitotic cells such as neurons where there is a decline in autophagic flux, a possible impairment of actin cytoskeleton and its dynamics and an accumulation of superfluous materials such as protein aggregates as

they cannot be diluted via cell division. Autophagy has been established as a modulator of yeast cell ageing mainly in chronological ageing models (Longo et al, 2012). In aged and diseased cells, actin filamentous aggregates such as Hirano bodies and cofilin rods have been observed in cases of neurodegenerative diseases including Alzheimer's and Huntingon's. Work performed by Gourlay and Ayscough (2005; 2006) demonstrated that the formation of actin aggregates in a mutant with defective actin dynamics was a trigger to hyperactivate the Ras/cAMP/PKA signaling cascade and resulted in increased apoptotic cell death. Furthermore, supplementation with latrunculin A, that sequesters actin monomers, prevented the formation of these aggregates and led to diminished ROS accumulation and reduced cell death. Similarly, knockout of an actin bundling protein, Scp1p, that had abnormal actin cytoskeleton morphology also attenuated ROS levels and markedly promoted replicative lifespan (Gourlay et al, 2004). The actin cytoskeleton has also been shown to be essential for the proper asymmetric segregation of protein aggregates between the mother and daughter yeast cells thus ensuring the next generation of pristine daughter cells where damaged molecules are preferentially retained by the mother cell (Liu et al, 2010).

Previous studies have reported that selective autophagy and not non-selective autophagy is impaired by the disruption of the actin cytoskeleton network (Hamasaki et al, 2005; Reggiori et al, 2005). Our data indicates increased *de novo* prion formation in an *atg19* deletion mutant, which is the receptor required for the cytoplasm-to-vacuole targeting (Cvt) selective autophagy pathway to occur. Interestingly, Arp2 provides the link between the actin cytoskeleton and the Cvt pathway by directing the movement of Atg9 to the pre-autophagosomal structure in the Cvt pathway (Monastyrska et al, 2008).

Treatment with latrunculin A was found to disrupt the movement of Atg9 vesicles as well as result in the defective localization of Atg11. In addition, latrunculin A treatment was also shown to impair the Cvt pathway (He et al, 2006). Similar observations were also found in a strain expressing a mutant form of actin, *Act1-159,* that had abnormal actin cytoskeleton morphology (He et al, 2006). Furthermore, pexophagy, which is the selective macroautophagy responsible for the degradation of peroxisomes, is also dependent on Atg11 and the Arp2/3 complex (Monastyrska et al, 2008). Thus, the impact of an *atg19* knockout and a mutant that disrupts Arp2/3 complex activity on *de novo* prion formation can be further characterized by performing prion formation assays on a double deletion mutant of *atg19* and component of the Arp2/3 complex such as *abp1*.

Prions are epigenetic regulators that are able to transmit phenotypes between successive generations. The [*PSI*$^{+}$] prion reduces translation termination efficiency at stop codons thus enabling uninterrupted translation by the ribosomes. This [*PSI*$^{+}$]-dependent feature allows the repertoire of unique proteins generated within cells that may have non-canonical functions or impact upon their signaling networks. How the presence of the [*PSI*$^{+}$] prion affects the diversity of proteins and longevity of cells would be an interesting avenue to further investigate. On the one hand, the production of non-native proteins by inefficient translation termination by [*PSI*$^{+}$] conditions may result in aggregation and disruption of activity of these proteins within the cell. The elevation of protein aggregation may in turn induce general defensive mechanisms such as autophagy as shown in our data and possibly other elements such as heat shock proteins and ROS scavengers. The connection between protein aggregation, cellular defense systems and chronological longevity of cells

presents interesting paradigms that require further elucidation. On the other hand, inefficient translation termination may result in the production of novel proteins with altered function/regulation that can either be beneficial or deleterious to the cell. Strategies to investigate these possibilities may include global transcriptomic and proteomic profiling in cells carrying prions and prion free cells at differential stages of chronological ageing. In addition, profiling of the expression levels of heat shock proteins and antioxidant proteins (superoxide dismutases, peroxiredoxins) and intracellular ROS levels should also be explored. These could be characterized using techniques such as qPCR, ribosome profiling, ROS markers and western blotting to detect expression levels of these proteins during chronological ageing in cells with different prion backgrounds.

Whether a protein forms a prion is dependent upon the presence of a prion forming domain that is usually non-essential to the overall function of the protein itself. The prion forming domain is capable of catalyzing aggregate formation even without the remainder of the protein being present (Kochneva-Pervukhova et al, 1998). It would be interesting to investigate whether the pro-chronological ageing phenotype observed in the presence of [*PSI*$^{+}$] in autophagy competent cells is dependent upon the prion forming domain of Sup35 alone or it requires the presence of the full length Sup35 protein. Mutants of the Sup35 protein lacking the prion forming domain or the middle domain essential for [*PSI*$^{+}$] propagation could be generated and assessed in chronological longevity experiments. If the Sup35 prion forming domain is required to elicit a pro-chronological lifespan phenotype, this would present an interesting paradigm for the biology of prion formation and yeast chronological ageing. Indeed, this would provide further evidence for prion formation as a

means to improve the adaptability of yeast cells during challenging conditions. Whether this effect extends to other fungal prions such as [*SWI*$^{+}$] or [*OCT*$^{+}$] that have wide-ranging modulatory effects on global gene expression also warrants further investigation.

Prions are unique proteinaceous entities capable of infection and self-replication. Autophagy, on the other hand, serves as part of the proteostasis network within the cell against aberrant protein accumulation that includes prions and prion precursors (Figure 6.2). Although prions have been regarded as toxic or non-beneficial to their host, the presence of the [*PSI*$^{+}$] prion in yeast may manifest positive outcomes to their yeast host during chronological ageing (Figure 6.2). The cortical actin cytoskeleton also serves as part of the framework that supports the aggregation of prion forming proteins and their maturation towards becoming fully-fledged prions that are self-perpetuating and transmissible (Figure 6.2). It is evident that a whole network of factors that affect prion formation and their accumulation needs further elucidation in order to help decipher the 'secret code' behind prion formation and their unique behaviour. The parallels found between prions and other protein agents that cause neurodegenerative diseases also points towards a greater paradigm of protein aggregation biology that needs to be more comprehensively understood in order to promote the development of more effective therapeutic interventions to tackle the debilitating diseases caused by these enigmatic protein entities.

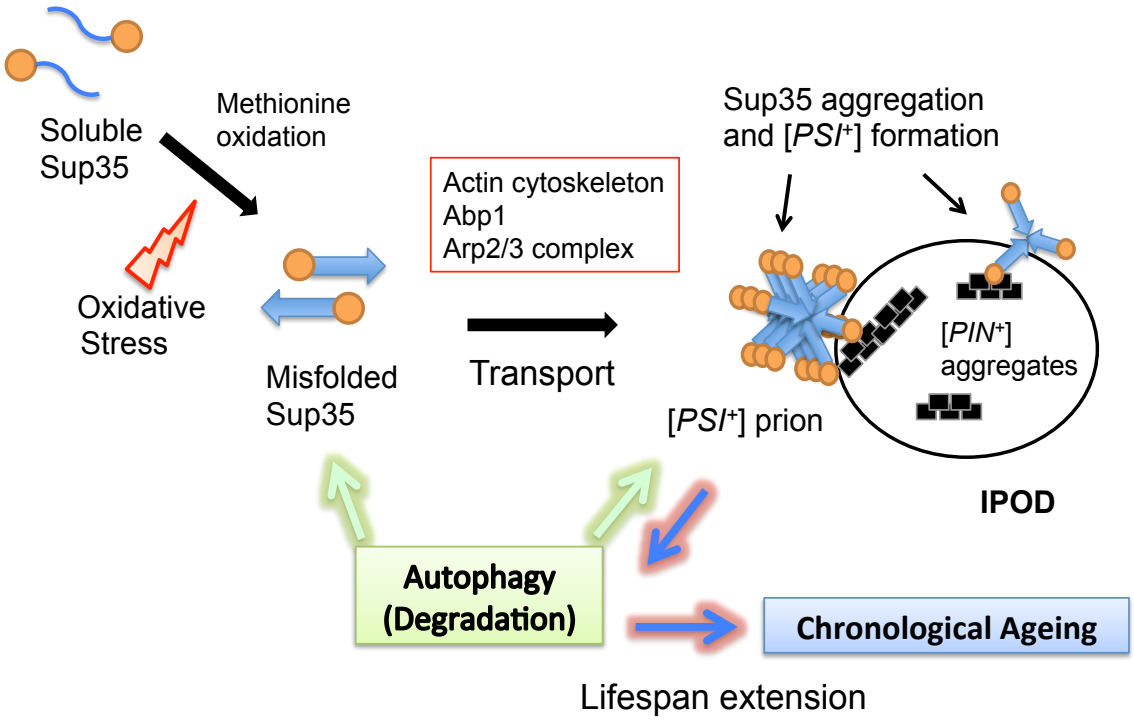

Figure 6.2: Model of the links between autophagy, ageing and the cortical actin cytoskeleton in relation to the [*PSI*$^+$] prion in yeast. Oxidative stress conditions induce oxidative damage on methionine residues of Sup35 leading to a higher propensity of Sup35 being converted into the misfolded form. The transport of misfolded Sup35 to the insoluble protein deposit (IPOD) via the actin cytoskeleton is promoted by components of the Arp2/3 complex and Abp1 (box with red outline). The IPOD is a sequestration site for [*PIN*$^+$] aggregates (black boxes) that serve as nucleation sites for misfolded Sup35 to template upon thus further promoting Sup35 aggregation as well as [*PSI*$^+$] prion formation. Conversely, the autophagy pathway (green box) exerts a protective role against [*PSI*$^+$] formation by facilitating the clearance of misfolded Sup35 as well as [*PSI*$^+$] prions (green arrows) which are ultimately degraded in the vacuole. During chronological ageing conditions (blue box), the formation of the [*PSI*$^+$] prion may result in enhanced autophagic flux (blue arrows) which in turn leads to increased lifespan extension in yeast.

7. Bibliography

Adams AE and Pringle JR (1984) Relationship of actin and tubulin distribution to bud growth in wild-type and morphogenetic-mutant Saccharomyces cerevisiae. *J Cell Biol* **98:** 934-945

Adams AE, Shen W, Lin CS, Leavitt J and Matsudaira P (1995) Isoform-specific complementation of the yeast sac6 null mutation by human fimbrin. *Mol Cell Biol* **15:** 69-75

Aguib Y, Heiseke A, Gilch S, Riemer C, Baier M, Schatzl HM and Ertmer A (2009) Autophagy induction by trehalose counteracts cellular prion infection. *Autophagy* **5:** 361-369

Aguilaniu H, Gustafsson L, Rigoulet M and Nystrom T (2003) Asymmetric inheritance of oxidatively damaged proteins during cytokinesis. *Science* **299:** 1751-1753

Aguzzi A (2008) Unraveling prion strains with cell biology and organic chemistry. *Proc Natl Acad Sci U S A* **105:** 11-12

Aguzzi A and O'Connor T (2010) Protein aggregation diseases: pathogenicity and therapeutic perspectives. *Nat Rev Drug Discov* **9:** 237-248

Alberti S, Halfmann R, King O, Kapila A and Lindquist S (2009) A systematic survey identifies prions and illuminates sequence features of prionogenic proteins. *Cell* **137:** 146-158

Alberti S, Halfmann R and Lindquist S (2010) Biochemical, cell biological, and genetic assays to analyze amyloid and prion aggregation in yeast. *Methods Enzymol* **470:** 709-734

Allen KD, Chernova TA, Tennant EP, Wilkinson KD and Chernoff YO (2007) Effects of ubiquitin system alterations on the formation and loss of a yeast prion. *J Biol Chem* **282:** 3004-3013

Allen KD, Wegrzyn RD, Chernova TA, Muller S, Newnam GP, Winslett PA, Wittich KB, Wilkinson KD and Chernoff YO (2005) Hsp70 chaperones as modulators of prion life cycle: novel effects of Ssa and Ssb on the Saccharomyces cerevisiae prion [PSI+]. *Genetics* **169:** 1227-1242

Alvers AL, Fishwick LK, Wood MS, Hu D, Chung HS, Dunn WA, Jr. and Aris JP (2009a) Autophagy and amino acid homeostasis are required for chronological longevity in Saccharomyces cerevisiae. *Aging Cell* **8:** 353-369

Alvers AL, Wood MS, Hu D, Kaywell AC, Dunn WA, Jr. and Aris JP (2009b) Autophagy is required for extension of yeast chronological life span by rapamycin. *Autophagy* **5:** 847-849

Amberg DC (1998) Three-dimensional imaging of the yeast actin cytoskeleton through the budding cell cycle. *Mol Biol Cell* **9:** 3259-3262

Anderson RM and Weindruch R (2012) The caloric restriction paradigm: implications for healthy human aging. *Am J Hum Biol* **24:** 101-106

Andersson V, Hanzen S, Liu B, Molin M and Nystrom T (2013) Enhancing protein disaggregation restores proteasome activity in aged cells. *Aging (Albany NY)* **5:** 802-812

Appleby BS, Appleby KK and Rabins PV (2007) Does the presentation of Creutzfeldt-Jakob disease vary by age or presumed etiology? A meta-analysis of the past 10 years. *J Neuropsychiatry Clin Neurosci* **19:** 428-435

Appleby BS and Lyketsos CG (2011) Rapidly progressive dementias and the treatment of human prion diseases. *Expert Opin Pharmacother* **12:** 1-12

Arslan F, Hong JY, Kanneganti V, Park SK and Liebman SW (2015) Heterologous aggregates promote de novo prion appearance via more than one mechanism. *PLoS Genet* **11:** e1004814

Ayscough KR, Stryker J, Pokala N, Sanders M, Crews P and Drubin DG (1997) High rates of actin filament turnover in budding yeast and roles for actin in establishment and maintenance of cell polarity revealed using the actin inhibitor latrunculin-A. *J Cell Biol* **137:** 399-416

Bailleul-Winslett PA, Newnam GP, Wegrzyn RD and Chernoff YO (2000) An antiprion effect of the anticytoskeletal drug latrunculin A in yeast. *Gene Expr* **9:** 145-156

Banerjee R, Beal MF and Thomas B (2010) Autophagy in neurodegenerative disorders: pathogenic roles and therapeutic implications. *Trends Neurosci* **33:** 541-549

Beckhouse AG, Grant CM, Rogers PJ, Dawes IW and Higgins VJ (2008) The adaptive response of anaerobically grown Saccharomyces cerevisiae to hydrogen peroxide is mediated by the Yap1 and Skn7 transcription factors. *FEMS Yeast Res* **8:** 1214-1222

Bence NF, Sampat RM and Kopito RR (2001) Impairment of the ubiquitin-proteasome system by protein aggregation. *Science* **292,:** 1552-1555

Berger Z, Ravikumar B, Menzies FM, Oroz LG, Underwood BR, Pangalos MN, Schmitt I, Wullner U, Evert BO, O'Kane CJ and Rubinsztein DC (2006) Rapamycin alleviates toxicity of different aggregate-prone proteins. *Hum Mol Genet* **15:** 433-442

Bizat N, Peyrin JM, Haik S, Cochois V, Beaudry P, Laplanche JL and Neri C (2010) Neuron dysfunction is induced by prion protein with an insertional mutation via a Fyn kinase and reversed by sirtuin activation in Caenorhabditis elegans. *J Neurosci* **30:** 5394-5403

Boellaard JW, Kao M, Schlote W and Diringer H (1991) Neuronal autophagy in experimental scrapie. *Acta Neuropathol* **82:** 225-228

Bonawitz ND, Chatenay-Lapointe M, Pan Y and Shadel GS (2007) Reduced TOR signaling extends chronological life span via increased respiration and upregulation of mitochondrial gene expression. *Cell Metab* **5:** 265-277

Borghouts C, Benguria A, Wawryn J and Jazwinski SM (2004) Rtg2 protein links metabolism and genome stability in yeast longevity. *Genetics* **166:** 765-777

Borras C, Monleon D, Lopez-Grueso R, Gambini J, Orlando L, Pallardo FV, Santos E, Vina J and Font de Mora J (2011) RasGrf1 deficiency delays aging in mice. *Aging (Albany NY)* **3:** 262-276

Bradley ME, Edskes HK, Hong JY, Wickner RB and Liebman SW (2002) Interactions among prions and prion "strains" in yeast. *Proc Natl Acad Sci U S A* **99 Suppl 4:** 16392-16399

Bradley ME and Liebman SW (2004) The Sup35 domains required for maintenance of weak, strong or undifferentiated yeast [PSI+] prions. *Mol Microbiol* **51:** 1649-1659

Brown DR, Qin K, Herms JW, Madlung A, Manson J, Strome R, Fraser PE, Kruck T, von Bohlen A, Schulz-Schaeffer W, Giese A, Westaway D and Kretzschmar H (1997) The cellular prion protein binds copper in vivo. *Nature* **390:** 684-687

Budovskaya YV, Stephan JS, Reggiori F, Klionsky DJ and Herman PK (2004) The Ras/cAMP-dependent protein kinase signaling pathway regulates an early step of the autophagy process in Saccharomyces cerevisiae. *J Biol Chem* **279:** 20663-20671

Burtner CR, Murakami CJ, Kennedy BK and Kaeberlein M (2009) A molecular mechanism of chronological aging in yeast. *Cell Cycle* **8:** 1256-1270

Caballero A, Ugidos A, Liu B, Oling D, Kvint K, Hao X, Mignat C, Nachin L, Molin M and Nystrom T (2011) Absence of mitochondrial translation control proteins extends life span by activating sirtuin-dependent silencing. *Mol Cell* **42:** 390-400

Canello T, Engelstein R, Moshel O, Xanthopoulos K, Juanes ME, Langeveld J, Sklaviadis T, Gasset M and Gabizon R (2008) Methionine sulfoxides on PrPSc: a prion-specific covalent signature. *Biochemistry* **47:** 8866-8873

Canello T, Frid K, Gabizon R, Lisa S, Friedler A, Moskovitz J and Gasset M (2010) Oxidation of Helix-3 methionines precedes the formation of PK resistant PrP. *PLoS Pathog* **6:** e1000977

Cebollero E, van der Vaart A, Zhao M, Rieter E, Klionsky DJ, Helms JB and Reggiori F (2012) Phosphatidylinositol-3-phosphate clearance plays a key role in autophagosome completion. *Curr Biol* **22:** 1545-1553

Chaudhuri B, Ingavale S and Bachhawat AK (1997) *apd1+,* a gene required for red pigment formation in *ade6* mutants of *schizosaccharomyces pombe,* encodes an enzyme required for glutathione biosynthesis: A role for glutathione and a glutathione-conjugate pump. *Genetics* **145:** 75-83

Chen JL, Lin HH, Kim KJ, Lin A, Ou JH and Ann DK (2009) PKC delta signaling: a dual role in regulating hypoxic stress-induced autophagy and apoptosis. *Autophagy* **5:** 244-246

Chen Q and Pollard TD (2013) Actin filament severing by cofilin dismantles actin patches and produces mother filaments for new patches. *Curr Biol* **23:** 1154-1162

Chen Y and Klionsky DJ (2011) The regulation of autophagy - unanswered questions. *J Cell Sci* **124:** 161-170

Cheong H and Klionsky DJ (2008) Dual role of Atg1 in regulation of autophagy-specific PAS assembly in Saccharomyces cerevisiae. *Autophagy* **4:** 724-726

Chernoff YO, Inge-Vechtomov SG, Derkach IL, Ptyushkina MV, Tarunina OV, Dagkesamanskaya AR and Ter-Avanesyan MD (1992) Dosage-dependent translational suppression in yeast Saccharomyces cerevisiae. *Yeast* **8:** 489-499

Chernoff YO, Lindquist SL, Ono B, Inge-Vechtomov SG and Liebman SW (1995) Role of the chaperone protein Hsp104 in propagation of the yeast prion-like factor [psi+]. *Science* **268:** 880-884

Chernova TA, Romanyuk AV, Karpova TS, Shanks JR, Ali M, Moffatt N, Howie RL, O'Dell A, McNally JG, Liebman SW, Chernoff YO and Wilkinson KD (2011) Prion induction by the short-lived, stress-induced protein Lsb2 is regulated by ubiquitination and association with the actin cytoskeleton. *Mol Cell* **43:** 242-252

Chernova TA, Wilkinson KD and Chernoff YO (2014) Physiological and environmental control of yeast prions. *FEMS Microbiol Rev* **38:** 326-344

Cherra SJ, 3rd and Chu CT (2008) Autophagy in neuroprotection and neurodegeneration: A question of balance. *Future Neurol* **3:** 309-323

Collinge J and Clarke AR (2007) A general model of prion strains and their pathogenicity. *Science* **318:** 930-936

Cornu M, Albert V and Hall MN (2013) mTOR in aging, metabolism, and cancer. *Curr Opin Genet Dev* **23:** 53-62

Costanzo M and Zurzolo C (2013) The cell biology of prion-like spread of protein aggregates: mechanisms and implication in neurodegeneration. *Biochem J* **452:** 1-17

Dang W, Steffen KK, Perry R, Dorsey JA, Johnson FB, Shilatifard A, Kaeberlein M, Kennedy BK and Berger SL (2009) Histone H4 lysine 16 acetylation regulates cellular lifespan. *Nature* **459:** 802-807

Dean RT, Fu S, Stocker R and Davies MJ (1997) Biochemistry and pathology of radical-mediated protein oxidation. *Biochem J* **324:** 1-18

Dearmond SJ and Bajsarowicz K (2010) PrPSc accumulation in neuronal plasma membranes links Notch-1 activation to dendritic degeneration in prion diseases. *Mol Neurodegener* **5:** 6

DeMarco ML and Daggett V (2005) Local environmental effects on the structure of the prion protein. *C R Biol* **328:** 847-862

Dennis PB, Jaeschke A, Saitoh M, Fowler B, Kozma SC and Thomas G (2001) Mammalian TOR: a homeostatic ATP sensor. *Science* **294:** 1102-1105

Derkatch IL, Bradley ME, Hong JY and Liebman SW (2001) Prions affect the appearance of other prions: the story of [PIN(+)]. *Cell* **106:** 171-182

Derkatch IL, Bradley ME, Masse SV, Zadorsky SP, Polozkov GV, Inge-Vechtomov SG and Liebman SW (2002) Dependence and independence of [PSI(+)] and [PIN(+)]: a two-prion system in yeast? *EMBO J* **19:** 1942-1952

Derkatch IL, Bradley ME, Zhou P, Chernoff YO and Liebman SW (1997) Genetic and environmental factors affecting the de novo appearance of the [PSI+] prion in Saccharomyces cerevisiae. *Genetics* **147:** 507-519

Derkatch IL, Chernoff YO, Kushnirov VV, Inge-Vechtomov SG and Liebman SW (1996) Genesis and variability of [PSI] prion factors in Saccharomyces cerevisiae. *Genetics* **144:** 1375-1386

Derkatch IL, Uptain SM, Outeiro TF, Krishnan R, Lindquist SL and Liebman SW (2004) Effects of Q/N-rich, polyQ, and non-polyQ amyloids on the de novo formation of the [PSI+] prion in yeast and aggregation of Sup35 in vitro. *Proc Natl Acad Sci U S A* **101:** 12934-12939

Dong J, Atwood CS, Anderson VE, Siedlak SL, Smith MA, Perry G and Carey PR (2003) Metal binding and oxidation of amyloid-beta within isolated senile plaque cores: Raman microscopic evidence. *Biochemistry* **42:** 2768-2773

Doronina VA, Staniforth GL, Speldewinde SH, Tuite MF and Grant CM (2015) Oxidative stress conditions increase the frequency of de novo formation of the yeast [PSI(+)] prion. *Mol Microbiol* **96:** 163-174

Eisenberg T, Knauer H, Schauer A, Buttner S, Ruckenstuhl C, Carmona-Gutierrez D, Ring J, Schroeder S, Magnes C, Antonacci L, Fussi H, Deszcz L, Hartl R, Schraml E, Criollo A, Megalou E, Weiskopf D, Laun P, Heeren G, Breitenbach M, Grubeck-Loebenstein B, Herker E, Fahrenkrog B, Frohlich KU, Sinner F, Tavernarakis N, Minois N, Kroemer G and Madeo F (2009) Induction of autophagy by spermidine promotes longevity. *Nat Cell Biol* **11:** 1305-1314

Elmallah MI, Borgmeyer U, Betzel C and Redecke L (2013) Impact of methionine oxidation as an initial event on the pathway of human prion protein conversion. *Prion* **7:** 404-411

Enns LC, Pettan-Brewer C and Ladiges W (2010) Protein kinase A is a target for aging and the aging heart. *Aging (Albany NY)* **2:** 238-243

Epple UD, Suriapranata I, Eskelinen EL and Thumm M (2001) Aut5/Cvt17p, a putative lipase essential for disintegration of autophagic bodies inside the vacuole. *J Bacteriol* **183:** 5942-5955

Erjavec N, Larsson L, Grantham J and Nystrom T (2007) Accelerated aging and failure to segregate damaged proteins in Sir2 mutants can be suppressed by overproducing the protein aggregation-remodeling factor Hsp104p. *Genes Dev* **21:** 2410-2421

Erjavec N and Nystrom T (2007) Sir2p-dependent protein segregation gives rise to a superior reactive oxygen species management in the progeny of Saccharomyces cerevisiae. *Proc Natl Acad Sci U S A* **104:** 10877-10881

Escusa-Toret S, Vonk WI and Frydman J (2013) Spatial sequestration of misfolded proteins by a dynamic chaperone pathway enhances cellular fitness during stress. *Nat Cell Biol* **15:** 1231-1243

Evangelista M, Pruyne D, Amberg DC, Boone C and Bretscher A (2002) Formins direct Arp2/3-independent actin filament assembly to polarize cell growth in yeast. *Nat Cell Biol* **4:** 260-269

Fabrizio P, Battistella L, Vardavas R, Gattazzo C, Liou LL, Diaspro A, Dossen JW, Gralla EB and Longo VD (2004) Superoxide is a mediator of an altruistic aging program in Saccharomyces cerevisiae. *J Cell Biol* **166:** 1055-1067

Fabrizio P, Li L and Longo VD (2005) Analysis of gene expression profile in yeast aging chronologically. *Mech Ageing Dev* **126:** 11-16

Fabrizio P and Longo VD (2003) The chronological life span of Saccharomyces cerevisiae. *Aging Cell* **2:** 73-81

Fabrizio P and Longo VD (2008) Chronological aging-induced apoptosis in yeast. *Biochim Biophys Acta* **1783:** 1280-1285

Fabrizio P, Pozza F, Pletcher SD, Gendron CM and Longo VD (2001) Regulation of longevity and stress resistance by Sch9 in yeast. *Science* **292:** 288-290

Feliciano D and Di Pietro SM (2012) SLAC, a complex between Sla1 and Las17, regulates actin polymerization during clathrin-mediated endocytosis. *Mol Biol Cell* **23:** 4256-4272

Ferreira PC, Ness F, Edwards SR, Cox BS and Tuite MF (2001) The elimination of the yeast [PSI+] prion by guanidine hydrochloride is the result of Hsp104 inactivation. *Mol Microbiol* **40:** 1357-1369

Filomeni G, Desideri E, Cardaci S, Rotilio G and Ciriolo MR (2010) Under the ROS...thiol network is the principal suspect for autophagy commitment. *Autophagy* **6:** 999-1005

Fontana L, Partridge L and Longo VD (2010) Extending healthy life span--from yeast to humans. *Science* **328:** 321-326

Friedman LG, Lachenmayer ML, Wang J, He L, Poulose SM, Komatsu M, Holstein GR and Yue Z (2012) Disrupted autophagy leads to dopaminergic axon and dendrite degeneration and promotes presynaptic accumulation of alpha-synuclein and LRRK2 in the brain. *J Neurosci* **32:** 7585-7593

Fujita N, Itoh T, Omori H, Fukuda M, Noda T and Yoshimori T (2008) The Atg16L complex specifies the site of LC3 lipidation for membrane biogenesis in autophagy. *Mol Biol Cell* **19:** 2092-2100

Galletta BJ, Mooren OL and Cooper JA (2010) Actin dynamics and endocytosis in yeast and mammals. *Curr Opin Biotechnol* **21:** 604-610

Ganusova EE, Ozolins LN, Bhagat S, Newnam GP, Wegrzyn RD, Sherman MY and Chernoff YO (2006) Modulation of prion formation, aggregation, and toxicity by the actin cytoskeleton in yeast. *Mol Cell Biol* **26:** 617-629

Garrido EO and Grant CM (2002) Role of thioredoxins in the response of *Saccharomyces cerevisiae* to oxidative stress induced by hydroperoxides. *Molec Microbiol* **43:** 993-1003

Gautschi M, Mun A, Ross S and Rospert S (2002) A functional chaperone triad on the yeast ribosome. *Proc Natl Acad Sci U S A* **99:** 4209-4214

Geng J and Klionsky DJ (2008) Quantitative regulation of vesicle formation in yeast nonspecific autophagy. *Autophagy* **4:** 955-957

Glover JR and Lindquist S (1998) Hsp104, Hsp70, and Hsp40: a novel chaperone system that rescues previously aggregated proteins. *Cell* **94:** 73-82

Goldberg AA, Bourque SD, Kyryakov P, Gregg C, Boukh-Viner T, Beach A, Burstein MT, Machkalyan G, Richard V, Rampersad S, Cyr D, Milijevic S and Titorenko VI (2009) Effect of calorie restriction on the metabolic history of chronologically aging yeast. *Exp Gerontol* **44:** 555-571

Gonzalez-Polo RA, Boya P, Pauleau AL, Jalil A, Larochette N, Souquere S, Eskelinen EL, Pierron G, Saftig P and Kroemer G (2005) The apoptosis/autophagy paradox: autophagic vacuolization before apoptotic death. *J Cell Sci* **118:** 3091-3102

Goode BL, Eskin JA and Wendland B (2015) Actin and endocytosis in budding yeast. *Genetics* **199:** 315-358

Goode BL, Rodal AA, Barnes G and Drubin DG (2001) Activation of the Arp2/3 complex by the actin filament binding protein Abp1p. *J Cell Biol* **153:** 627-634

Goold R, McKinnon C, Rabbanian S, Collinge J, Schiavo G and Tabrizi SJ (2013) Alternative fates of newly formed PrPSc upon prion conversion on the plasma membrane. *J Cell Sci* **126:** 3552-3562

Gourlay CW, Carpp LN, Timpson P, Winder SJ and Ayscough KR (2004) A role for the actin cytoskeleton in cell death and aging in yeast. *J Cell Biol* **164:** 803-809

Grant CM (2015) Sup35 methionine oxidation is a trigger for de novo [*PSI*+] prion formation. *Prion* **9:** 257-265

Grimminger-Marquardt V and Lashuel HA (2010) Structure and function of the molecular chaperone Hsp104 from yeast. *Biopolymers* **93:** 252-276

Hailey DW, Rambold AS, Satpute-Krishnan P, Mitra K, Sougrat R, Kim PK and Lippincott-Schwartz J (2010) Mitochondria supply membranes for autophagosome biogenesis during starvation. *Cell* **141:** 656-667

Halfmann R, Jarosz DF, Jones SK, Chang A, Lancaster AK and Lindquist S (2012) Prions are a common mechanism for phenotypic inheritance in wild yeasts. *Nature* **482:** 363-368

Hamasaki M, Noda T, Baba M and Ohsumi Y (2005) Starvation triggers the delivery of the endoplasmic reticulum to the vacuole via autophagy in yeast. *Traffic* **6:** 56-65

Hanada T, Noda NN, Satomi Y, Ichimura Y, Fujioka Y, Takao T, Inagaki F and Ohsumi Y (2007) The Atg12-Atg5 conjugate has a novel E3-like activity for protein lipidation in autophagy. *J Biol Chem* **282:** 37298-37302

Hara T, Nakamura K, Matsui M, Yamamoto A, Nakahara Y, Suzuki-Migishima R, Yokoyama M, Mishima K, Saito I, Okano H and Mizushima N (2006) Suppression of basal autophagy in neural cells causes neurodegenerative disease in mice. *Nature* **441:** 885-889

Harrison DE, Strong R, Sharp ZD, Nelson JF, Astle CM, Flurkey K, Nadon NL, Wilkinson JE, Frenkel K, Carter CS, Pahor M, Javors MA, Fernandez E and Miller RA (2009) Rapamycin fed late in life extends lifespan in genetically heterogeneous mice. *Nature* **460:** 392-395

Haynes CM, Titus EA and Cooper AA (2004) Degradation of misfolded proteins prevents ER-derived oxidative stress and cell death. *Molec Cell* **15:** 767-776.

He C, Baba M, Cao Y and Klionsky DJ (2008) Self-interaction is critical for Atg9 transport and function at the phagophore assembly site during autophagy. *Mol Biol Cell* **19:** 5506-5516

He C and Klionsky DJ (2009) Regulation mechanisms and signaling pathways of autophagy. *Annu Rev Genet* **43:** 67-93

He C, Song H, Yorimitsu T, Monastyrska I, Yen WL, Legakis JE and Klionsky DJ (2006) Recruitment of Atg9 to the preautophagosomal structure by Atg11 is essential for selective autophagy in budding yeast. *J Cell Biol* **175:** 925-935

Heiseke A, Aguib Y, Riemer C, Baier M and Schatzl HM (2009) Lithium induces clearance of protease resistant prion protein in prion-infected cells by induction of autophagy. *J Neurochem* **109:** 25-34

Heiseke A, Aguib Y and Schatzl HM (2010) Autophagy, prion infection and their mutual interactions. *Curr Issues Mol Biol* **12:** 87-97

Higgs HN and Pollard TD (2001) Regulation of actin filament network formation through ARP2/3 complex: activation by a diverse array of proteins. *Annu Rev Biochem* **70:** 649-676

Hohn A, Jung T and Grune T (2014) Pathophysiological importance of aggregated damaged proteins. *Free Radic Biol Med* **71:** 70-89

Homma T, Ishibashi D, Nakagaki T, Satoh K, Sano K, Atarashi R and Nishida N (2014) Increased expression of p62/SQSTM1 in prion diseases and its association with pathogenic prion protein. *Sci Rep* **4:** 4504

Hosoda N, Kobayashi T, Uchida N, Funakoshi Y, Kikuchi Y, Hoshino S and Katada T (2003) Translation termination factor eRF3 mediates mRNA decay through the regulation of deadenylation. *J Biol Chem* **278:** 38287-38291

Humphries CL, Balcer HI, D'Agostino JL, Winsor B, Drubin DG, Barnes G, Andrews BJ and Goode BL (2002) Direct regulation of Arp2/3 complex activity and function by the actin binding protein coronin. *J Cell Biol* **159:** 993-1004

Hutchins MU and Klionsky DJ (2001) Vacuolar localization of oligomeric alpha-mannosidase requires the cytoplasm to vacuole targeting and autophagy pathway components in Saccharomyces cerevisiae. *J Biol Chem* **276:** 20491-20498

Imai S, Johnson FB, Marciniak RA, McVey M, Park PU and Guarente L (2000) Sir2: an NAD-dependent histone deacetylase that connects chromatin silencing, metabolism, and aging. *Cold Spring Harb Symp Quant Biol* **65:** 297-302

Iwata A, Riley BE, Johnston JA and Kopito RR (2005) HDAC6 and microtubules are required for autophagic degradation of aggregated huntingtin. *J Biol Chem* **280:** 40282-40292

Jacobson T, Navarrete C, Sharma SK, Sideri TC, Ibstedt S, Priya S, Grant CM, Christen P, Goloubinoff P and Tamas MJ (2012) Arsenite interferes with protein folding and triggers formation of protein aggregates in yeast. *J Cell Sci* **125:** 5073-5083

Jang HH, Lee KO, Chi YH, Jung BG, Park SK, Park JH, Lee JR, Lee SS, Moon JC, Yun JW, Choi YO, Kim WY, Kang JS, Cheong GW, Yun DJ, Rhee.G., Cho MJ and Lee SY (2004) Two enzymes in one; two yeast peroxiredoxins display oxidative stress-dependent switching from a peroxidase to a molecular chaperone function. *Cell* **117:** 625-635

Jeong JK, Moon MH, Bae BC, Lee YJ, Seol JW, Kang HS, Kim JS, Kang SJ and Park SY (2012) Autophagy induced by resveratrol prevents human prion protein-mediated neurotoxicity. *Neurosci Res* **73:** 99-105

Jia K and Levine B (2007) Autophagy is required for dietary restriction-mediated life span extension in C. elegans. *Autophagy* **3:** 597-599

Joseph SB and Kirkpatrick M (2008) Effects of the [PSI+] prion on rates of adaptation in yeast. *J Evol Biol* **21:** 773-780

Joshi-Barr S, Bett C, Chiang WC, Trejo M, Goebel HH, Sikorska B, Liberski P, Raeber A, Lin JH, Masliah E and Sigurdson CJ (2014) De novo prion aggregates trigger autophagy in skeletal muscle. *J Virol* **88:** 2071-2082

Josse L, Marchante R, Zenthon J, von der Haar T and Tuite MF (2012) Probing the role of structural features of mouse PrP in yeast by expression as Sup35-PrP fusions. *Prion* **6:** 201-210

Juhasz G, Erdi B, Sass M and Neufeld TP (2007) Atg7-dependent autophagy promotes neuronal health, stress tolerance, and longevity but is dispensable for metamorphosis in Drosophila. *Genes Dev* **21:** 3061-3066

Jung G and Masison DC (2001) Guanidine hydrochloride inhibits Hsp104 activity in vivo: a possible explanation for its effect in curing yeast prions. *Curr Microbiol* **43:** 7-10

Kabani M, Redeker V and Melki R (2014) A role for the proteasome in the turnover of Sup35p and in [PSI(+)] prion propagation. *Mol Microbiol* **92:** 507-528

Kaeberlein M (2010) Lessons on longevity from budding yeast. *Nature* **464:** 513-519

Kaeberlein M, Hu D, Kerr EO, Tsuchiya M, Westman EA, Dang N, Fields S and Kennedy BK (2005) Increased life span due to calorie restriction in respiratory-deficient yeast. *PLoS Genet* **1:** e69

Kaeberlein M, McVey M and Guarente L (1999) The SIR2/3/4 complex and SIR2 alone promote longevity in Saccharomyces cerevisiae by two different mechanisms. *Genes Dev* **13:** 2570-2580

Kaganovich D, Kopito R and Frydman J (2008) Misfolded proteins partition between two distinct quality control compartments. *Nature* **454:** 1088-1095

Kaksonen M, Toret CP and Drubin DG (2005) A modular design for the clathrin- and actin-mediated endocytosis machinery. *Cell* **123:** 305-320

Kamada Y, Funakoshi T, Shintani T, Nagano K, Ohsumi M and Ohsumi Y (2000) Tor-mediated induction of autophagy via an Apg1 protein kinase complex. *J Cell Biol* **150:** 1507-1513

Karpova TS, McNally JG, Moltz SL and Cooper JA (1998) Assembly and function of the actin cytoskeleton of yeast: relationships between cables and patches. *J Cell Biol* **142:** 1501-1517

Kenyon CJ (2010) The genetics of ageing. *Nature* **464:** 504-512

Kiffin R, Bandyopadhyay U and Cuervo AM (2006) Oxidative stress and autophagy. *Antioxid Redox Signal* **8:** 152-162

Kihara A, Noda T, Ishihara N and Ohsumi Y (2001) Two distinct Vps34 phosphatidylinositol 3-kinase complexes function in autophagy and carboxypeptidase Y sorting in Saccharomyces cerevisiae. *J Cell Biol* **152:** 519-530

Kim DK, Cho ES, Seong JK and Um HD (2001) Adaptive concentrations of hydrogen peroxide suppress cell death by blocking the activation of SAPK/JNK pathway. *J Cell Sci* **114:** 4329-4334.

Kirchman PA, Kim S, Lai CY and Jazwinski SM (1999) Interorganelle signaling is a determinant of longevity in Saccharomyces cerevisiae. *Genetics* **152:** 179-190

Kirisako T, Baba M, Ishihara N, Miyazawa K, Ohsumi M, Yoshimori T, Noda T and Ohsumi Y (1999) Formation process of autophagosome is traced with Apg8/Aut7p in yeast. *J Cell Biol* **147:** 435-446

Kirisako T, Ichimura Y, Okada H, Kabeya Y, Mizushima N, Yoshimori T, Ohsumi M, Takao T, Noda T and Ohsumi Y (2000) The reversible modification regulates the membrane-binding state of Apg8/Aut7 essential for autophagy and the cytoplasm to vacuole targeting pathway. *J Cell Biol* **151:** 263-276

Kochneva-Pervukhova NV, Poznyakovski AI, Smirnov VN and Ter-Avanesyan MD (1998) C-terminal truncation of the Sup35 protein increases the frequency of de novo generation of a prion-based [PSI+] determinant in Saccharomyces cerevisiae. *Curr Genet* **34:** 146-151

Komatsu M, Waguri S, Chiba T, Murata S, Iwata J, Tanida I, Ueno T, Koike M, Uchiyama Y, Kominami E and Tanaka K (2006) Loss of autophagy in the central nervous system causes neurodegeneration in mice. *Nature* **441:** 880-884

Koplin A, Preissler S, Ilina Y, Koch M, Scior A, Erhardt M and Deuerling E (2010) A dual function for chaperones SSB-RAC and the NAC nascent polypeptide-associated complex on ribosomes. *J Cell Biol* **189:** 57-68

Kovacs GG and Budka H (2008) Prion diseases: from protein to cell pathology. *Am J Pathol* **172:** 555-565

Krick R, Tolstrup J, Appelles A, Henke S and Thumm M (2006) The relevance of the phosphatidylinositolphosphat-binding motif FRRGT of Atg18 and Atg21 for the Cvt pathway and autophagy. *FEBS Lett* **580:** 4632-4638

Kryndushkin DS, Alexandrov IM, Ter-Avanesyan MD and Kushnirov VV (2003) Yeast [PSI+] prion aggregates are formed by small Sup35 polymers fragmented by Hsp104. *J Biol Chem* **278:** 49636-49643

Kukulski W, Schorb M, Kaksonen M and Briggs JA (2012) Plasma membrane reshaping during endocytosis is revealed by time-resolved electron tomography. *Cell* **150:** 508-520

Kuma A, Mizushima N, Ishihara N and Ohsumi Y (2002) Formation of the approximately 350-kDa Apg12-Apg5.Apg16 multimeric complex, mediated by Apg16 oligomerization, is essential for autophagy in yeast. *J Biol Chem* **277:** 18619-18625

Kuwahara C, Takeuchi AM, Nishimura T, Haraguchi K, Kubosaki A, Matsumoto Y, Saeki K, Matsumoto Y, Yokoyama T, Itohara S and Onodera T (1999) Prions prevent neuronal cell-line death. *Nature* **400:** 225-226

Lancaster AK, Bardill JP, True HL and Masel J (2010) The spontaneous appearance rate of the yeast prion [PSI+] and its implications for the evolution of the evolvability properties of the [PSI+] system. *Genetics* **184:** 393-400

Lee J, Giordano S and Zhang J (2012) Autophagy, mitochondria and oxidative stress: cross-talk and redox signalling. *Biochem J* **441:** 523-540

Lee KJ, Panzera A, Rogawski D, Greene LE and Eisenberg E (2007) Cellular prion protein (PrPC) protects neuronal cells from the effect of huntingtin aggregation. *J Cell Sci* **120:** 2663-2671

Levine B and Kroemer G (2008) Autophagy in the pathogenesis of disease. *Cell* **132:** 27-42

Liberski PP, Sikorska B, Bratosiewicz-Wasik J, Gajdusek DC and Brown P (2004) Neuronal cell death in transmissible spongiform encephalopathies (prion diseases) revisited: from apoptosis to autophagy. *Int J Biochem Cell Biol* **36:** 2473-2490

Liebman SW and Chernoff YO (2012) Prions in yeast. *Genetics* **191:** 1041-1072

Lindstrom DL, Leverich CK, Henderson KA and Gottschling DE (2011) Replicative age induces mitotic recombination in the ribosomal RNA gene cluster of Saccharomyces cerevisiae. *PLoS Genet* **7:** e1002015

Lipinski MM, Hoffman G, Ng A, Zhou W, Py BF, Hsu E, Liu X, Eisenberg J, Liu J, Blenis J, Xavier RJ and Yuan J (2010) A genome-wide siRNA screen reveals multiple mTORC1 independent signaling pathways regulating autophagy under normal nutritional conditions. *Dev Cell* **18:** 1041-1052

Liu B, Larsson L, Caballero A, Hao X, Oling D, Grantham J and Nystrom T (2010) The polarisome is required for segregation and retrograde transport of protein aggregates. *Cell* **140:** 257-267

Longo VD and Fabrizio P (2002) Regulation of longevity and stress resistance: a molecular strategy conserved from yeast to humans? *Cell Mol Life Sci* **59:** 903-908

Longo VD, Gralla EB and Valentine JS (1996) Superoxide dismutase activity is essential for stationary phase survival in Saccharomyces cerevisiae. Mitochondrial production of toxic oxygen species in vivo. *J Biol Chem* **271:** 12275-12280

Longo VD, Shadel GS, Kaeberlein M and Kennedy B (2012) Replicative and chronological aging in Saccharomyces cerevisiae. *Cell Metab* **16:** 18-31

Lopez-Otin C, Blasco MA, Partridge L, Serrano M and Kroemer G (2013) The hallmarks of aging. *Cell* **153:** 1194-1217

Lund PM and Cox BS (1981) Reversion analysis of [psi-] mutations in Saccharomyces cerevisiae. *Genet Res* **37:** 173-182

Lynch-Day MA, Mao K, Wang K, Zhao M and Klionsky DJ (2012) The role of autophagy in Parkinson's disease. *Cold Spring Harb Perspect Med* **2:** a009357

Madeo F, Tavernarakis N and Kroemer G (2010) Can autophagy promote longevity? *Nat Cell Biol* **12:** 842-846

Maisonneuve E, Fraysse L, Lignon S, Capron L and Dukan S (2008) Carbonylated proteins are detectable only in a degradation-resistant aggregate state in Escherichia coli. *J Bacteriol* **190:** 6609-6614

Manogaran AL, Hong JY, Hufana J, Tyedmers J, Lindquist S and Liebman SW (2011) Prion formation and polyglutamine aggregation are controlled by two classes of genes. *PLoS Genet* **7:** e1001386

Manogaran AL, Kirkland KT and Liebman SW (2006) An engineered nonsense URA3 allele provides a versatile system to detect the presence, absence and appearance of the [PSI+] prion in Saccharomyces cerevisiae. *Yeast* **23:** 141-147

Matecic M, Smith DL, Pan X, Maqani N, Bekiranov S, Boeke JD and Smith JS (2010) A microarray-based genetic screen for yeast chronological aging factors. *PLoS Genet* **6:** e1000921

Mathur V, Taneja V, Sun Y and Liebman SW (2010) Analyzing the birth and propagation of two distinct prions, [PSI+] and [Het-s](y), in yeast. *Mol Biol Cell* **21:** 1449-1461

Matsuura A, Tsukada M, Wada Y and Ohsumi Y (1997) Apg1p, a novel protein kinase required for the autophagic process in Saccharomyces cerevisiae. *Gene* **192:** 245-250

Mazon MJ, Eraso P and Portillo F (2007) Efficient degradation of misfolded mutant Pma1 by endoplasmic reticulum-associated degradation requires Atg19 and the Cvt/autophagy pathway. *Mol Microbiol* **63:** 1069-1077

Medvedik O, Lamming DW, Kim KD and Sinclair DA (2007) MSN2 and MSN4 link calorie restriction and TOR to sirtuin-mediated lifespan extension in Saccharomyces cerevisiae. *PLoS Biol* **5:** e261

Meriin AB, Zhang X, He X, Newnam GP, Chernoff YO and Sherman MY (2002) Huntington toxicity in yeast model depends on polyglutamine aggregation mediated by a prion- like protein Rnq1. . *J Cell Biol* **157:** 997-1004

Merrifield CJ (2004) Seeing is believing: imaging actin dynamics at single sites of endocytosis. *Trends Cell Biol* **14:** 352-358

Mesquita A, Weinberger M, Silva A, Sampaio-Marques B, Almeida B, Leao C, Costa V, Rodrigues F, Burhans WC and Ludovico P (2010) Caloric restriction or catalase

inactivation extends yeast chronological lifespan by inducing H2O2 and superoxide dismutase activity. *Proc Natl Acad Sci U S A* **107:** 15123-15128

Michelot A, Grassart A, Okreglak V, Costanzo M, Boone C and Drubin DG (2013) Actin filament elongation in Arp2/3-derived networks is controlled by three distinct mechanisms. *Dev Cell* **24:** 182-195

Mijaljica D, Nazarko TY, Brumell JH, Huang WP, Komatsu M, Prescott M, Simonsen A, Yamamoto A, Zhang H, Klionsky DJ and Devenish RJ (2012) Receptor protein complexes are in control of autophagy. *Autophagy* **8:** 1701-1705

Milhavet O and Lehmann S (2002) Oxidative stress and the prion protein in transmissible spongiform encephalopathies. *Brain Res Brain Res Rev* **38:** 328-339

Mishra M, Huang J and Balasubramanian MK (2014) The yeast actin cytoskeleton. *FEMS Microbiol Rev* **38:** 213-227

Monastyrska I, He C, Geng J, Hoppe AD, Li Z and Klionsky DJ (2008) Arp2 links autophagic machinery with the actin cytoskeleton. *Mol Biol Cell* **19:** 1962-1975

Mooren OL, Galletta BJ and Cooper JA (2012) Roles for actin assembly in endocytosis. *Annu Rev Biochem* **81:** 661-686

Morselli E, Marino G, Bennetzen MV, Eisenberg T, Megalou E, Schroeder S, Cabrera S, Benit P, Rustin P, Criollo A, Kepp O, Galluzzi L, Shen S, Malik SA, Maiuri MC, Horio Y, Lopez-Otin C, Andersen JS, Tavernarakis N, Madeo F and Kroemer G (2011) Spermidine and resveratrol induce autophagy by distinct pathways converging on the acetylproteome. *J Cell Biol* **192:** 615-629

Morselli M, Pastor WA, Montanini B, Nee K, Ferrari R, Fu K, Bonora G, Rubbi L, Clark AT, Ottonello S, Jacobsen SE and Pellegrini M (2015) In vivo targeting of de novo DNA methylation by histone modifications in yeast and mouse. *Elife* **4:** e06205

Mortimer RK and Johnston JR (1959) Life span of individual yeast cells. *Nature* **183:** 1751-1752

Moseley JB and Goode BL (2006) The yeast actin cytoskeleton: from cellular function to biochemical mechanism. *Microbiol Mol Biol Rev* **70:** 605-645

Munhoz DC and Netto LE (2004) Cytosolic thioredoxin peroxidase I and II are important defenses of yeast against organic hydroperoxide insult: catalases and

peroxiredoxins cooperate in the decomposition of H2O2 by yeast. *J Biol Chem* **279:** 35219-35227

Nair U, Cao Y, Xie Z and Klionsky DJ (2010) Roles of the lipid-binding motifs of Atg18 and Atg21 in the cytoplasm to vacuole targeting pathway and autophagy. *J Biol Chem* **285:** 11476-11488

Nassif M, Matus S, Castillo K and Hetz C (2010) Amyotrophic lateral sclerosis pathogenesis: a journey through the secretory pathway. *Antioxid Redox Signal* **13:** 1955-1989

Ness F, Ferreira P, Cox BS and Tuite MF (2002) Guanidine hydrochloride inhibits the generation of prion "seeds" but not prion protein aggregation in yeast. *Mol Cell Biol* **22:** 5593-5605

Newby GA and Lindquist S (2013) Blessings in disguise: biological benefits of prion-like mechanisms. *Trends Cell Biol* **23:** 251-259

Newnam GP, Birchmore JL and Chernoff YO (2011) Destabilization and recovery of a yeast prion after mild heat shock. *J Mol Biol* **408:** 432-448

Newnam GP, Wegrzyn RD, Lindquist SL and Chernoff YO (1999) Antagonistic interactions between yeast chaperones Hsp104 and Hsp70 in prion curing. *Mol Cell Biol* **19:** 1325-1333

Noda T, Kim J, Huang WP, Baba M, Tokunaga C, Ohsumi Y and Klionsky DJ (2000) Apg9p/Cvt7p is an integral membrane protein required for transport vesicle formation in the Cvt and autophagy pathways. *J Cell Biol* **148:** 465-480

Noda T, Matsuura A, Wada Y and Ohsumi Y (1995) Novel system for monitoring autophagy in the yeast Saccharomyces cerevisiae. *Biochem Biophys Res Commun* **210:** 126-132

Nystrom T (2005) Role of oxidative carbonylation in protein quality control and senescence. *EMBO J* **24:** 1311-1317.

Ocampo A and Barrientos A (2011) Quick and reliable assessment of chronological life span in yeast cell populations by flow cytometry. *Mech Ageing Dev* **132:** 315-323

Oien DB, Canello T, Gabizon R, Gasset M, Lundquist BL, Burns JM and Moskovitz J (2009) Detection of oxidized methionine in selected proteins, cellular extracts and

blood serums by novel anti-methionine sulfoxide antibodies. *Arch Biochem Biophys* **485:** 35-40

Osherovich LZ, Cox BS, Tuite MF and Weissman JS (2004) Dissection and design of yeast prions. *PLoS Biol* **2:** E86

Osherovich LZ and Weissman JS (2001) Multiple Gln/Asn-rich prion domains confer susceptibility to induction of the yeast [PSI(+)] prion. *Cell* **106:** 183-194

Otzen D (2010) Functional amyloid: turning swords into plowshares. *Prion* **4:** 256-264

Pamplona R, Naudi A, Gavin R, Pastrana MA, Sajnani G, Ilieva EV, Del Rio JA, Portero-Otin M, Ferrer I and Requena JR (2008) Increased oxidation, glycoxidation, and lipoxidation of brain proteins in prion disease. *Free Radic Biol Med* **45:** 1159-1166

Pan Y, Schroeder EA, Ocampo A, Barrientos A and Shadel GS (2011) Regulation of yeast chronological life span by TORC1 via adaptive mitochondrial ROS signaling. *Cell Metab* **13:** 668-678

Park SG, Cha M-K, Jeong W and Kim I-H (2000) Distinct physiological functions of thiol peroxidase isoenzymes in *Saccharomyces cerevisiae*. *J Biol Chem* **275:** 5723-5732

Parzych KR and Klionsky DJ (2014) An overview of autophagy: morphology, mechanism, and regulation. *Antioxid Redox Signal* **20:** 460-473

Patel BK and Liebman SW (2007) "Prion-proof" for [PIN+]: infection with in vitro-made amyloid aggregates of Rnq1p-(132-405) induces [PIN+]. *J Mol Biol* **365:** 773-782

Patino MM, Liu JJ, Glover JR and Lindquist S (1995) Support for the prion hypothesis for inheritance of a phenotypic trait in yeast. *Science* **273:** 622-626.

Paushkin SV, Kushnirov VV, Smirnov VN and Ter-Avanesyan MD (1996) Propagation of the yeast prion-like [psi+] determinant is mediated by oligomerization of the SUP35-encoded polypeptide chain release factor. *EMBO J* **15:** 3127-3134

Pezza JA, Villali J, Sindi SS and Serio TR (2014) Amyloid-associated activity contributes to the severity and toxicity of a prion phenotype. *Nat Commun* **5:** 4384

Piper PW, Harris NL and MacLean M (2006) Preadaptation to efficient respiratory maintenance is essential both for maximal longevity and the retention of replicative potential in chronologically ageing yeast. *Mech Ageing Dev* **127:** 733-740

Pollard TD, Blanchoin L and Mullins RD (2000) Molecular mechanisms controlling actin filament dynamics in nonmuscle cells. *Annu Rev Biophys Biomol Struct* **29:** 545-576

Pollard TD and Cooper JA (2009) Actin, a central player in cell shape and movement. *Science* **326:** 1208-1212

Prusiner SB (1998) Prions. *Proc Natl Acad Sci U S A* **95:** 13363-13383

Prusiner SB (2013) Biology and genetics of prions causing neurodegeneration. *Annu Rev Genet* **47:** 601-623

Prusiner SB, Bolton DC, Groth DF, Bowman KA, Cochran SP and McKinley MP (1982) Further purification and characterization of scrapie prions. *Biochemistry* **21:** 6942-6950

Pyo JO, Yoo SM, Ahn HH, Nah J, Hong SH, Kam TI, Jung S and Jung YK (2013) Overexpression of Atg5 in mice activates autophagy and extends lifespan. *Nat Commun* **4:** 2300

Qin ZH, Wang Y, Kegel KB, Kazantsev A, Apostol BL, Thompson LM, Yoder J, Aronin N and DiFiglia M (2003) Autophagy regulates the processing of amino terminal huntingtin fragments. *Hum Mol Genet* **12:** 3231-3244

Rand JD and Grant CM (2006) The Thioredoxin System Protects Ribosomes against Stress-induced Aggregation. *Mol Biol Cell* **17:** 387-401.

Ravikumar B, Duden R and Rubinsztein DC (2002) Aggregate-prone proteins with polyglutamine and polyalanine expansions are degraded by autophagy. *Hum Mol Genet* **11:** 1107-1117

Ravikumar B, Sarkar S, Davies JE, Futter M, Garcia-Arencibia M, Green-Thompson ZW, Jimenez-Sanchez M, Korolchuk VI, Lichtenberg M, Luo S, Massey DC, Menzies FM, Moreau K, Narayanan U, Renna M, Siddiqi FH, Underwood BR, Winslow AR and Rubinsztein DC (2010) Regulation of mammalian autophagy in physiology and pathophysiology. *Physiol Rev* **90:** 1383-1435

Ravikumar B, Vacher C, Berger Z, Davies JE, Luo S, Oroz LG, Scaravilli F, Easton DF, Duden R, O'Kane CJ and Rubinsztein DC (2004) Inhibition of mTOR induces autophagy and reduces toxicity of polyglutamine expansions in fly and mouse models of Huntington disease. *Nat Genet* **36:** 585-595

Reggiori F and Klionsky DJ (2002) Autophagy in the eukaryotic cell. *Eukaryot Cell* **1:** 11-21

Reggiori F and Klionsky DJ (2013) Autophagic processes in yeast: mechanism, machinery and regulation. *Genetics* **194:** 341-361

Reggiori F, Monastyrska I, Shintani T and Klionsky DJ (2005) The actin cytoskeleton is required for selective types of autophagy, but not nonspecific autophagy, in the yeast Saccharomyces cerevisiae. *Mol Biol Cell* **16:** 5843-5856

Requena JR and Wille H (2014) The structure of the infectious prion protein: Experimental data and molecular models. *Prion* **8:** 60-66

Roth DM and Balch WE (2013) Q-bodies monitor the quinary state of the protein fold. *Nat Cell Biol* **15:** 1137-1139

Rubinsztein DC, DiFiglia M, Heintz N, Nixon RA, Qin ZH, Ravikumar B, Stefanis L and Tolkovsky A (2005) Autophagy and its possible roles in nervous system diseases, damage and repair. *Autophagy* **1:** 11-22

Rubinsztein DC, Marino G and Kroemer G (2011) Autophagy and aging. *Cell* **146:** 682-695

Sagot I, Rodal AA, Moseley J, Goode BL and Pellman D (2002) An actin nucleation mechanism mediated by Bni1 and profilin. *Nat Cell Biol* **4:** 626-631

Salih DA and Brunet A (2008) FoxO transcription factors in the maintenance of cellular homeostasis during aging. *Curr Opin Cell Biol* **20:** 126-136

Sarkar S, Floto RA, Berger Z, Imarisio S, Cordenier A, Pasco M, Cook LJ and Rubinsztein DC (2005) Lithium induces autophagy by inhibiting inositol monophosphatase. *J Cell Biol* **170:** 1101-1111

Sarkar S, Perlstein EO, Imarisio S, Pineau S, Cordenier A, Maglathlin RL, Webster JA, Lewis TA, O'Kane CJ, Schreiber SL and Rubinsztein DC (2007) Small molecules

enhance autophagy and reduce toxicity in Huntington's disease models. *Nat Chem Biol* **3:** 331-338

Saupe SJ (2007) A short history of small s: a prion of the fungus Podospora anserina. *Prion* **1:** 110-115

Scheibel T and Lindquist SL (2001) The role of conformational flexibility in prion propagation and maintenance for Sup35p. *Nat Struct Biol* **8:** 958-962

Scherz-Shouval R, Shvets E, Fass E, Shorer H, Gil L and Elazar Z (2007) Reactive oxygen species are essential for autophagy and specifically regulate the activity of Atg4. *EMBO J* **26:** 1749-1760

Schulz TJ, Zarse K, Voigt A, Urban N, Birringer M and Ristow M (2007) Glucose restriction extends Caenorhabditis elegans life span by inducing mitochondrial respiration and increasing oxidative stress. *Cell Metab* **6:** 280-293

Selman C, Tullet JM, Wieser D, Irvine E, Lingard SJ, Choudhury AI, Claret M, Al-Qassab H, Carmignac D, Ramadani F, Woods A, Robinson IC, Schuster E, Batterham RL, Kozma SC, Thomas G, Carling D, Okkenhaug K, Thornton JM, Partridge L, Gems D and Withers DJ (2009) Ribosomal protein S6 kinase 1 signaling regulates mammalian life span. *Science* **326:** 140-144

Shacka JJ, Roth KA and Zhang J (2008) The autophagy-lysosomal degradation pathway: role in neurodegenerative disease and therapy. *Front Biosci* **13:** 718-736

Shacter E, Williams JA, Lim M and Levine RL (1994) Differential susceptibility of plasma proteins to oxidative modification: examination by western blot immunoassay. *Free Radic Biol Med* **17:** 429-437.

Shewmaker F and Wickner RB (2006) Ageing in yeast does not enhance prion generation. *Yeast* **23:** 1123-1128

Shintani T, Mizushima N, Ogawa Y, Matsuura A, Noda T and Ohsumi Y (1999) Apg10p, a novel protein-conjugating enzyme essential for autophagy in yeast. *EMBO J* **18:** 5234-5241

Shorter J (2011) The mammalian disaggregase machinery: Hsp110 synergizes with Hsp70 and Hsp40 to catalyze protein disaggregation and reactivation in a cell-free system. *PLoS One* **6:** e26319

Sideri TC, Koloteva-Levine N, Tuite MF and Grant CM (2011) Methionine oxidation of Sup35 protein induces formation of the [PSI+] prion in a yeast peroxiredoxin mutant. *J Biol Chem* **286:** 38924-38931

Sideri TC, Stojanovski K, Tuite MF and Grant CM (2010) Ribosome-associated peroxiredoxins suppress oxidative stress-induced de novo formation of the [PSI+] prion in yeast. *Proc Natl Acad Sci U S A* **107:** 6394-6399

Sikorski RS and Hieter P (1989) A system of shuttle vectors and yeast host strains designed for efficient manipulation of DNA in Saccharomyces cerevisiae. *Genetics* **122:** 19-27

Simonsen A, Cumming RC, Brech A, Isakson P, Schubert DR and Finley KD (2008) Promoting basal levels of autophagy in the nervous system enhances longevity and oxidant resistance in adult Drosophila. *Autophagy* **4:** 176-184

Sinclair DA and Guarente L (1997) Extrachromosomal rDNA circles--a cause of aging in yeast. *Cell* **91:** 1033-1042

Sirotkin V, Berro J, Macmillan K, Zhao L and Pollard TD (2010) Quantitative analysis of the mechanism of endocytic actin patch assembly and disassembly in fission yeast. *Mol Biol Cell* **21:** 2894-2904

Smith DL, Jr., McClure JM, Matecic M and Smith JS (2007) Calorie restriction extends the chronological lifespan of Saccharomyces cerevisiae independently of the Sirtuins. *Aging Cell* **6:** 649-662

Sohal RS, Sohal BH and Orr WC (1995) Mitochondrial superoxide and hydrogen peroxide generation, protein oxidative damage, and longevity in different species of flies. *Free Radic Biol Med* **19:** 499-504

Sondheimer N and Lindquist S (2000) Rnq1: an epigenetic modifier of protein function in yeast. *Mol Cell* **5:** 163-172

Sontag EM, Vonk WI and Frydman J (2014) Sorting out the trash: the spatial nature of eukaryotic protein quality control. *Curr Opin Cell Biol* **26C:** 139-146

Soulard A, Friant S, Fitterer C, Orange C, Kaneva G, Mirey G and Winsor B (2005) The WASP/Las17p-interacting protein Bzz1p functions with Myo5p in an early stage of endocytosis. *Protoplasma* **226:** 89-101

Soulard A, Lechler T, Spiridonov V, Shevchenko A, Shevchenko A, Li R and Winsor B (2002) Saccharomyces cerevisiae Bzz1p is implicated with type I myosins in actin patch polarization and is able to recruit actin-polymerizing machinery in vitro. *Mol Cell Biol* **22:** 7889-7906

Speldewinde SH, Doronina VA and Grant CM (2015) Autophagy protects against de novo formation of the [PSI+] prion in yeast. *Mol Biol Cell* **26:** 4541-4551

Spokoini R, Moldavski O, Nahmias Y, England JL, Schuldiner M and Kaganovich D (2012) Confinement to organelle-associated inclusion structures mediates asymmetric inheritance of aggregated protein in budding yeast. *Cell Rep* **2:** 738-747

Stadtman ER and Levine RL (2000) Protein oxidation. *Ann N Y Acad Sci* **899:** 191-208

Stadtman ER, Van Remmen H, Richardson A, Wehr NB and Levine RL (2005) Methionine oxidation and aging. *Biochim Biophys Acta* **1703:** 135-140

Stephan JS, Yeh YY, Ramachandran V, Deminoff SJ and Herman PK (2009) The Tor and PKA signaling pathways independently target the Atg1/Atg13 protein kinase complex to control autophagy. *Proc Natl Acad Sci U S A* **106:** 17049-17054

Sun J, Molitor J and Tower J (2004) Effects of simultaneous over-expression of Cu/ZnSOD and MnSOD on Drosophila melanogaster life span. *Mech Ageing Dev* **125:** 341-349

Sun Y, Martin AC and Drubin DG (2006) Endocytic internalization in budding yeast requires coordinated actin nucleation and myosin motor activity. *Dev Cell* **11:** 33-46

Sundaram A and Grant CM (2014) Oxidant-specific regulation of protein synthesis in Candida albicans *Fungal Genet Biol* **67:** 15-23

Suzuki G, Shimazu N and Tanaka M (2012) A yeast prion, Mod5, promotes acquired drug resistance and cell survival under environmental stress. *Science* **336:** 355-359

Takahashi Y, Meyerkord CL and Wang HG (2009) Bif-1/endophilin B1: a candidate for crescent driving force in autophagy. *Cell Death Differ* **16:** 947-955

Tanaka M, Collins SR, Toyama BH and Weissman JS (2006) The physical basis of how prion conformations determine strain phenotypes. *Nature* **442:** 585-589

Taneja V, Maddelein ML, Talarek N, Saupe SJ and Liebman SW (2007) A non-Q/N-rich prion domain of a foreign prion, [Het-s], can propagate as a prion in yeast. *Mol Cell* **27:** 67-77

Tomoyasu T, Mogk A, Langen H, Goloubinoff P and Bukau B (2001) Genetic dissection of the roles of chaperones and proteases in protein folding and degradation in the Escherichia coli cytosol. *Mol Microbiol* **40:** 397-413

Treusch S and Lindquist S (2012) An intrinsically disordered yeast prion arrests the cell cycle by sequestering a spindle pole body component. *J Cell Biol* **197:** 369-379

Trotter EW, Collinson EJ, Dawes IW and Grant CM (2006) Old Yellow Enzymes protect against acrolein toxicity in the yeast Saccharomyces cerevisiae. . *Appl Environ Microbiol* **72:** 4885-4892

Trotter EW, Rand JD, Vickerstaff J and Grant CM (2008) The yeast Tsa1 peroxiredoxin is a ribosome-associated antioxidant. *Biochem J* **412:** 73-80

True HL, Berlin I and Lindquist SL (2004) Epigenetic regulation of translation reveals hidden genetic variation to produce complex traits. *Nature* **431:** 184-187

Tuite MF and Cox BS (2003) Propagation of yeast prions. *Nat Rev Mol Cell Biol* **4:** 878-890

Tuite MF and Cox BS (2007) The genetic control of the formation and propagation of the [PSI+] prion of yeast. *Prion* **1:** 101-109

Tuite MF, Marchante R and Kushnirov V (2011) Fungal prions: structure, function and propagation. *Top Curr Chem* **305:** 257-298

Tuite MF, Mundy CR and Cox BS (1981) Agents that cause a high frequency of genetic change from [psi+] to [psi-] in Saccharomyces cerevisiae. *Genetics* **98:** 691-711

Tuite MF and Serio TR (2010) The prion hypothesis: from biological anomaly to basic regulatory mechanism. *Nat Rev Mol Cell Biol* **11:** 823-833

Tyedmers J, Madariaga ML and Lindquist S (2008) Prion switching in response to environmental stress. *PLoS Biol* **6:** e294

Tyedmers J, Mogk A and Bukau B (2010a) Cellular strategies for controlling protein aggregation. *Nat Rev Mol Cell Biol* **11:** 777-788

Tyedmers J, Treusch S, Dong J, McCaffery JM, Bevis B and Lindquist S (2010b) Prion induction involves an ancient system for the sequestration of aggregated proteins and heritable changes in prion fragmentation. *Proc Natl Acad Sci U S A* **107:** 8633-8638

Ventruti A and Cuervo AM (2007) Autophagy and neurodegeneration. *Curr Neurol Neurosci Rep* **7:** 443-451

Verghese J, Abrams J, Wang Y and Morano KA (2012) Biology of the heat shock response and protein chaperones: budding yeast (Saccharomyces cerevisiae) as a model system. *Microbiol Mol Biol Rev* **76:** 115-158

Verhoef LG, Lindsten K, Masucci MG and Dantuma NP (2002) Aggregate formation inhibits proteasomal degradation of polyglutamine proteins. *Hum Mol Genet* **11:** 2689-2700

Vincent A, Newnam G and Liebman SW (1994) The yeast translational allosuppressor, SAL6: a new member of the PP1-like phosphatase family with a long serine-rich N-terminal extension. *Genetics* **138:** 597-608

Vishveshwara N, Bradley ME and Liebman SW (2009) Sequestration of essential proteins causes prion associated toxicity in yeast. *Mol Microbiol* **73:** 1101-1114

Vitrenko YA, Pavon ME, Stone SI and Liebman SW (2007) Propagation of the [PIN+] prion by fragments of Rnq1 fused to GFP. *Curr Genet* **51:** 309-319

Wang T, Lao U and Edgar BA (2009) TOR-mediated autophagy regulates cell death in Drosophila neurodegenerative disease. *J Cell Biol* **186:** 703-711

Wasko BM and Kaeberlein M (2014) Yeast replicative aging: a paradigm for defining conserved longevity interventions. *FEMS Yeast Res* **14:** 148-159

Webb JL, Ravikumar B, Atkins J, Skepper JN and Rubinsztein DC (2003) Alpha-Synuclein is degraded by both autophagy and the proteasome. *J Biol Chem* **278:** 25009-25013

Wei M, Fabrizio P, Hu J, Ge H, Cheng C, Li L and Longo VD (2008) Life span extension by calorie restriction depends on Rim15 and transcription factors downstream of Ras/PKA, Tor, and Sch9. *PLoS Genet* **4:** e13

Weids AJ and Grant CM (2014) The yeast peroxiredoxin Tsa1 protects against protein-aggregate-induced oxidative stress. *J Cell Sci* **127:** 1327-1335

Weinberg J and Drubin DG (2012) Clathrin-mediated endocytosis in budding yeast. *Trends Cell Biol* **22:** 1-13

Wen KK and Rubenstein PA (2005) Acceleration of yeast actin polymerization by yeast Arp2/3 complex does not require an Arp2/3-activating protein. *J Biol Chem* **280:** 24168-24174

Werner-Washburne M, Braun EL, Crawford ME and Peck VM (1996) Stationary phase in *Saccharomyces cerevisiae*. *Molec Microbiol* **19:** 1159-1166

Wickner RB (1994) [URE3] as an altered URE2 protein: evidence for a prion analog in Saccharomyces cerevisiae. *Science* **264:** 566-569

Wickner RB, Edskes HK, Kryndushkin D, McGlinchey R, Bateman D and Kelly A (2011) Prion diseases of yeast: amyloid structure and biology. *Semin Cell Dev Biol* **22:** 469-475

Wickner RB, Edskes HK, Shewmaker F and Nakayashiki T (2007) Prions of fungi: inherited structures and biological roles. *Nat Rev Microbiol* **5:** 611-618

Wickner RB, Shewmaker FP, Bateman DA, Edskes HK, Gorkovskiy A, Dayani Y and Bezsonov EE (2015) Yeast prions: structure, biology, and prion-handling systems. *Microbiol Mol Biol Rev* **79:** 1-17

Wierman MB and Smith JS (2014) Yeast sirtuins and the regulation of aging. *FEMS Yeast Res* **14:** 73-88

Wilkinson JE, Burmeister L, Brooks SV, Chan CC, Friedline S, Harrison DE, Hejtmancik JF, Nadon N, Strong R, Wood LK, Woodward MA and Miller RA (2012) Rapamycin slows aging in mice. *Aging Cell* **11:** 675-682

Winter D, Lechler T and Li R (1999) Activation of the yeast Arp2/3 complex by Bee1p, a WASP-family protein. *Curr Biol* **9:** 501-504

Winter D, Podtelejnikov AV, Mann M and Li R (1997) The complex containing actin-related proteins Arp2 and Arp3 is required for the motility and integrity of yeast actin patches. *Curr Biol* **7:** 519-529

Winzeler EA and *al. e* (1999) Functional Characterization of the S. cerevisiae Genome by Gene Deletion and Parallel Analysis. *Science* **285:** 901-906

Wirawan E, Vanden Berghe T, Lippens S, Agostinis P and Vandenabeele P (2012) Autophagy: for better or for worse. *Cell Res* **22:** 43-61

Wolschner C, Giese A, Kretzschmar HA, Huber R, Moroder L and Budisa N (2009) Design of anti- and pro-aggregation variants to assess the effects of methionine oxidation in human prion protein. *Proc Natl Acad Sci U S A* **106:** 7756-7761

Wong CM, Siu KL and Jin DY (2004) Peroxiredoxin-null yeast cells are hypersensitive to oxidative stress and are genomically unstable. *J Biol Chem* **22:** 23207-23213

Xie Z and Klionsky DJ (2007) Autophagosome formation: core machinery and adaptations. *Nat Cell Biol* **9:** 1102-1109

Yamin G, Glaser CB, Uversky VN and Fink AL (2003) Certain metals trigger fibrillation of methionine-oxidized alpha-synuclein. *J Biol Chem* **278:** 27630-27635

Yang HC and Pon LA (2002) Actin cable dynamics in budding yeast. *Proc Natl Acad Sci U S A* **99:** 751-756

Yang Z, Huang J, Geng J, Nair U and Klionsky DJ (2006) Atg22 recycles amino acids to link the degradative and recycling functions of autophagy. *Mol Biol Cell* **17:** 5094-5104

Yang Z and Klionsky DJ (2010) Mammalian autophagy: core molecular machinery and signaling regulation. *Curr Opin Cell Biol* **22:** 124-131

Yao Z, Delorme-Axford E, Backues SK and Klionsky DJ (2015) Atg41/Icy2 regulates autophagosome formation. *Autophagy* **11:** 2288-2299

Yla-Anttila P, Vihinen H, Jokitalo E and Eskelinen EL (2009) Monitoring autophagy by electron microscopy in Mammalian cells. *Methods Enzymol* **452:** 143-164

Yorimitsu T, He C, Wang K and Klionsky DJ (2009) Tap42-associated protein phosphatase type 2A negatively regulates induction of autophagy. *Autophagy* **5:** 616-624

Yorimitsu T and Klionsky DJ (2007) Endoplasmic reticulum stress: a new pathway to induce autophagy. *Autophagy* **3:** 160-162

Yorimitsu T, Zaman S, Broach JR and Klionsky DJ (2007) Protein kinase A and Sch9 cooperatively regulate induction of autophagy in Saccharomyces cerevisiae. *Mol Biol Cell* **18:** 4180-4189

Younan ND, Nadal RC, Davies P, Brown DR and Viles JH (2012) Methionine oxidation perturbs the structural core of the prion protein and suggests a generic misfolding pathway. *J Biol Chem* **287:** 28263-28275

Young JC (2010) Mechanisms of the Hsp70 chaperone system. *Biochem Cell Biol* **88:** 291-300

Yun SW, Gerlach M, Riederer P and Klein MA (2006) Oxidative stress in the brain at early preclinical stages of mouse scrapie. *Exp Neurol* **201:** 90-98

Zhou C, Slaughter BD, Unruh JR, Eldakak A, Rubinstein B and Li R (2011) Motility and segregation of Hsp104-associated protein aggregates in budding yeast. *Cell* **147:** 1186-1196

Zhou P, Derkatch IL and Liebman SW (2001) The relationship between visible intracellular aggregates that appear after overexpression of Sup35 and the yeast prion-like elements [PSI(+)] and [PIN(+)]. *Mol Microbiol* **39:** 37-46

8 Supplementary Materials.

Table 8.1 Strains used in this study. (All strains listed are in the 74D-694 strain background and in the [*PIN*$^+$][*psi*$^-$] prion background unless stated otherwise).

Strain	Genotype	Source
Wild-type	*MATa,* ade1-14*, ura3-52, leu2-3, 112, trp1-289, his3-200*	Grant strain collection
Wild-type [*PSI*$^+$]	*MATa,* ade1-14*, ura3-52, leu2-3, 112, trp1-289, his3-200*	Grant strain collection
atg1	*MATa,* ade1-14*, ura3-52, leu2-3, 112, trp1-289, his3-200, atg1::HIS3*	This study
atg1 [*PSI*$^+$]	*MATa,* ade1-14*, ura3-52, leu2-3, 112, trp1-289, his3-200, atg1::HIS3*	This study
atg4	*MATa,* ade1-14*, ura3-52, leu2-3, 112, trp1-289, his3-200, atg1::HIS3*	This study
atg7	*MATa,* ade1-14*, ura3-52, leu2-3, 112, trp1-289, his3-200, atg7::HIS3*	This study
atg8	*MATa,* ade1-14*, ura3-52, leu2-3, 112, trp1-289, his3-200, atg8::HIS3*	This study
atg8 [*PSI*$^+$]	*MATa,* ade1-14*, ura3-52, leu2-3, 112, trp1-289, his3-200, atg8::HIS3*	This study
atg9	*MATa,* ade1-14*, ura3-52, leu2-3, 112, trp1-289, his3-200, atg9::HIS3*	This study
atg10	*MATa,* ade1-14*, ura3-52, leu2-3, 112, trp1-289, his3-200, atg10::HIS3*	This study
atg11	*MATa,* ade1-14*, ura3-52, leu2-3, 112, trp1-289, his3-200, atg11::HIS3*	This study
atg12	*MATa,* ade1-14*, ura3-52, leu2-3, 112, trp1-289, his3-200, atg12::HIS3*	This study
atg14	*MATa,* ade1-14*, ura3-52, leu2-3, 112, trp1-289, his3-200, atg14::HIS3*	This study
atg15	*MATa,* ade1-14*, ura3-52, leu2-3, 112, trp1-289, his3-200, atg15::HIS3*	This study
atg19	*MATa,* ade1-14*, ura3-52, leu2-3, 112, trp1-289, his3-200, atg19::HIS3*	This study
atg19 [*PSI*$^+$]	*MATa,* ade1-14*, ura3-52, leu2-3, 112, trp1-289, his3-200, atg19::HIS3*	This study
atg32	*MATa,* ade1-14*, ura3-52, leu2-3, 112, trp1-289, his3-200, atg32::HIS3*	This study
tsa1 tsa2	*MATa,* ade1-14*, ura3-52, leu2-3, 112, trp1-289, his3-200, tsa1::LEU2, tsa2::KanMX*	Grant strain collection
ppq1	*MATa,* ade1-14*, ura3-52, leu2-3, 112, trp1-289, his3-200, ppq::TRP1*	Grant strain collection
TAP-tagged Sup35	*MATa, ade1-14, ura3-52, leu2-3, 112, trp1-289, his3-200, his3-200, SUP35*-TAP (*TRP1*)	Grant strain collection
tsa1 tsa2 TAP-tagged Sup35	*MATa,* ade1-14*, ura3-52, leu2-3, 112, trp1-289, his3-200, tsa1::LEU2, tsa2::KanMX, SUP35*-TAP (*TRP1*)	Grant strain collection
atg1 TAP-tagged Sup35	*MATa, ade1-14, ura3-52, leu2-3, 112,, trp1-289, his3-200, atg1::HIS3, SUP35*-TAP (*TRP1*)	This study
abp1	*MATa,* ade1-14*, ura3-52, leu2-3, 112, trp1-289, his3-200, abp1::HIS3*	This study
abp1 TAP-	*MATa, ade1-14, ura3-52, leu2-3, 112,, trp1-*	This study

tagged Sup35	*289, his3-200, atg14::HIS3, SUP35*-TAP (*TRP1*)	
crn1	*MATa,* ade1-14*, ura3-52, leu2-3, 112, trp1-289, his3-200, crn1::HIS3*	This study
pan1	*MATa,* ade1-14*, ura3-52, leu2-3, 112, trp1-289, his3-200, pan1::HIS3*	This study

Table 8.2 Oligonucleotide used in this study. [The deletion mutants were generated in the 74D-694 strain background using a PCR-based homologous gene replacement strategy. Forward and reverse primers were designed with additional sequences homologous to the *HIS3* selectable marker from the pRS413 vector as described previously (Sikorski and Hieter, 1989)].

Gene	Sequence	Purpose
ABP1	TATTTAGACGTTACTTTGATATCTCTG TCC ATGAGAGCACTTATTTTAGGCGTTTCGGT GATGAC	Forward tagging of *HIS3* cassette
ABP1	CTCTACTCTAGTTAAAAGGTTTACTAC TGAATATATCAGACCTAATGACGCAAA TGAGTTCCTGATGCGGTATTTTCTCCT	Reverse tagging of *HIS3* cassette
ABP1	ATGTATAGTACGCGTTAGGACATCTATAA TAA	Forward verification primer
ATG1	CAAATCTCTTTTACAACACCAGACGAGAA ATTAAGAAAATGGGAGACATTAACGTTTC GGTGATGAC	Forward tagging of *HIS3* cassette
ATG1	GTACTTAATAAGAAAACCATATTATGCATC ACTTAATTTTGGTGGTTCATCTTCTTCCTG ATGCGGTATTTTCTCCT	Reverse tagging of *HIS3* cassette
ATG1	ATTTCATCACCTTTAAGTTAAGTACCAAG	Forward verification primer
ATG4	CACTTCTTCCTTCTAGAAACTCTGCGCAG GCCTAATTGTTGTTGTTTTGTTCAGCGTTT CGGTGATGAC	Forward tagging of *HIS3* cassette
ATG4	CTTCAAGTTTGAATTGCGATGACTAGGCA TTTTGGACTTCGACACTAGTTCCTGATGC GGTATTTTCTCCT	Reverse tagging of *HIS3* cassette
ATG4	CACCTTCTCCTAGTGGTATAGAAGAGTTA T	Forward verification primer
ATG7	CAACAAATATAAGATAATCAAGAATAAAAT GTCGTCAGAAAGGGTCCGTTTCGGTGAT GAC	Forward tagging of *HIS3* cassette
ATG7	GTGGCACCACAATATGTACCAATGCTATT ATATGCAAAATATTAAGCTTCCTGATGCG GTATTTTCTCCT	Reverse tagging of *HIS3* cassette

ATG7	GATGTAAAATGTACTTTATGGAAGAACAAG	Forward verification primer
ATG9	AATGTTATTCTAGTTATTGTTACCCAGTTTCGGAACTTTAGGGGAGCCACACTTTAAACCGTTTCGGTGATGAC	Forward tagging of *HIS3* cassette
ATG9	GGCCCAACTAAAGAAGGAACGTAAATTCACTATGAAAGAAATCCGTAAAGACGCCTTCCTGATGCGGTATTTTCTCCT	Reverse tagging of *HIS3* cassette
ATG9	GGTAAAATAGTAGTCACACCTCAAATCTAAT	Forward verification primer
ATG10	CCCGGTCTGTATATATGTCCATCATAGGCGACAAGGTGTTCTAGTATCTTCAGGCGTTTCGGTGATGAC	Forward tagging of *HIS3* cassette
ATG10	GCTTCGCTAGGTGCGACGACGACTGATTCTATTGGGTTATCCGACACATCATCAGTTCCTGATGCGGTATTTTCTCCT	Reverse tagging of *HIS3* cassette
ATG10	TATACGTTAGGCGTTTATGTTTACTCTCTAT	Forward verification primer
ATG11	GCTTGCCATGGAGAGCCTTTTTATCGCTTTTGGCTACCCGGTTTCTTGGTAGGCGTTTCGGTGATGAC	Forward tagging of *HIS3* cassette
ATG11	TCAATGAATGTTAATCTGACTTGGATAGGCATTTTACCTGATGAGCCACATTCCTGATGCGGTATTTTCTCCT	Reverse tagging of *HIS3* cassette
ATG11	TAATCTCTTGTGAAACTTTGTTCTTCAT	Forward verification primer
ATG12	CGTACATCCCTAACTGTATATTCTACAGTAGAGTGAACCAATGACAGTATGAGTAGCGTTTCGGTGATGAC	Forward tagging of *HIS3* cassette
ATG12	GGATTTTTGATCGACTGTAGGTTTTCTTCTTAGACCATTCCAGCGCCCGGGTATTTAACTTCCTGATGCGGTATTTTCTCCT	Reverse tagging of *HIS3* cassette
ATG12	TTAGTGTCTGAGTATCGTATTGAATGTCTA	Forward verification primer
ATG14	GGGAAAGGACCAAATACAAAAGTGATTAGAAGGATAACGAGTAGAGAAAAAGGGCGTTTCGGTGATGAC	Forward tagging of *HIS3* cassette
ATG14	GCTTATTACACTGGCTGCTATTGTTTATGACTGACTACATGCAACTTTATACACTTCCTGATGCGGTATTTTCTCCT	Reverse tagging of *HIS3* cassette
ATG14	TAAATAATACGTGTAATTGTTTTCCTTACG	Forward verification primer
ATG15	GACACTCAAATCAGTGTCAACCTTTTGGATAAGTCAAAGAAAGTACGCCGCTGCCGTT	Forward tagging of *HIS3* cassette

	TCGGTGATGAC	
ATG15	GCACCTGACTGACGCCTTTCACTTTAAAG CAGTATTAATATATCTTCTCGTGTCGTTCC TGATGCGGTATTTTCTCCT	Reverse tagging of *HIS3* cassette
ATG15	GTATCTCTACTATATTGTTGTTCGCTGAAG	Forward verification primer
ATG19	GCGGCGGCACTTGCTTCAGTAACGCCCA AAGGAGAGTTCTGGTAAATGAACAACTCC GTTTCGGTGATGAC	Forward tagging of *HIS3* cassette
ATG19	CTCATTGCTGTATAAAAATAGAGTTTGACC TAGAGTTCTTCCCAAGTCAGGGCTTCCTG ATGCGGTATTTTCTCCT	Reverse tagging of *HIS3* cassette
ATG19	ATCTATAAATTCTTGCCAAATATTGTCTTT	Forward verification primer
ATG32	TGGCACTTGTTTCGTGCTTTCTCAAATATC TTAGATCACCGTCTGTCTAGAGCCGTTTC GGTGATGAC	Forward tagging of *HIS3* cassette
ATG32	CTATCACTTCTGTTTCTCTCACTGCGTATC TATATTCCCCGTTTGGTTCCTTTCCTTAAT TACCTTCCTGATGCGGTATTTTCTCCT	Reverse tagging of *HIS3* cassette
ATG32	ATACCACTCTTATACAGTATGCACGATATT	Forward verification primer
CRN1	CTCGAAGAAAATAAAGTAGATTCATGTAC ACGTATATCAAAAGAGTACAGCGTTTCGG TGATGAC	Forward tagging of *HIS3* cassette
CRN1	GATTCACTTTCTAAGTGCATTATTATCGCC GCCGTCTTATGTACATTACTTCCTGATGC GGTATTTTCTCCT	Reverse tagging of *HIS3* cassette
CRN1	AGATTCATGTACACGTATATCAAAAGAGT A	Forward verification primer
HIS3	CGACAACTGCGTACGGCCTG	Reverse internal primer for verification of tagged genes
PAN1	GCTTGATCACATGACACGTCGACGATATT TTTTTCTTGTTAGGGGCAAAAGTTGGTATT GCGTTTCGGTGATGAC	Forward tagging of *HIS3* cassette
PAN1	GGATCAACGGTCAACGATTCTAGCAGTCG ATAATTTAAATGGATTTAAAATTGGCGGTA GTTCCTGATGCGGTATTTTCTCCT	Reverse tagging of *HIS3* cassette
PAN1	GTTTACCAGAGATATAGAAACCTTAAACG	Forward verification primer

Table 8.3 Plasmids used in this study. [The selection marker for each plasmid is included in brackets (all plasmids are ampicillin resistant, Amp^R)].

Lab number	Description	Source
9	pRS413 (*HIS3*)	Lab strain
341	p6442, *CUP1-SUP35NM-GFP* (*URA3*)	Patino et al 1995
383	2 micron, *GAL1-RNQ1-EFGP* (*URA3*)	Meriin et al 2002
396	p1513, *CEN2 LEU2 ura3–14 ori* (*LEU2*)	Manogaran et al 2011
559	pESC-*GFP-Ubc9*^{ts} (*URA3*)	Escusa-Toret et al 2013
566	pUKC1809, *GAL1-SUP35* (*LEU2*)	Josse et al 2012
587	pRS415-*GPD-CFP-ATG8* (*LEU2*)	Tyedmers et al 2010a
588	pRS415-*GPD-CFP-ATG14* (*LEU2*)	Tyedmers et al 2010a
600	pRS415-*GAL1-SUP35NM-RFP* (*LEU2*)	Arslan et al 2015
616	pRS416-*GFP-Atg8* (*URA3*)	Noda et al 1995

Table 8.4 Primary antibodies used in this study.

Target	**Secondary**	**Source**	**Concentration**
Abp1	Mouse	Abcam	1:10000
Act1	Mouse	Thermo Scientific	1:10000
Arp3	Mouse	Santa Cruz Biotechnology	1:5000
DNPH	Rabbit	Dako	1:5000
GFP	Rabbit	Life technologies	1:10000
Methionine sulphoxide	Rabbit	Novus Biologicals	1:1000
Pgk1	Rabbit	Thermo Scientific	1:10000
Sap190	Rabbit	Lab stock	1:5000
Sup35	Rabbit	Gift from Mick Tuite	1:10000
Tef1	Rabbit	Lab stock	1:5000
Tsa1	Rabbit	Lab stock	1:5000

Table 8.5 Secondary antibodies used in this study.

Description	**Source**	**Concentration**
Goat Anti-Rabbit IgG Horseradish Peroxidase Conjugate	Sigma	1:10000
Goat Anti-Mouse IgG Horseradish Peroxidase Conjugate	Promega	1:10000
Donkey Anti-Goat IgG Horseradish Peroxidase Conjugate	Promega	1:10000
Goat Anti-Rabbit Li-Cor	Li-Cor	1:10000
Goat Anti-Mouse Li-Cor	Li-Cor	1:10000
Donkey Anti-Goat Li-Cor	Li-Cor	1:10000